



universität  
wien

# DISSERTATION

Titel der Dissertation

**Detection and characterization of *PAX5* aberrations in childhood  
acute lymphoblastic leukemia**

angestrebter akademischer Grad

Doktorin der Naturwissenschaften (Dr. rer.nat.)

Verfasserin / Verfasser:	Karin Nebral
Matrikel-Nummer:	9604391
Dissertationsgebiet (lt. Studienblatt):	442 Anthropologie
Betreuerin / Betreuer:	Univ.-Prof. Dr. Oskar A. Haas

Wien, am 04. November 2008

<b>Contents</b>	<b>pages</b>
<b>Abbreviations</b>	3
<b>Abstract</b>	6
<b>Chapter 1</b>	8
1. Introduction	8
1.1. Hematopoiesis	8
1.2. Lymphoid development	10
1.2.1. B-cell development and the role of PAX5	11
1.3. Acute lymphoblastic leukemia	15
1.4. The PAX gene family in oncogenesis	17
1.5. PAX5 aberrations in B-cell malignancies	20
1.5.1. PAX5 aberrations in lymphoma	20
1.5.2. PAX5 aberrations in acute lymphoblastic leukemia	21
1.5.2.1. Deletions and Mutations	21
1.5.2.2. PAX5 fusions in ALL	23
<b>Chapter 2</b>	25
Identification of PML as novel PAX5 fusion partner in childhood acute lymphoblastic leukemia	
<b>Chapter 3</b>	39
Incidence and diversity of PAX5 fusion genes in childhood acute lymphoblastic leukemia	
<b>Chapter 4</b>	65
Monoallelic loss and frequent mutation of the second allele of <i>PAX5</i> in dic(9;20) childhood acute lymphoblastic leukemia	
<b>Chapter 5</b>	74
5. Additional Methods and Results	74
5.1. Establishment and validation of automated FISH screening	74
5.1.1. Analysis of control samples	80
5.1.2. Validation of the FISH assay in <i>PAX5</i> -rearranged samples	82
5.1.3. Novel PAX5 positive cases - Metafer 4 Metacyte analysis	83

---

5.2. Detailed analysis of selected cases	86
5.2.1. PAX5 rearranged cases	87
5.2.2. <i>PAX5</i> deletions	94
<b>Chapter 6</b> _____	101
6. Discussion	101
<b>Chapter 7</b> _____	106
7. References	106
<b>Chapter 8</b> _____	113
8. Appendix	113
8.1. <i>ETV6-NCOA2</i> fusion defines a new entity of T-lymphoid/myeloid progenitor acute leukemia	113
8.2. Additional FISH clones	121
8.3. Additional PCR primers	123
<b>Deutsche Zusammenfassung</b> _____	125
<b>Curriculum Vitae</b> _____	127
<b>Danksagung</b> _____	129

---

## ABBREVIATIONS

ALL	acute lymphoblastic leukemia
BAC	bacterial artificial chromosome
BCP	B-cell precursor
BCR	B-cell receptor
CLP	common lymphoid progenitor
CML	chronic myelogenous leukemia
CMLP	common myelo-lymphoid progenitor
CMP	common myeloid progenitor
CY3	cyanine 3
DLBCL	diffuse large B-cell lymphoma
EFS	event-free survival
ELP	earliest lymphocyte progenitor
FAB	French-American-British
FISH	fluorescence in situ hybridization
FITC	fluorescein isothiocyanate
GC B-cell	germinal center B-cells
GMP	granulocyte/macrophage progenitor
HLH	helix–loop–helix
HSC	hematopoietic stem cell
Ig	immunoglobulin
LIN	lineage
LMPP	lymphoid-primed multipotent progenitor
LSK	LIN <sup>−</sup> SCA1 <sup>+</sup> KIT <sup>hi</sup>
MkEP	megakaryocyte/erythroid progenitor
MPP	multipotent progenitor
RACE	rapid amplification of cDNA ends
RT-PCR	reverse-transcription polymerase chain reaction
SAGA	Spt–Ada–Gcn5 acetyltransferase
shRNA	short hairpin RNA
SNP	single nucleotide polymorphism
SSP DNA	salmon sperm DNA

Human and mouse gene nomenclature according to the *HUGO Gene Nomenclature Committee* (<http://www.genenames.org>) and the *Mouse Genome Informatics* (<http://www.informatics.jax.org/>), respectively. Mouse protein nomenclature according to *The Universal Protein Resource (UniProt)* (<http://www.uniprot.org/uniprot>).

Human gene symbols are *ITALICIZED*, with all letters UPPERCASE, whereas mouse gene symbols are written in *Italics* with the first letter capitalized followed by lowercase letters. Protein designations are the same as the gene symbol, but NOT ITALICIZED and all letters UPPERCASE. However, to differentiate between human and mouse proteins they are often indicated in UPPERCASE and Lowercase, respectively [e.g. PAX5 (human) and Pax5 (mouse)].

### Genes (human)

ABL1	c-abl oncogene 1, receptor tyrosine kinase
ATXN1 (SCA1)	ataxin 1
AUTS2	autism susceptibility candidate 2
BCL11B	B-cell CLL/lymphoma 11B (zinc finger protein)
BCR	breakpoint cluster region
BDNF	brain-derived neurotrophic factor
BLNK	B-cell linker
BRD1	bromodomain containing 1
BTG1	B-cell translocation gene 1, anti-proliferative
C20orf112	chromosome 20 open reading frame 112
CCR2	chemokine (C-C motif) receptor 2
CD19	CD19 molecule
CD22	CD22 molecule
CD28	CD28 molecule
CD72	CD72 molecule
CD79A (mb-1, Ig $\alpha$ )	CD79a molecule, immunoglobulin-associated alpha
CD79B (Ig $\beta$ , B29)	CD79b molecule, immunoglobulin-associated beta
CDKN2A	cyclin-dependent kinase inhibitor 2A (melanoma, p16, inhibits CDK4)
CDKN2B	cyclin-dependent kinase inhibitor 2B (p15, inhibits CDK4)
CEBPA (C/EBP $\alpha$ )	CCAAT/enhancer binding protein (C/EBP), alpha
CR2 (CD21)	complement component (3d/Epstein Barr virus) receptor 2
CREBBP (CBP)	CREB binding protein
CSF1R (GM-CSFR $\alpha$ )	colony stimulating factor 1 receptor
DACH1	dachshund homolog 1
EBF1	early B-cell factor 1
ELN	elastin
ERG	v-ets erythroblastosis virus E26 oncogene homolog (avian)
ETS1	v-ets erythroblastosis virus E26 oncogene homolog 1 (avian)
ETV6 (TEL)	ets variant gene 6 (TEL oncogene)
FLT3	FMS-related tyrosine kinase 3
FOXO1 (FKHR)	forkhead box O1
FOXP1	forkhead box P1
GATA1	GATA binding protein 1 (globin transcription factor 1)
GATA3	GATA binding protein 3
HIPK1	homeodomain interacting protein kinase 1
IGH@ (IgH)	immunoglobulin heavy locus
IGJ	immunoglobulin J polypeptide, linker protein for immunoglobulin alpha and mu polypeptides
IGK@ (IgK)	immunoglobulin kappa locus
Igll1( $\lambda$ 5)	immunoglobulin lambda-like polypeptide 1
IKZF1 (Ikaros)	IKAROS family zinc finger 1 (Ikaros)
IKZF3 (Aiolos)	IKAROS family zinc finger 3 (Aiolos)
IL7	interleukin 7
IL7R (IL-7R $\alpha$ )	interleukin 7 receptor
IRF4	interferon regulatory factor 4

---

IRF8	interferon regulatory factor 8
JAK2	janus kinase 2
KIT (C-Kit, CD117)	v-kit Hardy-Zuckerman 4 feline sarcoma viral oncogene homolog
LEF1	lymphoid enhancer-binding factor 1
LMO1	LIM domain only 1 (rhombotin 1)
LMO2	LIM domain only 2 (rhombotin-like 1)
MLL	myeloid/lymphoid or mixed-lineage leukemia (trithorax homolog, Drosophila)
MYC (c-Myc)	v-myc myelocytomatosis viral oncogene homolog (avian)
NOTCH1	Notch homolog 1, translocation-associated (Drosophila)
NUP98	nucleoporin 98kDa
PAX5	paired box 5
PBX1	pre-B-cell leukemia homeobox 1
PLCG2 (PLC $\gamma$ 2)	phospholipase C, gamma 2 (phosphatidylinositol-specific)
PML	promyelocytic leukemia
POM121	POM121 membrane glycoprotein
PPARG (PPAR $\gamma$ 1)	peroxisome proliferator-activated receptor gamma
PRDM1 (BLIMP1)	PR domain containing 1, with ZNF domain
PRKCB (PKC $\beta$ )	protein kinase C, beta
RAG1	protein: BSAP, B-cell lineage specific activator protein
RAG2	recombination-activation gene 1
RB1	recombination activating gene 2
RCSD1	retinoblastoma 1
RUNX1 (AML1)	RCSD domain containing 1
RUNX1T1 (ETO)	runt-related transcription factor 1
SCA1	runt-related transcription factor 1; translocated to, 1 (cyclin D-related)
SCL (TAL1)	stem cell antigen 1
SPI1 (PU.1)	T-cell acute lymphocytic leukemia 1
SPIB	spleen focus forming virus (SFFV) proviral integration oncogene spi1
STAT5	Spi-B transcription factor (Spi-1/PU.1 related)
TCF3 (E2A)	signal transducer and activator of transcription 5A
THY-1 (CD90)	transcription factor 3 (E2A immunoglobulin enhancer binding factors E12/E47)
TP53 (p53)	Thy-1 cell surface antigen
VCAM1	tumor protein p53
VPREB1 (VpreB)	vascular cell-adhesion molecule 1
WT1	pre-B lymphocyte gene 1
XBP1	Wilms tumor 1
ZCCHC7	X-box binding protein 1
ZNF521	zinc finger, CCHC domain containing 7
	zinc finger protein 521

### Mouse genes & proteins

Ets1	E26 avian leukemia oncogene 1, 5' domain
Igh	protein: Protein C-ets-1
Ikzf1 (Ikaros)	immunoglobulin heavy chain complex
Ikzf3 (Aiolos)	IKAROS family zinc finger 1
Plcg2	protein: DNA-binding protein Ikaros
Prkcb (Prkcb1)	IKAROS family zinc finger 3
Sfp1 (PU.1)	protein: Zinc finger protein Aiolos
Tcfe2a (E2A, TCF3)	phospholipase C, gamma 2
	protein: PLC $\gamma$ 2
	protein kinase C, beta 1
	protein: PKC $\beta$
	SFFV proviral integration 1
	protein: Transcription factor PU.1
	transcription factor E2a
	protein: Transcription factor E2-alpha

---

## ABSTRACT

*PAX5*, a master regulator of B-cell development, was recently shown to be involved in several B-cell malignancy-associated genetic alterations, such as point mutations, deletions, and, of particular interest in the context of my work, also gene rearrangements. In B-cell non-Hodgkin's-Lymphoma with a t(9;14)(p13;q32), for instance, *PAX5* is juxtaposed to the *IGH* locus, which results in an inappropriate over-expression of *PAX5*. In B-cell precursor acute lymphoblastic leukemia (BCP-ALL), on the other hand, *PAX5* can fuse to several different partner genes such as *FOXP1* (3p13), *AUTS2* (7q11), *ELN* (7q11), *ETV6* (12p13), *ZNF521* (18q11), and *C20orf112* (20q11), thereby generating fusion transcripts that encode chimeric proteins. Therefore, the aim of this study was to screen childhood ALL samples for *PAX5* rearrangements and to determine their incidence and the types of *PAX5* gene fusions in a systematic and population-based fashion.

To identify all potential *PAX5*-affecting breakpoints, including even those that result in juxtaposition of *PAX5* under the regulatory elements of a partner gene, a novel dual-color split-apart fluorescence in situ hybridization (FISH) assay with BAC clones flanking the *PAX5* gene was employed. All samples with suspicious FISH patterns were further analyzed with *PAX5* exon-specific cosmid clones. In order to facilitate high-throughput screening, interphase FISH analysis was performed using an automated spot counting system (Metafer4-Metacyte, Metasystems). Novel fusion partners were identified by FISH, 3'- or 5'-RACE (Rapid Amplification of cDNA ends) and the presence of specific hybrid transcripts was verified by RT-PCR (Reverse Transcription-PCR) and sequence analysis.

A *PAX5* rearrangement-indicating FISH pattern was observed in 10 (2.2%) of 446 children with *de novo* ALL registered in the Austrian ALL-BFM 2000 and Interfant-99 studies. Out of these 10 patients, one case was previously shown to harbor a *PAX5-ETV6* fusion, in one the recently described *PAX5-C20orf112* gene fusion was found and, despite all efforts, the fusion partner remained unidentified in another one. However, in seven cases we succeeded to identify six new *PAX5* in-frame fusions with *HIPK1* (1p13), *POM121* (7q11), *JAK2* (9p24), *DACH1* (13q21), *PML* (15q24), or *BRD1* (22q13.33). Apart from two *PAX5-JAK2*-positive cases, every other fusion gene was non-recurring. Moreover, at least in childhood ALL we did not find any evidence for *PAX5* activating translocations. Given the large variety of recovered *PAX5* fusion partners, our custom-made dual-color/two-step FISH screening approach has proven to be an appropriate and efficient tool for the reliable detection of *PAX5* gene fusions.

The results of this study show that *PAX5* rearrangements occur with a frequency of approximately 2.5% exclusively in BCP-ALL and fuse *PAX5* to a broad range of different partner genes comprising transcription factors, structural proteins, and even a tyrosine kinase. All hypothetical fusion proteins retain at least the *PAX5* paired DNA-binding domain,

---

which is joined to the C-terminal region or even the entire protein of the fusion partner. Thus, all PAX5 chimeric proteins are predicted to retain the ability to bind to PAX5 target genes suggesting that they act as aberrant transcription factors, which may antagonize intrinsic PAX5 transcriptional activity, and hence, may contribute to the pathogenesis of BCP-ALL.



## CHAPTER 1

### 1. INTRODUCTION

#### 1.1. Hematopoiesis

Hematopoiesis, the formation of the blood cellular components, is initiated in the fetal liver and postnatal bone marrow and all types of blood cells derive from hematopoietic stem cells (HSCs). Extensive proliferation occurs during differentiation into all lineages, which comprise the **myeloid** (including macrophages, granulocytes and polymorphonuclear cells such as neutrophils, basophils and eosinophils), the **erythroid-megakaryocyte** (including erythrocyte and platelets derived from megakaryocytes), and the **lymphoid** (B-cells, T-cells, natural killer cells, and dendritic cells) lineage (Fig. 1) (Katsura, 2002).

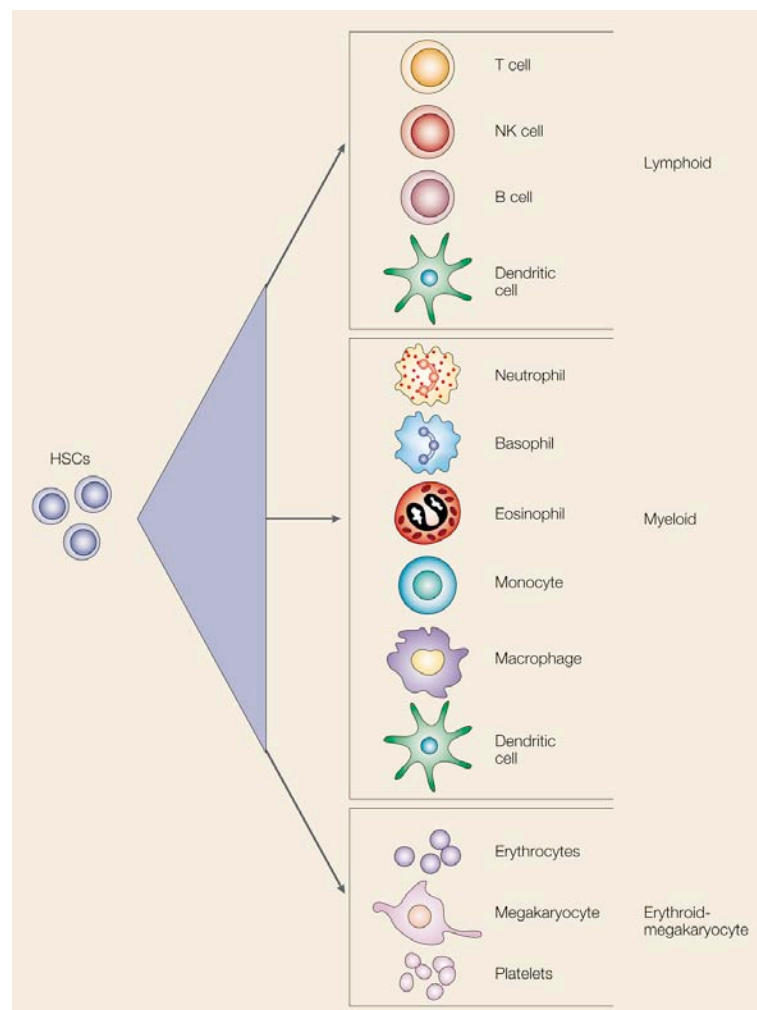


**Figure 1. Hematopoietic cell classifications.** Figure taken from Katsura, 2002.

The lineage differentiation processes during hematopoiesis are still under debate and currently various models are proposed, which almost all are based on experimental evidence of mice studies. The classic paradigm implies that blood-cell formation proceeds along an ordered pathway with binary decision steps, and that a single route is given for each major cell type. However, recent findings suggest that more dynamic alternative developmental pathways are generating myeloid and lymphoid cells.

Stem cells and all early progenitors are found within the LIN<sup>-</sup> SCA1<sup>+</sup> KIT<sup>hi</sup> subset (LSK subset) and are defined by the capacity of self-renewal and the capability of differentiation into all hematopoietic cell lineages. In one of the models, HSCs are subdivided into long-term HSCs (Thy-1<sup>low</sup>Flt3<sup>-</sup>), short-term HSCs (Thy-1<sup>low</sup>Flt3<sup>+</sup>), and multipotent progenitors (MPPs) (Thy-1<sup>-</sup>Flt3<sup>+</sup>), which differentiate into common lymphoid progenitors (CLP) as well as common myeloid progenitors (CMP) that generate the granulocytic-macrophage (GM) and the megakaryocytic-erythroid (MegE) lineages (Fig. 2A) (Kondo *et al*, 1997; Akashi *et al*, 2000; Laiosa *et al*, 2006). Short-term HSCs and MPPs sustain the full lympho-myeloid lineage potential of long-term HSCs, but have reduced self renewal capacity, which coincides with Flt3 expression. This concept implicates that the first lineage commitment step of adult HSCs results in an immediate and complete separation of myelopoiesis and lymphopoiesis (Fig. 2A) (Adolfsson *et al*, 2005; Welner *et al*, 2008).

In contrast, Katsura and co-workers detected bipotential myeloid/T-cell (p-MT) and myeloid/B-cell (p-MB) progenitor stages and proposed a model, in which T- and B-cells arise from a multipotent myeloid/T/B-cell progenitor and are produced through intermediate p-MT and p-MB stages. The existence of a common myelo-lymphoid progenitor (CMLP or p-MTP) also indicates that the erythroid potential is shut off at an early stage before branching towards T and B progenitors (Katsura, 2002). Furthermore, Adolfsson *et al* demonstrated that LSK Flt3<sup>+</sup> HSCs sustain granulocyte, monocyte, and B- and T-cell potentials but lack a megakaryocytic-erythroid lineage potential (lymphoid-primed multipotent progenitors, LMPPs) revising the generally accepted concept of hematopoiesis (Fig. 2B) (Adolfsson *et al*, 2005). A summary of the currently existing models and a potential composite model as well as the expression of several key factors during lineage differentiation (described below) is shown in Figure 2.

Although at low levels, hematopoietic multipotential progenitors (MPPs) and HSCs promiscuously express genes of disparate lineages. This phenomenon, which is termed lineage priming, suggests that the fate of immature cells is not predetermined and that lineage selection extinguishes alternative potentials (Miyamoto *et al*, 2002; Laiosa *et al*, 2006; Mansson *et al*, 2007; Orkin & Zon, 2008). The coexistence of different transcriptional programs in progenitor cells, followed by the stepwise extinction of all except for one of them, is therefore a defining feature of the hematopoietic system (Laiosa *et al*, 2006). It was shown,

that hematopoietic progenitors as well as differentiated cells can be redirected into other lineages upon ectopic cytokine signaling or forced expression of lineage-specific transcription factors (Laiosa *et al*, 2006), which also challenges the model of an unidirectional differentiation process.

The important transcription factors implicated in early hematopoietic development and formation of HSCs include GATA-1, SPI1 (PU.1), CEBPA (C/EBP $\alpha$ ), NOTCH1, and GATA-3 (Laiosa *et al*, 2006) as well as RUNX1, MLL, SCL (TAL-1), LMO2, and ETV6 (Orkin & Zon, 2008). Moreover, many genes commonly expressed in T- and B-cells are not active in HSCs, thus, HSCs more closely resemble myeloid than lymphoid precursors (Laiosa *et al*, 2006; Welner *et al*, 2008).

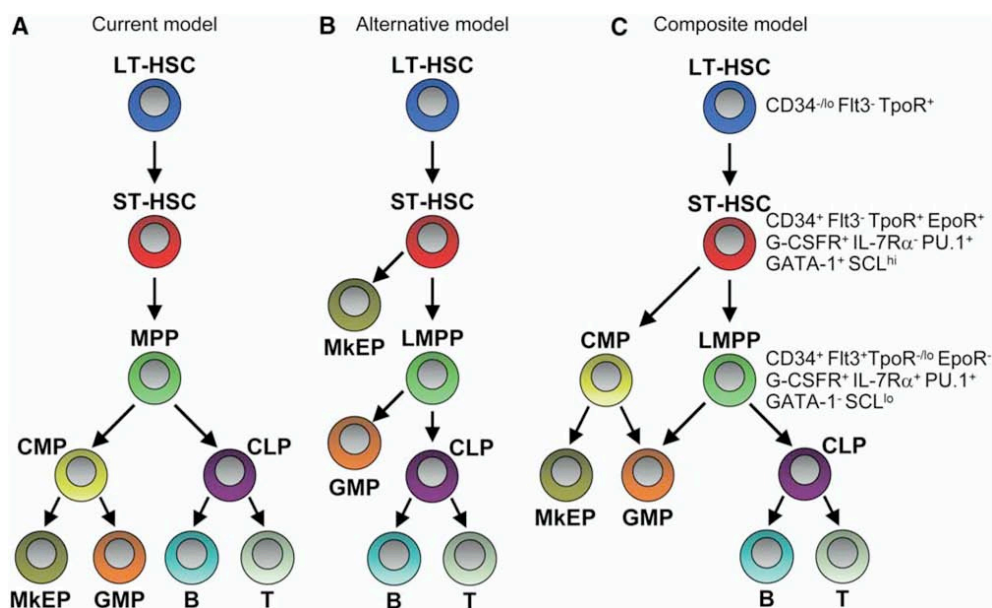


**Figure 2. Models for Hematopoietic Stem Cell and Blood Lineage Commitment (Adolfsson *et al*, 2005).** (A) Model supported through the identification of CMPs and CLPs (Kondo *et al*, 1997; Akashi *et al*, 2000). (B) Alternative model by Adolfsson *et al*, 2005. (C) Composite model incorporating experimental evidence for models (A) and (B). LT-HSC, long-term hematopoietic stem cell; ST-HSC, short-term hematopoietic stem cell; MPP, multipotent progenitor; LMPP, lymphoid-primed multipotent progenitor; CLP, common lymphoid progenitor; CMP, common myeloid progenitor; GMP, granulocyte/macrophage progenitor; MkEP, megakaryocyte/erythroid progenitor; B, B-cell; T, T-cell. Figure taken from Adolfsson *et al*, 2005.

## 1.2. Lymphoid development

One of the key players for initiation of lymphoid development is FLT3, which is progressively upregulated from long-term HSCs towards MPPs, accompanied by a loss of VCAM1 expression. In addition to high FLT3 expression, RAG1 is activated in LMPPs characterizing the emergence of the earliest lymphocyte progenitors (ELPs) (Welner *et al*, 2008). ELPs are the precursors of CLPs, which give rise to B- and T-lymphocytes, natural killer cells, and dendritic cells. In early lymphoid development important factors are IKZF1 (Ikaros) and SPI1

(PU.1). Ikaros-deficient mice lack ELPs, but also alterations in the myeloid lineages have been observed, which might be explained by the expression of distinct *Ikzf1* (Ikaros) isoforms in different lineages and cooperation with the lymphoid-restricted Ikaros family member Aiolos (*Ikzf3*) (Laiosa *et al*, 2006; Welner *et al*, 2008). Ikaros may activate *Flt3* and repress *CSF1R* (*GM-CSFR $\alpha$* ) and, thus, promote lymphoid cell fate. In contrast, loss of SPI1 (PU.1) inhibits B lineage and myelomonocytic cell formation as well as T-cell and dendritic cell formation, and PU.1-deficient mice lack expression of *IL7R* (*IL-7R $\alpha$* ) and *EBF1* (Laiosa *et al*, 2006).

GATA-3 and NOTCH1 drive lymphoid progenitors versus a T lineage differentiation, whereas entry of CLPs into the B-cell lineage critically depends on signaling of the IL7-receptor (IL7R), as well as expression of the transcription factors TCF3 (E2A), EBF1 and **PAX5** (Laiosa *et al*, 2006).

### 1.2.1. B-cell development and the role of PAX5

The hallmark of B-cell development is the stepwise expression and assembly of components of the functional receptor for antigen, the B-cell receptor (BCR). Assembly of the pre-BCR requires the rearrangement of immunoglobulin heavy chain (*IGH@*) genes, which proceeds in two steps: (1) diversity (D) and joining (J) segments are assembled (D-J rearrangements), and (2) variable regions are joined to D-J segments to create mature V(D)J joints (Maier & Hagman, 2002). Additionally, the pre-BCR complex is composed of the surrogate light chains Igll1 ( $\lambda 5$ ) and VPREB1 (VpreB) as well as of the signal-transducing proteins CD79A (Ig $\alpha$ ) and CD79B (Ig $\beta$ ) (Schebesta *et al*, 2002).

The helix-loop-helix transcription factors TCF3 (E2A) and EBF1 coordinately regulate B-cell specific genes, such as components of the BCR, and in the absence of TCF3 (E2A) or EBF1 B-cell differentiation is blocked at the uncommitted pre-pro-B-cell stage (the first identifiable B-cell-specified progenitor stage arising from CLPs) (O'Riordan & Grosschedl, 1999; Nutt & Kee, 2007). Moreover, E2A-deficient CLPs and pre-pro-B-cells fail to undergo D<sub>H</sub>-J<sub>H</sub> rearrangements at the *Igh* and V <sub>$\kappa$</sub> -J <sub>$\kappa$</sub>  recombination at the *Igk* (*Ig $\kappa$* ) locus (Kwon *et al*, 2008). E2A activates *Ebf1*, which in turn activates *Pax5* and, thus, promotes the B-cell transcriptional program (Nutt & Kee, 2007). Furthermore, E2A is required to maintain the expression of *Ebf1*, *Pax5*, and the B-cell gene program in pro-B-cells, whereas it is largely dispensable for the formation and function of mature B-lymphocytes and plasma cells (Kwon *et al*, 2008).

Ebf1-deficient mice lack expression of most B-cell genes including *Cd79a* (*mb-1*, Ig $\alpha$ ), *Cd79b* (Ig $\beta$ , B29), *Igll1* ( $\lambda 5$ ), *Vpreb1* (VpreB), and *Rag1*, and do not undergo any *Igh* gene recombinations (Lin & Grosschedl, 1995). *Ebf1* is controlled through two promoters, a distal

( $\alpha$ ) and a proximal ( $\beta$ ). The *Ebf1* $\alpha$  promoter is regulated by TCF3 (E2A) and STAT5 (which is activated by IL7R signaling) and, intriguingly, also contains an EBF1 binding site suggesting an autoregulatory function for EBF1. The *Ebf1* $\beta$  promoter is controlled by Ets1, PU.1 and Pax5, whose expression itself is dependent on EBF1 (Roessler *et al*, 2007). Thus, EBF1 regulates its own expression directly through induction of the *Ebf1* $\alpha$  promoter and indirectly through upregulation of *Pax5* (Nutt & Kee, 2007; Roessler *et al*, 2007). The synergistic activity of E2A and EBF1 is required for B-cell specification, and both indirectly control B-cell development by induction of the B-cell commitment factor Pax5 (Nutt & Kee, 2007). However, activation of the B-cell specific transcription program is not sufficient to commit early progenitors to the B-lymphoid lineage without Pax5.

In the absence of Pax5, B-cell development is arrested at the early pro-B (pre-BI) cell stage, which is characterized by the expression of early B-cell markers and a markedly reduced frequency of V<sub>H</sub>-to-D<sub>H</sub>J<sub>H</sub> immunoglobulin rearrangements (Nutt *et al*, 1997). *Pax5*<sup>-/-</sup> pro-B-cells are not committed to the B-lymphoid lineage yet, they can be cultivated indefinitely *in vitro* in the presence of interleukin 7 and stroma but are unable to differentiate into mature B-cells. Upon stimulation with the appropriate cytokines *Pax5*<sup>-/-</sup> pro-B-cells can be differentiated into a broad spectrum of hematopoietic cell types *in vitro* and only restoration of Pax5 expression suppresses the multilineage potential of these cells (Fig. 3) (Nutt *et al*, 1999a). Conditional *Pax5* inactivation in committed pro-B-cells reverts lineage commitment and results in retrodifferentiation of B-lymphocytes to an uncommitted progenitor stage (Fig. 3), and these cells can completely restore thymocyte development *in vivo* in *Rag2*-deficient mice (Mikkola *et al*, 2002). Upon conditional *Pax5* deletion in mice mature B-cells from peripheral lymphoid organs are capable to dedifferentiate *in vivo* back to early uncommitted progenitors in the bone marrow, which rescues T lymphopoiesis in the thymus of T-cell-deficient mice (Cobaleda *et al*, 2007a).

Stages of B-cell development, the corresponding status of V(D)J recombination, and the approximate points at which B-cell lymphopoiesis is arrested in mice upon deletion of key regulatory factors are summarized in Figure 4.

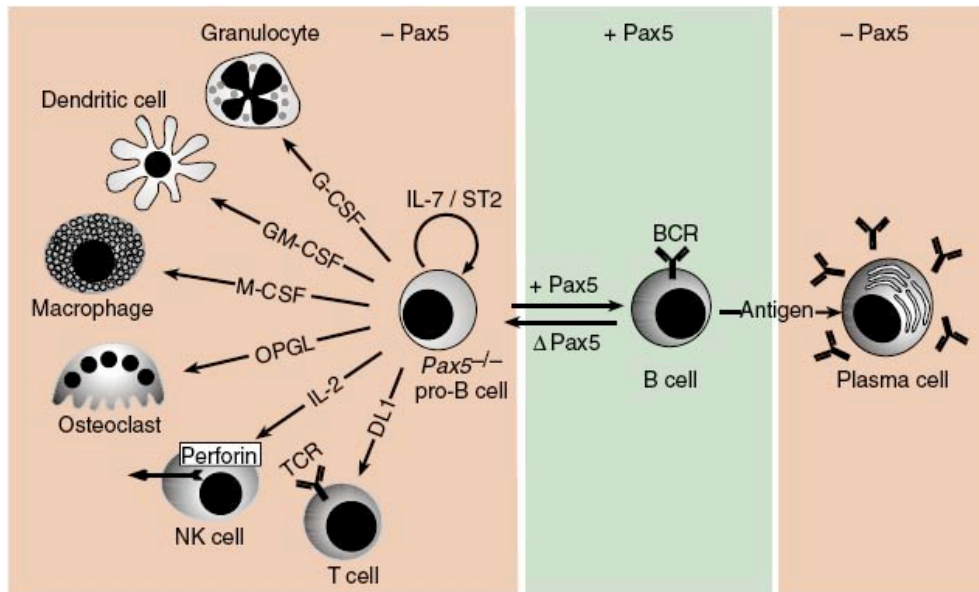


**Figure 3. B-cell lineage commitment by Pax5 (Cobaleda *et al*, 2007b).** Uncommitted  $Pax5^{-/-}$  pro-B-cells are able to differentiate into several hematopoietic cell types. The cytokines required for *in vitro* differentiation are indicated. Conditional  $Pax5$  deletion ( $\Delta Pax5$ ) results in retrodifferentiation of B-lymphocytes to an uncommitted progenitor cell stage. During terminal plasma cell differentiation  $Pax5$  is physiologically downregulated. OPG, osteoprotegerin ligand (also known as RANKL or TRANCE); ST2, stromal ST2 cells; TCR, T-cell receptor. Figure taken from Cobaleda *et al*, 2007.

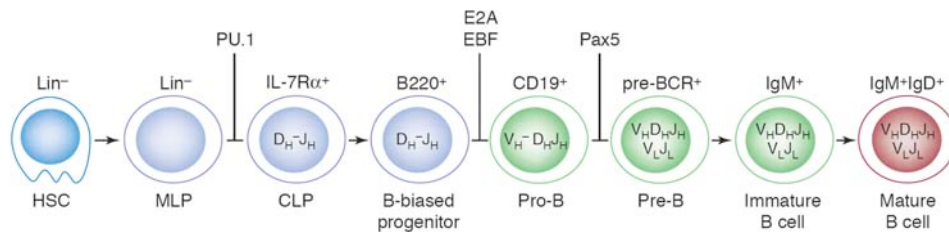


**Figure 4. B-cell developmental stages (Hagman & Lukin, 2005).** Progressive stages of B-cell lymphopoiesis are shown. Cell designations are indicated below, the status of V(D)J recombination is shown within each cell type and characteristic cell surface markers are depicted above each cell. The approximate points at which B-cell lymphopoiesis is arrested in  $PU.1^{-/-}$ ,  $TCF3$  ( $E2A^{-/-}$ ),  $EBF1$  ( $EBF^{-/-}$ ) and  $Pax5^{-/-}$  mice are designated above the cells. HSC, hematopoietic stem cell; MLP, multi-lineage progenitor; CLP, common lymphoid progenitor, Pro-B, pro-B-cell; Pre-B, pre-B-cell. Figure taken from Hagman *et al*, 2005.

At the molecular level, Pax5 fulfills a dual role by activating B-cell-specific genes and simultaneously repressing lineage-inappropriate genes to initiate B-lineage differentiation (Nutt *et al*, 1999a). In this context, the Pax5 paired domain functions as bipartite DNA-binding region, which binds to the distinct half-site of the degenerate Pax5 recognition sequence (Czerny *et al*, 1993; Garvie *et al*, 2001). Transcriptional regulation of Pax5 target genes is determined by the interaction of distinct partner proteins with the central and C-terminal protein interaction motifs of Pax5 (Cobaleda *et al*, 2007b). The partial homeodomain associates with the TATA-binding protein of the basal transcription machinery, while the transactivation domain regulates gene transcription most likely by interacting with histone acetyltransferases such as the coactivator CREBBP (CBP) or SAGA complex. In contrast, corepressors of the Groucho protein family, which are part of a larger histone deacetylase complex, convert Pax5 from a transcriptional activator to a repressor by binding to the octapeptide motif (Cobaleda *et al*, 2007b).

Pax5 target gene activation plays an essential role in controlling signal transduction from the pre-BCR and BCR, which constitute important checkpoints in B-cell development (Schebesta *et al*, 2007). Pax5 promotes V<sub>H</sub>-D<sub>H</sub> recombination at the *Igh* locus (Fuxa *et al*, 2004), it activates expression of *Cd79a* (*Igα*) (Fitzsimmons *et al*, 1996), *Cd19* (Kozmik *et al*, 1992; Nutt *et al*, 1998), *Cr2* (*Cd21*) (Horcher *et al*, 2001), *Cd72* (Ying *et al*, 1998; Horcher *et al*, 2001), and *Blnk* (SLP-65) (Schebesta *et al*, 2002) and, thus, facilitates pre-BCR signaling. Comprehensive gene expression analysis identified additional Pax5-activated genes, which are implicated in the control of signaling from the pre-BCR on the cell surface to transcription in the nucleus at multiple levels (Schebesta *et al*, 2007). Moreover, it was shown that Pax5 regulates genes involved in B-cell adhesion and migration, such as cell-surface receptors and intracellular signal transducers, which leads to a remodeling of the actin cytoskeleton. Pax5 also activates a number of transcription factors involved in B-cell differentiation, including *Ikzf3* (*Aiolos*), *Spib*, *Irf4*, *Irf8*, *Lef1*, and *Ebf1* suggesting that Pax5 activity initiates a downstream transcriptional cascade that reinforces the B-cell program (Schebesta *et al*, 2007; Pridans *et al*, 2008).

Besides the activation of B-cell specific genes Pax5 concurrently represses lineage-inappropriate genes, which become reactivated in *Pax5*<sup>-/-</sup> pro-B-cells (Nutt *et al*, 1999a; Delogu *et al*, 2006). Global transcriptional profiling of *Pax5*<sup>-/-</sup> pro-B-cells identified >100 genes repressed by Pax5 including genes implicated in cell-cell communication, cell adhesion, migration, nuclear processes, and cellular metabolism at B-cell commitment (Delogu *et al*, 2006). Importantly, many genes repressed by Pax5 are normally expressed in non-B-cell lineages, which underlines the lineage promiscuity of *Pax5*<sup>-/-</sup> pro-B-cells. As an example, Pax5 represses cell surface receptors *Csf1r* (*M-CSFR*) and *Notch1*, associated with macrophage and T-cell development, respectively, rendering committed B-lymphocytes

unresponsive to lineage-inappropriate signals (Nutt *et al*, 1999a; Souabni *et al*, 2002; Nutt & Kee, 2007). Furthermore, Pax5 represses genes that are required to maintain stem cell or multipotent progenitor fate such as *Atxn1* (*Sca1*) and *Flt3* (Delogu *et al*, 2006).

Terminal differentiation of mature B-cells into antibody-secreting cells is antigen-driven and represents a crucial component of the immune response. The physiological downregulation of *Pax5* upon antigen stimulation followed by the reactivation of Pax5-repressed plasma cell-specific genes including *Xbp1*, *Igj*, *Cd28*, *Ccr2*, and *Prdm1* (*Blimp1*) seems to be the initial event in plasma cell differentiation (Delogu *et al*, 2006; Kallies *et al*, 2007). Final plasma cell differentiation requires the expression of functional *Prdm1* (*Blimp1*), which represses *Pax5* and, hence, the B-cell program by a feedback mechanism (Kallies *et al*, 2007).

Thus, comprehensive analysis of just a small number of key transcription factors involved in B-cell differentiation has revealed that the transcriptional network controlling B-cell specification and commitment is not a simple linear cascade but involves multiple combinatorial inputs and feedback loops (Nutt & Kee, 2007).

### 1.3. Acute lymphoblastic leukemia

Acute lymphoblastic leukemia (ALL) is the most common leukemia in children accounting for approximately 80% of pediatric cases (Martinez-Climent, 1997). In ALL, the B- or T-cell lineage can be affected, and in children the most common immunophenotype is B-cell precursor (BCP) ALL, followed by T-cell, and mature B-cell ALL. The group of BCP-ALL has a good prognosis with an event-free survival (EFS) of approximately 80% in children between 1-18 years, whereas in infants (children <1 year of age) the outcome is worse with an EFS of 28-45% (Armstrong & Look, 2005; Pieters *et al*, 2007). About 15% of childhood ALL cases are diagnosed with T-ALL and this group of patients was historically linked to a poor prognosis (Aifantis *et al*, 2008). However, owing to the application of intensive chemotherapy regimens, nowadays also in T-ALL cure rates of approximately 75% are achieved. Nevertheless, in about 25% of the patients treatment failure occurs and the outcome of these patients remains dismal (Goldberg *et al*, 2003; Einsiedel *et al*, 2005).

Recurrent genetic abnormalities are a hallmark of acute leukemia and provide insights into the molecular mechanisms of leukemogenesis (Armstrong & Look, 2005). The most frequent targets of genetic alterations involved in hematological disorders are genes controlling transcription and tyrosine kinases (Mitelman *et al*, 2004). The large variety of genetic alterations includes point mutations and deletions, but the main genetic characteristics of acute leukemia are translocations and numerical chromosome imbalances resulting in hyper- or hypodiploidy (Fig. 5). These chromosomally defined subtypes also show distinctive patterns of global gene expression in microarray analysis (Greaves & Wiemels, 2003).



Chromosome translocations either result in inappropriate expression of an oncogene by juxtaposition of the entire coding sequence under constitutive activated regulatory elements of a partner gene or more commonly in leukemia in the formation of a chimeric fusion gene with novel properties. An increasing number of promiscuous genes (e.g. *MLL*, *ETV6* or *NUP98*) that recombine with numerous different partner genes have been identified and, thus, the number of fusion genes exceeds the number of affected genes. So far, in ALL 1139 balanced aberrations have been described, 155 of which are recurrent resulting in 82 distinct gene fusions (Mitelman *et al*, 2007).

In childhood BCP-ALL the most common genetic rearrangement is the t(12;21)(p13;q22), which fuses *ETV6* to *RUNX1* and is present in about 25% of BCP-ALL cases (Fig. 5) (Armstrong & Look, 2005). Other commonly found chromosomal aberrations in childhood ALL are the t(1;19)(q23;p13)/*E2A-PBX1* (*TCF3-PBX1*), the t(9;22)(q34;q11)/*BCR-ABL1*, and hyperdiploidy (presence of >46 chromosomes), which is often associated with a *FLT3* mutation (Fig. 5) (Armstrong & Look, 2005). Rearrangements of the *MLL* gene occur in up to 80% of infant ALL and are associated with a pro-B ALL phenotype (Attarbaschi *et al*, 2006; O'Neil & Look, 2007; Pieters *et al*, 2007).

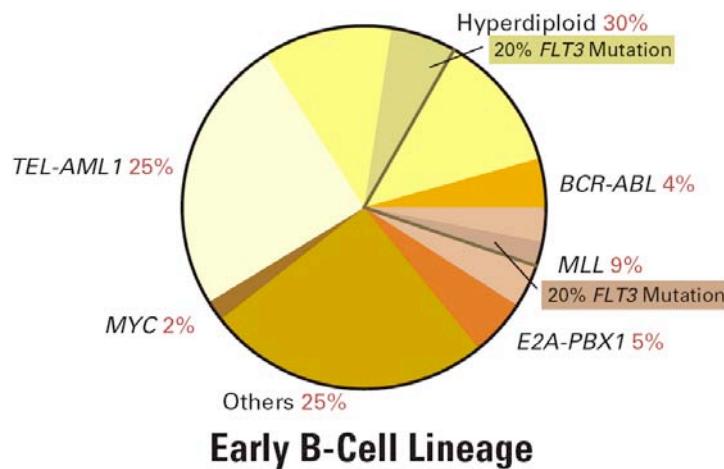


**Figure 5. Chromosomal abnormalities in acute lymphoblastic leukemia (Armstrong & Look, 2005).** The relative frequencies of chromosomal aberrations found in childhood B-ALL are depicted. Figure taken from Armstrong & Look, 2005.

Recently, pediatric ALL was further characterized by genome-wide analyses using high-resolution SNP arrays and DNA sequencing, which uncovered that in about 40% of BCP-ALL genes implicated in B-cell development and differentiation are targets of mutations, deletions or structural rearrangements (Mullighan *et al*, 2007a). These genes comprised *IKZF1* (*Ikaros*), *IKZF3* (*Aiolos*), *LEF1*, *EBF1*, *TCF3* (*E2A*), and *PAX5* (Kuiper *et al*, 2007; Mullighan *et al*, 2007a). In addition to microdeletions in transcription factors involved in B-lineage

development, recurrent deletion of *BTG1* a negative effector of B-cell proliferation was observed. Moreover, other genes frequently affected by copy number losses were those controlling G1/S cell cycle progression (e.g. *CDKN2A*, *CDKN2B*, and *RB1*), and such deletions were detected in 54% of BCP-ALL and 86% of T-ALL, respectively (Kuiper *et al*, 2007).

Many pediatric leukemias originate *in utero*, which was demonstrated by sequence analysis of the unique genomic breakpoints of chromosomal rearrangements of concordant leukemia in monozygotic twins, and from screening of Guthrie cards (Fasching *et al*, 2000; Panzer-Grumayer *et al*, 2002; Greaves & Wiemels, 2003). In contrast to BCP-ALL, analysis of neonatal blood spots for leukemia specific rearrangements showed that most T-ALL cases are more likely initiated postnatally (Fischer *et al*, 2007). Interestingly, the *ETV6-RUNX1* and the *RUNX1-RUNX1T1* (*AML1-ETO*) fusion genes could be detected 100 times more often in blood samples from healthy newborns as the risk of the corresponding leukemia (Mori *et al*, 2002).

In transgenic mouse models it was shown that particular fusion genes can initiate, but seldom complete leukemogenesis and, thus, require cooperating mutations similar to the Knudson two-step model for non-inheritable pediatric solid tumors (Knudson, 1992; Bernardin *et al*, 2002; Greaves & Wiemels, 2003; Tsuzuki *et al*, 2004). For instance, *ETV6-RUNX1* positive leukemia is often associated with additional genetic changes, such as deletions of the second *ETV6* allele, *PAX5*, *CDKN2A*, or *BTG1*, which may represent one of the secondary rate-limiting hits in leukemogenesis (Greaves & Wiemels, 2003; Mullighan *et al*, 2007a; Tsuzuki *et al*, 2007). In a recent study of monozygotic twins – one twin had BCP-ALL while the other one was healthy – a tumor-propagating *ETV6-RUNX1* positive cell population could be isolated from both twins. The *ETV6-RUNX1* positive leukemic blasts of the twin diagnosed with full-blown BCP-ALL showed a deletion of the second *ETV6* allele, whereas the *ETV6-RUNX1* positive cells of the healthy twin harbored one intact copy of *ETV6* (Hong *et al*, 2008). These data strongly support the notion that inactivation of the second unrearranged *ETV6* allele indeed represents a crucial cooperating mutation (Hong *et al*, 2008).

#### 1.4. The PAX gene family in oncogenesis

The mammalian paired box or PAX transcription factor family comprises nine members and is characterized by a highly conserved paired box DNA binding domain. Mouse and human *PAX* genes are classified into four paralogous groups according to the presence of two additional motifs, namely a conserved octapeptide and a complete or truncated homeodomain (Fig. 6) (Bouchard *et al*, 2003). Additionally, all members of the *PAX* gene family contain regions rich in proline, serine, and threonine residues (PST-rich) at the

C-terminal end (Fig. 6), which comprises a transactivation and an inhibitory domain, a characteristic feature of inducible transcription factors.

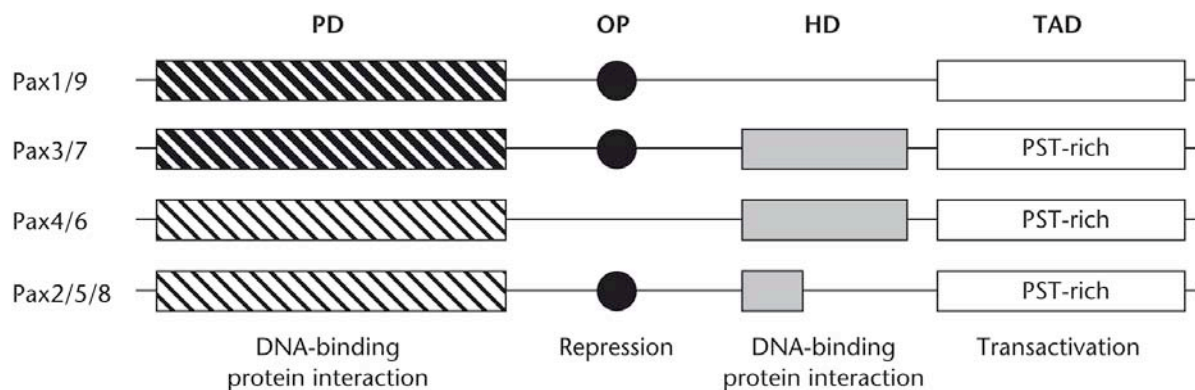


**Figure 6. Structure and classification of mammalian Pax proteins (Bouchard *et al*, 2003).** Pax proteins are classified according to their protein domains. PD, paired domain; HD, homeodomain; OP, conserved octapeptide, TAD, transactivation domain; PST, proline-serine-threonine. Figure taken from Bouchard *et al*, 2003.

The PAX family has been conserved throughout metazoan evolution and controls tissue development and differentiation processes during embryonic development including proliferation, stem-cell self-renewal, apoptosis, cell migration and invasion within a variety of cell lineages (Barr, 1997; Robson *et al*, 2006). The important developmental role of the PAX genes is further emphasized by the association of mutations with heritable murine and human developmental defects (Barr, 1997). Moreover, the cellular activities controlled by the PAX genes are also fundamental targets for the development of neoplasia (Barr, 1997). Therefore, the PAX genes are intriguing candidates to contribute to tumorigenesis in specific cell lineages, and indeed, some members of the PAX gene family have been shown to be involved in tumor development (Robson *et al*, 2006).

**PAX3** and **PAX7** are expressed during early neural and myogenic development. In alveolar rhabdomyosarcoma (ARMS), a pediatric soft tissue tumor related to the striated muscle lineage, the PAX3 and PAX7 genes are fused to the FOXO1 (FKHR) gene through the translocations t(2;13)(q35;q14) and t(1;13)(p36;q14), respectively (Galili *et al*, 1993; Davis *et al*, 1994). The t(2;13)(q35;q14)/PAX3-FKHR (PAX3-FOXO1) rearrangement is the most prevalent finding in ARMS detected in about 70% of cases, whereas the t(1;13)(p36;q14) is found in a smaller subset of cases. The chimeric fusion proteins contain the PAX3/PAX7 paired domain, the octapeptide and the homeodomain fused to the FOXO1 (FKHR) transcriptional activation domain. The PAX3-FOXO1 and PAX7-FOXO1 proteins function as transcription factors that activate genes containing a PAX3/PAX7 DNA-binding site in a more potent manner than the corresponding wild-type proteins (Barr, 2001). Moreover, both fusions are consistently overexpressed relative to the respective wild-type PAX transcripts.

Overexpression of the *PAX7-FOXO1* fusion results mainly from *in vivo* amplification of the fusion gene, whereas in case of *PAX3-FOXO1* the increase in transcriptional rate is copy number independent (Barr, 2001).

Furthermore, alternative tumor-specific *PAX3* and *PAX7* isoforms are predominantly expressed in Ewing's sarcoma and in embryonal rhabdomyosarcoma, and melanoma cell lines, respectively (Barr *et al*, 1999). In squamous cell lung carcinoma *PAX7* is frequently amplified (Racz *et al*, 2000) and in N-type neuroblastoma cell lines (with high *N-MYC* expression and/or amplification) two isoforms of *PAX3* are expressed at abnormally high levels (Harris *et al*, 2002; Wang *et al*, 2008).

**PAX2** is required for kidney, eye and ear development and in the mammary glands, whereas **PAX8** controls thyroid development, but is also expressed during kidney organogenesis (Bouchard *et al*, 2003; Robson *et al*, 2006). In thyroid follicular carcinomas *PAX8* is fused to *PPARG* (*PPAR $\gamma$ 1*) as a result of the translocation t(2;3)(q13;p25) generating a chimeric fusion gene that contains the paired box, octapeptide, and partial homeodomain of *PAX8* fused to the entire *PPARG* (*PPAR $\gamma$ 1*) protein including all nuclear receptor domains (Kroll *et al*, 2000). The *PAX8-PPARG* (*PAX8-PPAR $\gamma$ 1*) fusion is expressed at higher levels as endogenous *PPARG* (*PPAR $\gamma$ 1*) and it might act in a dominant negative manner over wild-type *PPARG* (*PPAR $\gamma$ 1*), which is implicated in growth inhibition and promotes differentiation of cancer cell lines (Kroll *et al*, 2000). Moreover, in carcinomas of the kidney, prostate, breast, ovary, and in blastemal tissues in Wilms' tumor and Kaposi sarcoma unattenuated tumor-associated expression of *PAX2* and/or *PAX8* was observed (Robson *et al*, 2006).

**PAX5** expression is critically required for very early brain development but transcriptionally downregulated before birth. In astrocytoma, glioblastoma, medullablastoma, small cell lung cancer (neural-crest derived tumor) and N-type neuroblastoma (a malignant subset), but not in S-type cells (a benign subset), *PAX5* is ectopically expressed during tumor development (Stuart *et al*, 1995b; Baumann Kubetzko *et al*, 2004; Robson *et al*, 2006). Moreover, it was shown that *PAX5* expression levels correlate with or promote neoplastic tumor growth in astrocytoma and neuroblastoma, respectively (Stuart *et al*, 1995b; Baumann Kubetzko *et al*, 2004). Furthermore, in astrocytoma the expression of *PAX5* is inversely proportional to the expression of *TP53* (*p53*), whose transcriptional activity can be repressed by binding of *PAX5* to the *TP53* (*p53*) promoter (Stuart *et al*, 1995a).

The involvement of *PAX5* in B-cell malignancies is described in section 1.5.

**PAX6**, a master regulator of eye development, is frequently expressed in brain, breast and other cancer cell lines (Muratovska *et al*, 2003). However, in glioblastoma a tumor-suppressor function for *PAX6* was suggested and also in malignant astrocytic gliomas high levels of *PAX6* expression correlate with improved prognosis (Robson *et al*, 2006).

**PAX9** expression was also widely detected in cancer cell lines (Muratovska *et al*, 2003). On the other hand decreased **PAX9** expression correlates with increasing malignancy of oesophageal carcinomas and epithelial dysplasia (Robson *et al*, 2006).

In summary, **PAX** genes seem to exhibit a pivotal role in the oncogenesis of several tumors arising from those tissues, in which they exert a developmental stage-dependent function during embryogenesis and differentiation (Lang *et al*, 2007; Wang *et al*, 2008). Because of their normal function in development, it is assumed that re-expression of **PAX** genes in malignant neoplasms promotes tumor development and progression by increasing proliferation and motility, while inhibiting apoptosis (Baumann Kubetzko *et al*, 2004).

## 1.5. PAX5 aberrations in B-cell malignancies

### 1.5.1. PAX5 aberrations in lymphoma

In non-Hodgkin lymphoma **PAX5** is involved in the rare translocation t(9;14)(p13;q32) resulting in a juxtaposition of the intact **PAX5** coding sequence to regulatory elements of the **IGH@** locus, which leads to inappropriate **PAX5** expression (Busslinger *et al*, 1996; Iida *et al*, 1996). The breakpoints within the **PAX5** and **IGH@** loci are variable and, thus, the deregulation of **PAX5** occurs in two different ways: (1) In the KIS-1 cell line, which was established from a patient with diffuse large-cell lymphoma, the breakpoint at 9p13 occurs 1.8kb upstream of exon 1A of **PAX5** and juxtaposes **PAX5** in a head-to-head orientation in close proximity to the potent **IGH@** gene E $\mu$  enhancer (Busslinger *et al*, 1996). Thus, deregulation of **PAX5** transcription is caused by enhancer insertion. (2) In variant translocations, which were cloned from a patients with lymphoplasmacytoid lymphoma (Iida *et al*, 1996) and a splenic marginal zone lymphoma (Morrison *et al*, 1998), the breakpoints arise in the non-coding sequence and the 3' region of exon 1B of **PAX5**, respectively. In both cases the rearrangement translocates the **PAX5** gene into the S $\mu$  region of the **IGH@** gene in a head-to-head position, which leads to replacement of the **PAX5** promoters by an antisense promoter of the S $\mu$  region.

In a transgenic mouse model a **Pax5** minigene was inserted into the **Igh** locus to mimic the t(9;14)(p13;q32)/**PAX5-IGH@** rearrangement (Souabni *et al*, 2007). This knock-in mouse corresponds to a germline rather than a somatic mutation and therefore, curiously, the mice developed T-cell lymphomas. Nevertheless, this data identified **Pax5** as a potent oncogene, in that ectopic **Pax5** expression interferes with normal T-cell development and deregulated the T-cell transcription program (Souabni *et al*, 2007). Conversely, in mice experiments biallelic **Pax5** deletion in mature B-cells resulted in the development of aggressive lymphoma, which were by gene expression analysis characterized as progenitor cell tumors.

Moreover, in respect to their expression profile of Pax5 target genes these cells were indistinguishable from *Pax5*<sup>-/-</sup> pro-B-cells (Cobaleda *et al*, 2007a).

In follicular lymphoma, PAX5 and MYC are the only transcription factors consistently overexpressed as compared to their putative normal counterparts, germinal center B-cells (Husson *et al*, 2002). Furthermore, in diffuse large B-cell lymphoma (DLBCL) and to a lesser extent in Burkitt and follicular lymphomas, *PAX5* showed a high frequency of somatic hypermutations, which cluster downstream of both transcription initiation sites, predominantly around exon 1B (Pasqualucci *et al*, 2001). Such hypermutations of *PAX5* have not been detected in normal germinal-center B-cells, naïve B-cells and control fibroblasts and, thus, may cause PAX5 malfunction in these diseases (Pasqualucci *et al*, 2001). However, as the alternatively transcribed exon 1A and the second *PAX5* allele mainly escape somatic hypermutations, the role of these hypermutations for lymphoma formation is doubtful (Cobaleda *et al*, 2007b).

Recent work also addressed the role of PAX5 during lymphomagenesis (Cozma *et al*, 2007). It was shown that activation of *Pax5* significantly upregulated components of the BCR signaling, such as Cd79a, Cd19, Blnk, PKC $\beta$ , and PLC $\gamma$ 2, and that this activation stimulated tumor growth. Moreover, knock down of *Pax5* expression in DLBCL cell lines by sh-RNA decreased the growth rate of these cell lines. The contribution of *Pax5* to neoplastic growth appears to correlate with its ability to maintain expression of BCR components. Thus, interference with BCR signaling downstream of Cd79a either by overexpression of Cd22 or by pharmacological inhibition may represent a therapeutic option (Cozma *et al*, 2007).

## **1.5.2. PAX5 aberrations in acute lymphoblastic leukemia**

### **1.5.2.1. Deletions and Mutations**

By genome-wide SNP array analysis of childhood ALL frequent deletions of the *PAX5* gene were detected (Kawamata *et al*, 2007; Kuiper *et al*, 2007; Mullighan *et al*, 2007a). Deletions were found in about 30% of all cases and comprised focal intragenic *PAX5* deletions (13%), broader deletions involving *PAX5* and a variable number of flanking genes (3,6%), large 9p deletions including the 3' portion of *PAX5* (2,6%), and deletions of the whole 9p arm or complete loss of one chromosome 9 (9,9%) (Fig. 7) (Mullighan *et al*, 2007a). The focal *PAX5* deletions affect only a subset of *PAX5* exons (Fig. 7) resulting in expression of internally deleted transcripts. These transcripts, the so-called hypermorphic alleles, encode proteins lacking either the PAX5 paired domain and/or transcriptional regulatory domains or lead to truncated mutants.

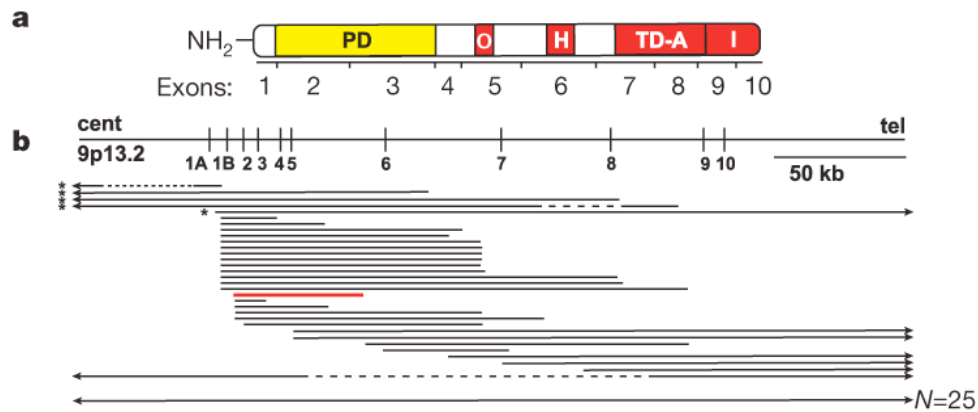


**Figure 7. PAX5 deletions.** (a) Schematic representation of *PAX5* exons and corresponding domains. H, homeodomain-like; I, transactivation, inhibitory; O, octapeptide; PD, paired domain; TD-A, transactivation, activating. (b) *PAX5* aberrations: hemizygous deletions, solid lines; homozygous deletions, dashed lines; amplification, red line. Deletions that stretch beyond the region shown are arrowed. \*shows a deletion confined to *PAX5*. Figure and Legend taken from Mullighan *et al*, 2007.

In several cases also *PAX5* point mutations, which mainly comprise frameshift, splice site or missense mutations and clustered in exons encoding the paired domain or the transcriptional regulatory domains were found (Fig. 8). Mutations affecting the paired domain are suggested to impair the DNA-binding function of *PAX5* and mutations in the transactivation domain may alter transcriptional regulatory functions. Indeed, an impaired function of *PAX5* mutants was shown in luciferase-based reporter assays and a reduced DNA-binding activity for *PAX5* variants with mutations or deletions of the paired-domain was demonstrated. However, in leukemic blasts no correlation between *PAX5* mutation status and *CD19* and *CD79A* expression was observed (Mullighan *et al*, 2007a).

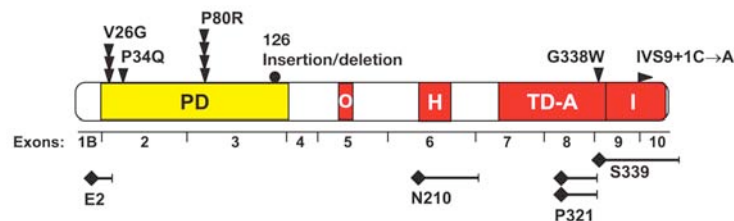


**Figure 8. PAX5 mutations detected by Mullighan *et al*, 2007.** Location of missense (downward pointing arrowheads), insertion/ deletion (filled circles), frameshift (filled diamonds) and splice-site (right-pointing arrowhead) mutations. Figure and Legend taken from Mullighan *et al*, 2007.

Intriguingly, the type and frequency of *PAX5* aberrations varied among the genetic subtypes of ALL: all hypodiploid cases showed loss of one *PAX5* allele and about 50% of the cases harbored concomitant mutations in the second *PAX5* allele, whereas 28% of *ETV6-RUNX1* positive cases displayed focal mono-allelic deletions but lacked *PAX5* mutations (Mullighan

*et al*, 2007a). The high frequency of *PAX5* deletions in *ETV6-RUNX1* BCP-ALL suggests that they may represent 'second hit' mutations cooperating in the pathogenesis of this leukemia subtype.

In addition, recent analysis of *BCR-ABL1* positive pediatric and adult ALL by SNP microarrays identified *IKZF1* (Ikaros) deletions in >80% of cases and in about 50% deletions of *PAX5* and *CDKN2A*, which mostly coincided with *IKZF1* deletions (Mullighan *et al*, 2008). Strikingly, these deletions were found in *BCR-ABL1* positive ALL and CML blast crisis, but were not detected in chronic-phase CML (Mullighan *et al*, 2008). Together these data indicate that alterations in Ikaros possibly in conjunction with haploinsufficiency of *PAX5* may contribute to the arrested B-lymphoid maturation in *BCR-ABL1* positive ALL.

### 1.5.2.2. *PAX5* fusions in ALL

In 2001 the first chimeric *PAX5* fusion gene in a case of ALL with a t(9;12)(q11;p13) resulting in a *PAX5-ETV6* fusion was identified (Cazzaniga *et al*, 2001). Subsequently, it was shown that the *PAX5-ETV6* fusion defines the cytogenetic entity dic(9;12)(p13;p13), which occurs in about 1% of childhood ALL (Strehl *et al*, 2003). The *PAX5-ETV6* rearrangement fuses exon 4 of *PAX5* to exon 3 of *ETV6*, thus, the fusion protein contains the *PAX5* DNA-binding paired domain and the HLH and ETS-binding domains of *ETV6*. The *PAX5-ETV6* chimeric protein most likely acts as an aberrant transcription factor, probably as transcriptional repressor, which recruits transcriptional cofactors through the *ETV6* regulatory elements (Fazio *et al*, 2008). In addition, *PAX5-ETV6* functions as strong competitive inhibitor of wild-type *PAX5* in co-transfection and co-transduction experiments (Mullighan *et al*, 2007a).

Six years after the first description of this *PAX5* rearrangement in ALL, several other *PAX5* fusion partners were identified, namely *AUTS2*, *C20orf112* (Kawamata *et al*, 2008), *ELN* (Bousquet *et al*, 2007), *FOXP1*, and *ZNF521* (Mullighan *et al*, 2007a). All breakpoints described in these novel *PAX5* fusions occurred within *PAX5* intron 5 or downstream of it fusing at least the *PAX5* DNA-binding paired domain to the C-terminal region or nearly the entire protein of the fusion partner. It is assumed, that *PAX5* fusion proteins act as transcriptional repressors, which antagonize the *PAX5* activity provided by the normal wild-type allele (Cobaleda *et al*, 2007b).





## CHAPTER 2

### IDENTIFICATION OF *PML* AS NOVEL *PAX5* FUSION PARTNER IN CHILDHOOD ACUTE LYMPHOBLASTIC LEUKEMIA

Karin Nebral<sup>1</sup>, Margit König<sup>1</sup>, Lana Harder<sup>2</sup>, Reiner Siebert<sup>2</sup>, Oskar Haas<sup>3</sup>, Sabine Strehl<sup>1</sup>

British Journal of Haematology. 2007;139:269-274.

<sup>1</sup>CCRI, Children's Cancer Research Institute, St. Anna Kinderkrebsforschung, Kinderspitalgasse 6, A-1090 Vienna, Austria

<sup>2</sup>Institute of Human Genetics, University Hospital Schleswig-Holstein, Campus Kiel, Schwanenweg 24, D-24105 Kiel, Germany

<sup>3</sup>St. Anna Children's Hospital, Kinderspitalgasse 6, A-1090 Vienna, Austria

## Summary

*PAX5* encodes the B-cell lineage specific activator protein (BSAP) and is required for B-cell development and maintenance. In B-cell precursor acute lymphoblastic leukemia (ALL), *PAX5* is involved in several chromosome translocations that fuse the N-terminal paired DNA-binding domain of *PAX5* with the C-terminal regulatory sequences of *ETV6*, *FOXP1*, *ZNF521* or *ELN*. Herein, we describe the identification of a novel recurrent t(9;15)(p13;q24) in two cases of childhood ALL, which results in an in-frame fusion of *PAX5* to the promyelocytic leukemia (*PML*) gene. The putative *PAX5-PML* fusion gene encodes a chimeric protein that retains the paired domain, the octapeptid and the partial homeodomain of *PAX5*, and virtually the whole *PML* protein. The steadily increasing number of *PAX5* rearrangements suggests that *PAX5* is not only crucial for B-cell lymphopoiesis but also for the development of B-cell malignancies.

**Key Words:** *PAX5*, *PML*, fusion transcript, childhood acute lymphoblastic leukemia, t(9;15)(p13;q24).

## Introduction

PAX5 is a member of the paired box (PAX) family, a group of nine highly conserved transcription factors that are implicated in brain development and organogenesis (Bouchard *et al*, 2003). *PAX5* encodes the only PAX protein expressed within the hematopoietic system, the B-cell lineage specific activator protein (BSAP) that is required for B-cell commitment and maintenance. At the molecular level, Pax5 fulfils a dual role by activating B-cell specific genes and simultaneously repressing lineage-inappropriate genes (Nutt *et al*, 1999).

In the bone marrow, *Pax5* is exclusively expressed from the pro-B to the mature B-cell stage and is down regulated during terminal differentiation into plasma cells (Nutt *et al*, 1998). In the absence of *Pax5* in homozygous mutant mice, B-cell development is arrested at an early pro-B (pre-BI) cell stage (Urbanek *et al*, 1994; Nutt *et al*, 1999). Expression of *Pax5* is also essential for maintaining B-cell identity as upon conditional inactivation using a *CD19*-driven *Cre-loxP* system that allows for tissue-specific deletion of *Pax5* (Horcher *et al*, 2001), committed pro-B cells with a restricted B-lymphoid fate convert into progenitors with multilineage potential (Mikkola *et al*, 2002). Restoration of *Pax5* expression suppresses the hematopoietic pluripotency of *Pax5*<sup>-/-</sup> pro-B cells while simultaneously promoting their development to mature B-cells. (Nutt *et al*, 1999) Together, these data render *Pax5* as the critical B-lineage commitment factor (Cobaleda *et al*, 2007).

Chromosomal translocations affecting *PAX5* have been described in different types of B-cell malignancies. The t(9;14)(p13;q32) translocation, which is mainly associated with B-cell non-Hodgkin-Lymphoma (B-NHL) results in the juxtaposition of *PAX5* to the immunoglobulin heavy-chain (*IGH@*) locus, and thus, brings *PAX5* under the control of potent enhancers or promoters from the *IGH@* locus leading to elevated *PAX5* expression (Busslinger *et al*, 1996; Morrison *et al*, 1998). In B-cell precursor acute lymphoblastic leukemia (ALL) *PAX5* rearrangements involve several different partner genes including *ETV6* (12p13), *FOXP1* (3p14), *ZNF521* (18q11), and *ELN* (7q11) (Cazzaniga *et al*, 2001; Strehl *et al*, 2003; Bousquet *et al*, 2007; Mullighan *et al*, 2007).

PAX5 consists of a N-terminal paired domain, which is a bipartite DNA-binding region and a C-terminal proline-serine-threonine-rich region that harbors a transactivation domain. The central region contains an octapeptide capable of recruiting members of the Groucho proteins, a family of transcriptional corepressors that are required for many developmental processes, including lateral inhibition, segmentation, sex determination, dorsal/ventral pattern formation, terminal pattern formation and eye development (Chen & Courey, 2000; Eberhard *et al*, 2000), and a partial homeodomain functioning as a protein-protein interaction motif (Bouchard *et al*, 2003). The evolutionary highly conserved paired box domain that is shared by all PAX genes is retained in every fusion protein involving other members of the PAX family, namely PAX3, PAX7, and PAX8, which are affected by tumor-specific translocations

in alveolar rhabdomyosarcoma and thyroid follicular carcinoma ( Kroll *et al*, 2000; Barr, 2001). Each of the *PAX5* chimeric genes identified so far also encodes a fusion protein that maintains the paired-box DNA-binding domain that is fused to the DNA-binding and transcriptional regulatory domains of the partner protein (Cazzaniga *et al*, 2001; Strehl *et al*, 2003; Bousquet *et al*, 2007; Mullighan *et al*, 2007). *PAX5* fusion proteins may contribute to leukemogenesis by acting as constitutive repressor, and thus interfering with normal *PAX5* function (Cobaleda *et al*, 2007).

This study identified a novel recurrent t(9;15)(p13;q24) in two cases of childhood B-ALL, which results in the fusion of the 5' region of *PAX5* to almost the entire promyelocytic leukemia (*PML*) gene.

## Material and Methods

### Case History

Patient 1, a 9-months-old infant suffering from continuous fever, otorrhoe and hepatomegaly was diagnosed with ALL. The bone marrow (BM) showed 99% blast cell infiltration and 63% in the peripheral blood (PB). Immunophenotyping was performed on BM cells by means of flow cytometry with a panel of monoclonal antibodies. The blast cells were positive for CD19, CD79a, CD10, CD22, CD34, TdT, and HLA-DR typical for B-II-ALL (common-ALL). Cytogenetic analysis revealed a 46,XX,add(9)(p13)[8]/46,XX[14] karyotype. The patient was treated according to the ALL - Berlin-Frankfurt-Münster (BFM) 2000 Interfant protocol and is in complete remission more than 4 years from diagnosis.

Patient 2 was diagnosed with ALL at 19.5 months of age, following a 1-month period of pneumonic complaints. Immunophenotyping revealed a B-II-ALL positive for CD19, CD10, CD22, TdT, and HLA-DR. Treatment was performed according to the ALL-BFM 86 protocol (Reiter *et al*, 1994) and the patient achieved remission after 40 d, but relapsed 2 years and 3 months after diagnosis. At relapse biopsy of the testis showed infiltration with ALL blast cells and in the BM 45% of lymphoblasts were detected. Cytogenetic analysis showed a 46,XY,t(9;15)(p21;q25)[12] karyotype in the testis and a 46,XY,t(9;15)(p21;q25)[3]/46,XY,add(1)(p?)[3] in the BM. The patient was treated with high-dose methotrexate, but died of progressive disease.

### Conventional and molecular cytogenetics

Cytogenetic analysis was performed using standard methods and karyotypes were described according to the International System for Human Cytogenetic Nomenclature (Shaffer & Tommerup, 2005). *PAX5* rearrangements were detected using exon-specific cosmid cos-hPAX5-1 (exons 2-5) and cos-hPAX5-3 (exons 9-10) (Busslinger *et al*, 1996). In addition, the LSI *PML-RARA* dual-color, dual-fusion-translocation probe (Vysis, Downers Grove, IL, USA) and the BAC clone RP11-2M12 (The Sanger Institute, Cambridge, United Kingdom) encompassing the whole *PML* gene were used. To ensure analysis of abnormal metaphases, whole chromosome painting (WCP) probes were combined with gene-specific probes. The 24-color-fluorescence in situ hybridization (FISH) analysis was performed with the Spectra Vysion probe (Vysis, Downers Grove, IL, USA). Probes were differentially labeled by nick translation either with digoxigenin-11-dUTP or biotin-16-dUTP (Roche Diagnostics, Vienna, Austria). Slides for FISH were prepared from the methanol/acetic acid-fixed cell suspension used for cytogenetic analysis and FISH was performed as previously described (Konig *et al*, 2002). Samples were evaluated using an Axioplan fluorescence microscope (Zeiss, Vienna, Austria) equipped with the appropriate filter sets. Images were

taken with a CCD camera (Photometrix, Tucson, AZ) using the IPLabs software (Vysis, Downers Grove, IL, USA).

### *Reverse-Transcription-PCR analysis*

Total RNA was isolated from cryopreserved mononuclear cells (MNCs) of the BM obtained from patient 1 at diagnosis, and from methanol/acetic acid-fixed cell suspension of BM cells obtained from patient 2 at relapse as previously described (Strehl *et al*, 2001). RNA extraction was performed using the peqGOLD Total RNA kit (peqLab, Biotechnologie GmbH, Erlangen, Germany) according to the manufacturer's recommendations. RNA was reverse transcribed with 200 Units Moloney-murine leukaemia virus (M-MLV) reverse transcriptase (Invitrogen, Lofer, Austria) and 100 pmol random hexamers (GE Healthcare, Vienna, Austria) at 42°C for 1 h. Reverse-transcription polymerase chain reaction (RT-PCR) were performed using Hot Start Taq polymerase (Qiagen, Vienna, Austria) according to the manufacturer's instructions, with annealing at 61-63°C for 30 s, elongation at 72°C for 30-45 s for 30-40 cycles. Primer sequences are listed in Table 1.

## **Results**

### *Conventional and molecular cytogenetics*

Cytogenetic analysis of patient 1 showed a 46,XX,add(9)(p13). To determine the chromosomal origin of the extra material on 9p, 24-color FISH was performed. This analysis revealed a t(9;15) (Fig 1B, inset), and subsequent FISH using the *PAX5* exon-specific cosmid detected a separation of the probes (Fig 1A) suggesting involvement of *PAX5* in the t(9;15).

To narrow down the precise breakpoint at 15q, FISH-based chromosome walking with various locus-specific BAC clones located at 15q24-25 was performed (data not shown). Hybridization of the *PML*-specific BAC RP11-2M12 in combination with a whole chromosome painting probe specific for chromosome 9 to ensure hybridization of aberrant metaphases resulted in a split signal of *PML* (Fig 1B) providing compelling evidence that *PAX5* was fused to *PML*. Thus, the karyotype was refined as t(9;15)(p13;q24).

In the second patient (patient 2), cytogenetic analysis revealed a similar aberration, namely a t(9;15)(p21;q25). Also in this case, FISH analysis using the *PML-RARA* and the *PML*-specific BAC probes showed disruption of *PML*. Subsequent hybridization with the *PAX5* exon-specific cosmid showed a deletion of the *PAX5* 3'-end (data not shown) indicating that this patient also displayed a *PAX5-PML* fusion, associated with a deletion of the *PAX5* 3'-end.

### RT-PCR analysis

Fusion gene-specific RT-PCR experiments using primers located in *PAX5* exon 5 and *PML* exon 2 detected chimeric *PAX5-PML* transcripts in both patients (Fig 2A, left), but not in normal peripheral blood used as a negative control. Sequence analyses identified exactly the same in-frame fusion between *PAX5* exon 6 and *PML* exon 2 in both patients (Fig 2B and C). The PML protein consists of a RING domain followed by additional zinc fingers (B-boxes) and an  $\alpha$ -helical coiled-coil motif (collectively referred to as RBCC domain) (Bernardi & Pandolfi, 2003). Thus, the putative *PAX5-PML* chimeric fusion protein consists of the paired domain, the octapeptide and the partial homeodomain of *PAX5*, and almost the entire *PML* protein lacking only the 5' proline-rich region (Fig 2D). Amplification of the reciprocal *PML-PAX5* fusion transcript using different primer combinations failed, which indicate that the *PAX5-PML* fusion is responsible for leukemogenesis. These data are in concordance with the deletion of the *PAX5* 3'-end detected in patient 2 by FISH analysis. According to the FISH data, the second alleles of both genes involved in the translocation were retained and expression of normal *PAX5* and *PML* transcripts was verified by RT-PCR (Fig 1A, right; analysis was performed only for patient 1, because there was a lack of material for patient 2).

### Discussion

In this study, we report the identification of a novel recurrent t(9;15)(p13;q24), which results in a fusion of the B-cell specific transcription factor *PAX5* and the *PML* gene. The putative *PAX5-PML* fusion protein fuses the paired domain, the octapeptide, and the homeodomain of *PAX5* to almost the entire *PML* protein. Lack of reciprocal transcripts strongly suggest that *PAX5-PML* and not *PML-PAX5* is responsible for leukemogenesis.

The second known translocation involving *PML*, the t(15;17)(q22;q21), fuses *PML* to the retinoic acid receptor alpha (*RARA*), and is the genetic hallmark of acute promyelocytic leukemia (APL). The *PML-RARA* protein functions as an aberrant retinoid receptor with altered DNA-binding properties as compared to wild-type *RARA* and acts as a constitutive transcriptional repressor of *RARA* target genes (Lo-Coco & Ammatuna, 2006). As approximately 20-30% of APL lack expression of the reciprocal *RARA-PML*, *PML-RARA* must be the chimeric protein that is critical for the development of APL (Melnick & Licht, 1999; Lo-Coco & Ammatuna, 2006).

*PML* is detected in the nucleus in multiprotein complexes termed *PML* nuclear bodies (NBs), which are implicated in the regulation of transcription, apoptosis, DNA repair, control of genomic stability, tumor suppression, cellular senescence, and anti-viral response (Zhong *et al*, 2000; Dellaire & Bazett-Jones, 2004). In this respect, a specific feature of *PML-RARA* positive cells is the delocalization of *PML* from the *PML*-NBs to a microspeckled nuclear pattern and relocalization of *PML* to the NBs upon ATRA treatment (Melnick & Licht, 1999)



In the PAX5-PML fusion protein almost the entire PML is retained, and thus the chimeric fusion protein might heterodimerize with normal PML resulting in impaired PML function. In this regard, the PML-NBs play a key role in the regulation and functional activation of a number of proapoptotic/tumor suppressive transcription factors (Bernardi & Pandolfi, 2003). Thus, one might speculate that impairment of PML by the PAX5-PML fusion may exert a survival advantage by interfering with cellular apoptotic programs. To date it remains elusive whether PAX5-PML has *per se* transforming potential or additional mutations are required for the development of overt leukemia. Thus, impairment of PML, which is known to be involved in genome stability (Bernardi & Pandolfi, 2003) may facilitate the accumulation of additional mutations.

On the other hand, *PAX5*, as a master regulator of B-cell development, is indispensable for B-lineage commitment and continuous expression is required to maintain B-cell fate (Nutt *et al*, 2001; Mikkola *et al*, 2002; Busslinger 2004). A common feature of most PAX5 chimeric proteins described to date, is the fusion of the paired box DNA-binding domain of PAX5 with C-terminal regulatory sequences of a second transcription factor implicated in B-cell development or hematopoietic malignancy. Thus, the fusion proteins are predicted to retain the ability to bind to PAX5 transcriptional targets without providing normal transcriptional regulatory functions (Cobaleda *et al*, 2007; Mullighan *et al*, 2007). Indeed, in transient transfection assays *PAX5-ETV6* and *PAX5-FOXP1* competitively inhibit the transcriptional activation of wild-type *PAX5* (Mullighan *et al*, 2007). However, no transcriptional regulatory function for the *PAX5* partner *ELN*, which encodes an extracellular matrix protein that is the main component of elastic fibers, has been demonstrated. Nevertheless, the PAX5-ELN fusion protein also acts in a dominant-negative manner over PAX5 in *in vitro* CD19 reporter gene assays (Bousquet *et al*, 2007). Thus, it is highly likely that the PAX5-PML chimera also operates as an aberrant transcription factor exerting a repressor activity antagonizing normal PAX5 function.

Yet, analyses of the effects of *PAX5-ELN* on *PAX5* endogenous targets resulted in conflicting data, as in DG75 (Burkitt lymphoma) transfected cells, the expression of the *PAX5* target genes *BLNK*, *CD79A* and *LEF1* was downregulated, whereas *CD19* and *BLK* remained unaffected. In contrast, *PAX5-ELN* leukemic pre-B-cells showed exactly the opposite expression pattern. These data suggest that, in case of *PAX5* fusions, regulation of *PAX5* target gene transcription may be cellular context-dependent (Bousquet *et al*, 2007).

Although *PAX5* fusions seem to account for just about 2% of childhood ALL (Mullighan *et al*, 2007; unpublished observation) and the functional consequences of all PAX5 chimaeric proteins need to be elucidated in more detail, the increasing number of PAX5-involving rearrangements renders this critical B-cell-specific transcription factor not only crucial for

normal B-cell lymphopoiesis but it may also be considered as a major player in leukaemogenesis.

## Acknowledgements

We thank Meinrad Busslinger (IMP, Vienna, Austria) for kindly providing the *PAX5* cosmid probes, and Claudia Becher (Campus Kiel, Kiel, Germany) and Elisabeth Lang (St. Anna Kinderkrebsforschung, Vienna, Austria) for excellent technical assistance.

*Grant support:* This work was supported by the Austrian Ministry of Science and Research (GEN-AU II, GZ 200.136/1-VI/1/2005), the St. Anna Kinderkrebsforschung and the Kinderkrebs-Initiative Buchholz/Holm-Seppensen.

## References

- Barr, F.G. (2001) Gene fusions involving PAX and FOX family members in alveolar rhabdomyosarcoma. *Oncogene*, **20**, 5736-5746.
- Bernardi, R. & Pandolfi, P.P. (2003) Role of PML and the PML-nuclear body in the control of programmed cell death. *Oncogene*, **22**, 9048-9057.
- Bouchard, M., Schleiffer, A., Eisenhaber, F., and Busslinger, M. (2003) Evolution and function of Pax genes. In: *Encyclopedia of the Human Genome* (ed. by D. Cooper), pp. 1-7. Nature Publishing Group, UK, London.
- Bousquet, M., Broccardo, C., Quelen, C., Meggetto, F., Kuhlein, E., Delsol, G., Dastugue, N. & Brousset, P. (2007) A novel PAX5-ELN fusion protein identified in B-cell acute lymphoblastic leukemia acts as a dominant negative on wild-type PAX5. *Blood*, **109**, 3417-3423.
- Busslinger, M. (2004) Transcriptional control of early B cell development. *Annual Review of Immunology*, **22**, 55-79.
- Busslinger, M., Klix, N., Pfeffer, P., Graninger, P.G. & Kozmik, Z. (1996) Deregulation of PAX-5 by translocation of the Emu enhancer of the IgH locus adjacent to two alternative PAX-5 promoters in a diffuse large-cell lymphoma. *The Proceedings of the National Academy of Science of the United States of America*, **93**, 6129-6134.
- Cazzaniga, G., Daniotti, M., Tosi, S., Giudici, G., Aloisi, A., Pogliani, E., Kearney, L. & Biondi, A. (2001) The paired box domain gene PAX5 is fused to ETV6/TEL in an acute lymphoblastic leukemia case. *Cancer Research*, **61**, 4666-4670.
- Chen, G. & Courey, A.J. (2000) Groucho/TLE family proteins and transcriptional repression. *Gene*, **249**, 1-16.
- Cobaleda, C., Schebesta, A., Delogu, A. & Busslinger, M. (2007) Pax5: the guardian of B cell identity and function. *Nature Immunology*, **8**, 463-470.
- Dellaire, G. & Bazett-Jones, D.P. (2004) PML nuclear bodies: dynamic sensors of DNA damage and cellular stress. *Bioessays*, **26**, 963-977.
- Eberhard, D., Jimenez, G., Heavey, B. & Busslinger, M. (2000) Transcriptional repression by Pax5 (BSAP) through interaction with corepressors of the Groucho family. *The EMBO Journal*, **19**, 2292-2303.
- Horcher, M., Souabni, A. & Busslinger, M. (2001) Pax5/BSAP maintains the identity of B cells in late B lymphopoiesis. *Immunity*, **14**, 779-790.
- Konig, M., Reichel, M., Marschalek, R., Haas, O.A. & Strehl, S. (2002) A highly specific and sensitive fluorescence in situ hybridization assay for the detection of t(4;11)(q21;q23) and concurrent submicroscopic deletions in acute leukaemias. *British Journal of Haematology*, **116**, 758-764.

- Kroll, T.G., Sarraf, P., Pecciarini, L., Chen, C.J., Mueller, E., Spiegelman, B.M. & Fletcher, J.A. (2000) PAX8-PPARgamma1 fusion oncogene in human thyroid carcinoma [corrected]. *Science*, **289**, 1357-1360.
- Lo-Coco, F. & Ammatuna, E. (2006) The biology of acute promyelocytic leukemia and its impact on diagnosis and treatment. *Hematology (American Society of Hematology Education Program)*, **514**, 156-161.
- Melnick, A. & Licht, J.D. (1999) Deconstructing a disease: RARalpha, its fusion partners, and their roles in the pathogenesis of acute promyelocytic leukemia. *Blood*, **93**, 3167-3215.
- Mikkola, I., Heavey, B., Horcher, M. & Busslinger, M. (2002) Reversion of B cell commitment upon loss of Pax5 expression. *Science*, **297**, 110-113.
- Morrison, A.M., Jager, U., Chott, A., Schebesta, M., Haas, O.A. & Busslinger, M. (1998) Deregulated PAX-5 transcription from a translocated IgH promoter in marginal zone lymphoma. *Blood*, **92**, 3865-3878.
- Mullighan, C.G., Goorha, S., Radtke, I., Miller, C.B., Coustan-Smith, E., Dalton, J.D., Girtman, K., Mathew, S., Ma, J., Pounds, S.B., Su, X., Pui, C.H., Relling, M.V., Evans, W.E., Shurtleff, S.A. & Downing, J.R. (2007) Genome-wide analysis of genetic alterations in acute lymphoblastic leukaemia. *Nature*, **446**, 758-764.
- Nutt, S.L., Morrison, A.M., Dorfler, P., Rolink, A. & Busslinger, M. (1998) Identification of BSAP (Pax-5) target genes in early B-cell development by loss- and gain-of-function experiments. *The EMBO Journal*, **17**, 2319-2333.
- Nutt, S.L., Heavey, B., Rolink, A.G. & Busslinger, M. (1999) Commitment to the B-lymphoid lineage depends on the transcription factor Pax5. *Nature*, **401**, 556-562.
- Nutt, S.L., Eberhard, D., Horcher, M., Rolink, A.G. & Busslinger, M. (2001) Pax5 determines the identity of B cells from the beginning to the end of B-lymphopoiesis. *International Reviews of Immunology*, **20**, 65-82.
- Reiter, A., Schrappe, M., Ludwig, W.D., Hiddemann, W., Sauter, S., Henze, G., Zimmermann, M., Lampert, F., Havers, W. & Niethammer, D. (1994) Chemotherapy in 998 unselected childhood acute lymphoblastic leukemia patients. Results and conclusions of the multicenter trial ALL-BFM 86. *Blood*, **84**, 3122-3133.
- Shaffer L.G. & Tommerup N. (eds). (2005): *An International System for Human Cytogenetic Nomenclature (ISCN)*. S. Karger, Basel.
- Strehl, S., Konig, M., Mann, G. & Haas, O.A. (2001) Multiplex reverse transcriptase-polymerase chain reaction screening in childhood acute myeloblastic leukemia. *Blood*, **97**, 805-808.
- Strehl, S., Konig, M., Dworzak, M.N., Kalwak, K. & Haas, O.A. (2003) PAX5/ETV6 fusion defines cytogenetic entity dic(9;12)(p13;p13). *Leukemia*, **17**, 1121-1123.
- Urbanek, P., Wang, Z.Q., Fetka, I., Wagner, E.F. & Busslinger, M. (1994) Complete block of early B cell differentiation and altered patterning of the posterior midbrain in mice lacking Pax5/BSAP. *Cell*, **79**, 901-912.
- Zhong, S., Salomoni, P. & Pandolfi, P.P. (2000) The transcriptional role of PML and the nuclear body. *Nature Cell Biology*, **2**, E85-90.

## Tables

**Table 1. Oligonucleotide Primer Sequences**

Primer	Oligonucleotide sequence	Direction	Gene/Exon <sup>1</sup>	Transcript
PAX5ex5-F1	TACTCCATCAGCGGCATCC	sense	PAX5/5	PAX5-PML
PMLex2-R1	CGCACTCAAAGCACCAAGAAG	antisense	PML/2	
PAX5ex5-F1	TACTCCATCAGCGGCATCC	sense	PAX5/5	PAX5
PAX5ex7-R1	GGCCTTCATGTCGTCCAG	antisense	PAX5/7	
PMLex1-F1	CTCAAGGGACTCAGCCAACTG	sense	PML/1	PML
PMLex2-R1	CGCACTCAAAGCACCAAGAAG	antisense	PML/2	

<sup>1</sup>Exon nomenclature according to the Ensembl Genome Browser exon information (<http://www.ensembl.org/>).

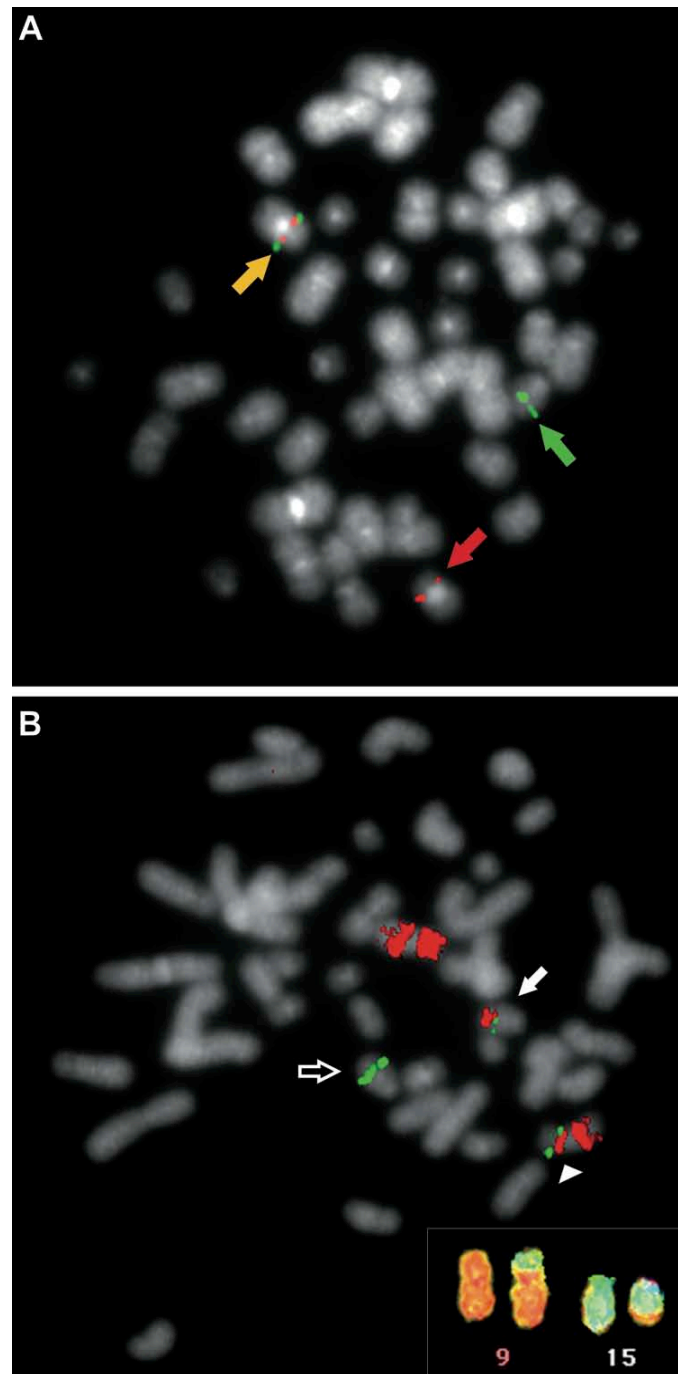


**Figure 1. Fluorescence *in situ* hybridization (FISH) analysis of patient 1.**

**(A)** Metaphase hybridized with exon-specific *PAX5* probes cos-hPAX5-1 (red) and cos-hPAX5-3 (green) showing a disruption of *PAX5*. Arrows indicate the normal chromosome 9 (orange), the derivative chromosome 9 (red) and the derivative chromosome 15 (green). **(B)** 24-color FISH analysis showing the t(9;15) (inset). Metaphase analysis using probes WCP 9 (red) and RP11-2M12 (green) encompassing the whole promyelocytic leukemia (*PML*) gene and displaying a disruption of *PML*. The filled arrow is pointing to derivative chromosome 15, the arrowhead to derivative chromosome 9, and the open arrow to the normal chromosome 15.

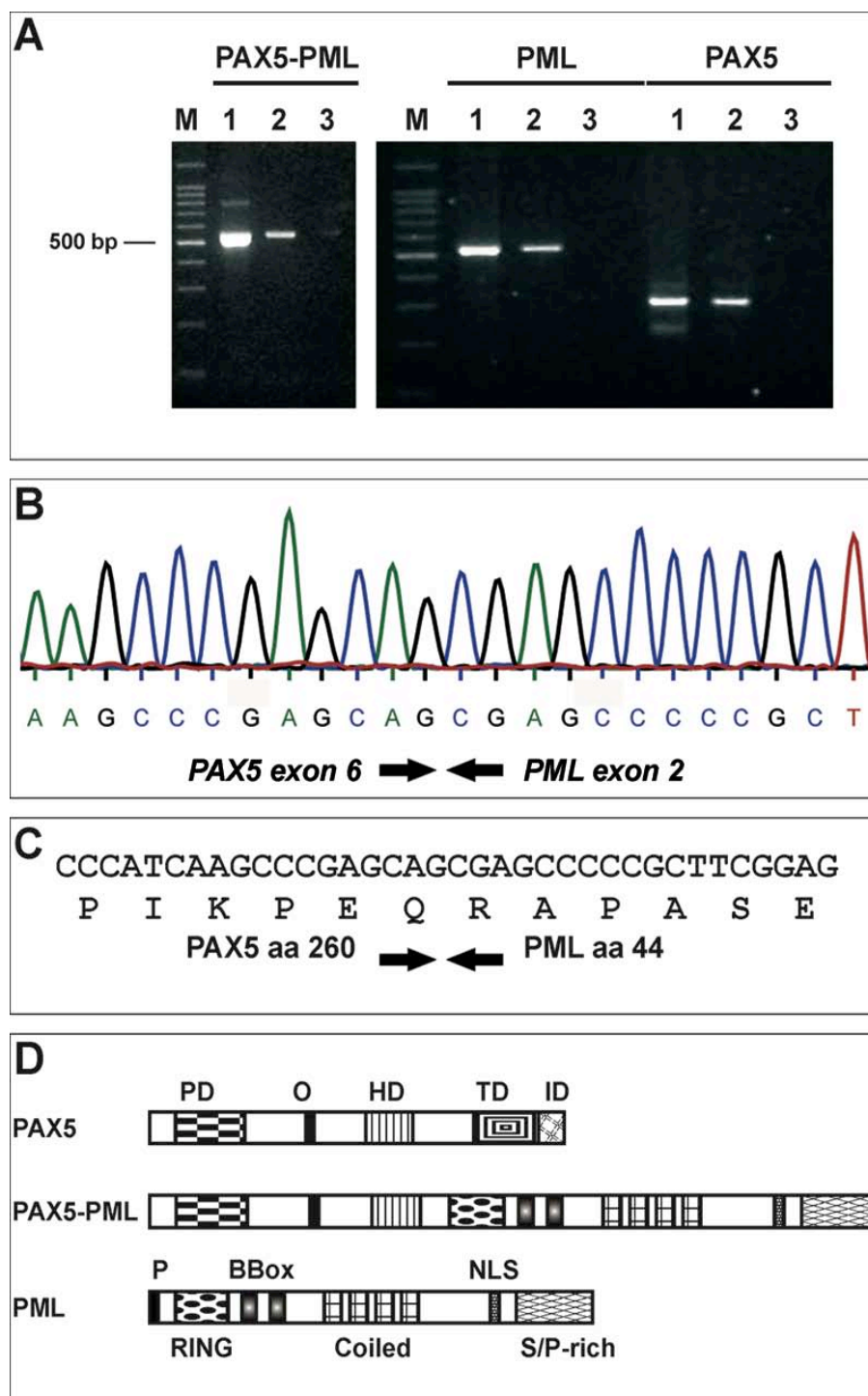


**Figure 2. Reverse-transcription polymerase chain reaction (RT-PCR) analysis.**

**(A)** RT-PCR of the *PAX5-PML* fusion transcript (left) and the normal *PML* and *PAX5* alleles. M, molecular weight marker, 100 bp ladder; lane 1, patient 1; lane 2, patient 2; lane 3, negative control (left). lanes 1, patient 1; lanes 2, normal control; lanes 3, negative control (right). **(B)** Sequence analysis of the *PAX5-PML* transcript showing a fusion of *PAX5* exon 6 to *PML* exon 2. **(C)** Partial nucleotide and amino acid sequence of the *PAX5-PML* chimera. **(D)** Schematic representation of the *PAX5* and *PML* wild-type proteins and the putative chimeric *PAX5-PML* protein. PD, paired domain; O, conserved octapeptide; HD, homeobox domain; TD, transactivation domain; ID, inhibitory domain; P, proline-rich sequence; RING, 'really interesting new gene' finger; BBOX, B box zinc fingers; COILED, coiled-coil domain; NLS, nuclear localization signal; S/P-rich, serine/proline-rich region;



## CHAPTER 3

### INCIDENCE AND DIVERSITY OF *PAX5* FUSION GENES IN CHILDHOOD ACUTE LYMPHOBLASTIC LEUKEMIA

Karin Nebral<sup>1</sup>, Dagmar Denk<sup>1</sup>, Andishe Attarbaschi<sup>2</sup>, Margit König<sup>1</sup>, Georg Mann<sup>2</sup>,  
Oskar A. Haas<sup>2</sup>, and Sabine Strehl<sup>1</sup>

Leukemia. 2008. In press.

<sup>1</sup>CCRI, Children's Cancer Research Institute, St. Anna Kinderkrebsforschung, Vienna, Austria;

<sup>2</sup>Department of Pediatric Hematology and Oncology, St. Anna Children's Hospital, Vienna, Austria



## Abstract

*PAX5*, a master regulator of B-cell development, was recently shown to be involved in several leukemia-associated rearrangements, which result in fusion genes encoding chimeric proteins that antagonize *PAX5* transcriptional activity. In a population-based fluorescence *in situ* hybridization (FISH) screening study of 446 childhood acute lymphoblastic leukemia (ALL) patients we now show that *PAX5* rearrangements occur at an incidence of about 2.5% of B-cell precursor leukemia (BCP-ALL). Identification of several novel *PAX5* partner genes including *POM121*, *BRD1*, *DACH1*, *HIPK1*, and *JAK2* brings the number of distinct *PAX5* in-frame fusions to at least twelve. Our data show that these not only comprise transcription factors but also structural proteins and genes involved in signal transduction, which at least in part have not been implicated in tumorigenesis.

## Keywords

*PAX5* rearrangements, fusion genes, FISH screening, B-cell precursor acute lymphoblastic leukemia

## Introduction

The transcription factor *Pax5* encodes the B-cell lineage specific activator protein (BSAP) and is a master regulator of B-cell development. Within the hematopoietic system, *Pax5* is exclusively expressed in the B-lymphoid lineage and is required for progression beyond the pro-B cell stage.<sup>1</sup> *Pax5* is not only indispensable for B-lineage commitment, but its continuous expression is also essential to maintain this fate.<sup>1-3</sup> During B-cell lineage commitment, *Pax5* fulfils a dual role by repressing B-lineage inappropriate genes and simultaneously activating B-lineage-specific genes.<sup>4-6</sup> Loss of *Pax5* expression in pro-B cells by conditional gene inactivation arrests B-cell development at an early pro-B cell stage and reverts committed B-cell precursors with a restricted B-lymphoid potential to progenitors with self-renewal capacity and hematopoietic pluripotency.<sup>2,4</sup> The restoration of *Pax5* expression suppresses the multilineage potential of *Pax5*<sup>-/-</sup> pro-B cells while simultaneously promoting their differentiation to mature B-cells.<sup>4</sup>

The essential role of *Pax5* for proper B-cell development renders *PAX5* also an intriguing candidate to be involved in B-cell neoplasia. The t(9;14)(p13;q32) found in a subset of B-cell non-Hodgkin's lymphoma juxtaposes the intact coding sequence of *PAX5* under the control of the *IGH@* locus, leading to inappropriate expression of *PAX5*.<sup>7,8</sup> Recently, it was also shown that deletion, amplification, point mutation and structural rearrangements in genes encoding regulators of B-lymphocyte development and differentiation occur in 40% of B-progenitor ALL.<sup>9</sup> Amongst the affected genes, *PAX5* was the most frequent target of somatic mutation, being altered in about 32% of the cases.<sup>9</sup> In ALL *PAX5* is involved in different translocations that result in fusion genes encoding chimeric proteins with novel functions. So far, *ETV6*,<sup>10,11</sup> *ELN*,<sup>12</sup> *FOXP1*,<sup>9</sup> *ZNF521*,<sup>9</sup> *PML*,<sup>13</sup> *AUTS2*,<sup>14</sup> and *C20orf112*<sup>14</sup> were identified as *PAX5* fusion partners.

In this population-based FISH screening study of 446 consecutive childhood ALL cases, we determined that in B-cell precursor ALL (BCP-ALL) *PAX5* rearrangements occur at an incidence of about 2.5%. The subsequent identification of the partner genes discovered five novel in-frame *PAX5* fusions to *HIPK1*, *POM121*, *JAK2*, *DACH1*, and *BRD1*, a set of genes with diverse functions including not only transcription factors but also structural proteins and even a tyrosine kinase.

## Materials and Methods

### Patients

Between June 1999 and December 2007, 486 infants and children with *de novo* acute lymphoblastic leukemia (ALL) were registered in the Austrian ALL-BFM 2000 (n=475) and Interfant-99<sup>15</sup> (n=11) studies. The 486 patients also include those only registered but

subsequently for various reasons not treated accordingly. The patients comprised n=65 with T-ALL and n=414 with B-cell leukemia including all immunophenotypes: pro-B ALL (n=20), cALL (n=268), pre-B ALL (n=118), mature ALL (n=5); and (n=3) without specific classification. Further, the study included 4 biphenotypic and one NK-cell leukemia, as well as two ALLs, which were not analyzed in detail. Based on successful routine diagnostic work-up by cytogenetics, FISH and RT-PCR approaches, the n=421 ALLs (excluding only the n=65 T-ALL cases) consisted of 126/400 (31.5%) with high hyperdiploidy (> 50 chromosomes), 38/400 (9.5%) with low hyperdiploidy (47-50 chromosomes), 18/400 (4.5%) with hypodiploidy (< 46 chromosomes) and 113/421 (26.8%) *ETV6-RUNX1*, 12/418 (2.9%) *TCF3-PBX1* (*E2A-PBX1*), 7/421 (1.7%) *BCR-ABL1*, and 11/421 (2.6%) *MLL* positive cases. The entire patient cohort consisted of 272 male and 214 female patients, and the age distribution ranged from 0.18 – 19.3 years (median = 5.6 years). Written informed consent was obtained from the patients, their parents or their legal guardians that surplus material not required for diagnostic purposes may be used for accompanying cancer research projects.

Out of these 486 patients from 454 (93.4%) sufficient material for FISH analysis was available. FISH analysis was successful in 446 (98.2%) of the analyzed cases, while in 8 (1.8%) poor quality of the fixed cells and, thus, insufficient hybridization efficiency precluded unambiguous evaluation of the FISH pattern.

### **FISH approach for the detection of PAX5 rearrangements**

*PAX5* rearrangements were detected using *PAX5* flanking BAC clones RP11-12P15 and RP11-220I1 (obtained from Pieter de Jong, BACPAC Resources, Children's Hospital and Research Center Oakland, CA, USA). Direct involvement of *PAX5* was verified using the exon-specific cosmid cos-hPAX5-1 (exons 2-5) and cos-hPAX5-3 (exons 9-10)<sup>7</sup>. For metaphase analysis also RP11-465P6 and RP11-84P7 were applied (obtained from M. Rocchi, Department of Cytogenetics, University of Bari, Bari, Italy). Exact clone positions relative to *PAX5* are illustrated in Supplementary Figure S1.

BAC and cosmid DNA was isolated using the PSI-Clone BAC DNA Kit (emp Biotech, Berlin, Germany) and the QIAprep Spin Miniprep Kit (Qiagen, Vienna, Austria), respectively. BAC and cosmid DNA was then amplified with the TempliPhi Amplification Kit (GE Healthcare, Vienna, Austria) according to the manufacturer's recommendations. Slides for FISH were prepared from the methanol/acetic acid-fixed cell suspensions used for cytogenetic analysis and incubated in Nonidet P40 (Sigma-Aldrich, Vienna Austria) 0.4% / 2xSSC at 37°C for 1 hour and then immediately dehydrated through an ascending ethanol series followed by 3 minutes of pepsin digestion. FISH was essentially performed as previously described.<sup>16</sup>

Metaphase images were acquired with a Zeiss Axioplan 2 Imaging fluorescence microscope (Zeiss, Göttingen, Germany) equipped with appropriate filter sets using a Zeiss AxioCam

MRm CCD camera and the Isis version 5.0 SR-6 FISH Imaging System (MetaSystems, Altlußheim, Germany). High-throughput automated interphase FISH spot counting was accomplished using the Axioplan 2 microscope coupled to the Metafer4-Metacyte system, Version V 3.1.122 (MetaSystems). Following automated analyses of 300-400 nuclei per case, each sample was manually reevaluated. Based on the analysis of normal controls and leukemia samples with normal *PAX5* status, separation of differentially labeled clones was considered when the distance between the signals was > 10 pixel.

### Identification of *PAX5* fusion partners

*PAX5* fusion partners were identified by rapid amplification of cDNA ends (RACE) or fluorescence *in situ* hybridization (FISH) analysis.

**RACE.** Total RNA was extracted from mononuclear cells isolated from bone marrow using the PeqGOLD total RNA Kit (Peqlab Biotechnology, Erlangen, Germany) including an on column DNase digestion step. 300 ng – 2 µg of total RNA were reverse transcribed using the AMV Reverse Transcriptase and the cDNA synthesis primer provided with the Marathon Kit (Takara Bio Europe/Clontech, Saint-Germain-en-Laye, France) followed by second-strand cDNA synthesis according to the manufacturer's instructions. Ligation of the Marathon cDNA Adaptor to the ds-cDNA was performed overnight at 16°C. Appropriately diluted adapter-ligated ds-cDNA was amplified using the *PAX5* gene-specific forward primer PAX5ex2-3-F1 (5'-TCTTGGCAGGTATTATGAGACAGGAAG-3') or the reverse primer PAX5ex6-7-R1 (5'-TGGCTGAATACTCTGTGGTCTGCTC-3') and the adaptor primer AP1 (5'-CCATCCTAATACGACTCACTATAGGGC-3'). A nested PCR reaction was done with the *PAX5*-specific primers PAX5ex3-F2 (5'-CAGAGCGGGTGTGTGACAATGAC-3') or PAX5ex6-R1 (5'-CTGCTGCTGTGTGAACAAGTCTCC-3') and the AP2 (5'-ACTCACTATAGGGCTC GAGCGGC-3') universal primer. PCRs were carried out with a T3000 thermocycler (Biometra, Göttingen, Germany) using the following cycling parameters: 95°C initial denaturation for 1 minute; 5 cycles of 94°C for 15 seconds, 72°C for 5-8 minutes; 5 cycles of 94°C for 15 seconds, 70°C for 5-8 minutes; 25 cycles of 94°C for 15 seconds, 68°C for 5-8 minutes.

RACE products were cut out from the gels, extracted using the PeqGOLD Gel Extraction Kit (Peqlab Biotechnology) and directly sequenced or cloned into the pGEM-T Easy vector (Promega, Mannheim, Germany) and sequenced. Sequencing was performed by Eurofins MWG Operon (Ebersberg, Germany).

**FISH.** The *PAX5-C20orf112* fusion was detected using RP11-431F4 and RP11-465P6 (M. Rocchi) encompassing the complete *PAX5* gene (Supplementary Figure S1) in combination with RP5-1184F4 (Wellcome Trust Sanger Institute; <http://www.sanger.ac.uk>), which spans the *C20orf112* locus.

### Reverse Transcription-PCR Analysis

Total RNA was reverse transcribed using 2µg of random hexamers (Amersham) and 200 units Moloney-murine leukemia virus (M-MLV) reverse transcriptase (Invitrogen, Lofer, Austria) at 42°C for 60 minutes. RT-PCR reactions were carried out using Hot Start Taq (Qiagen): initial denaturation at 95°C for 14 minutes, 38-42 cycles at 95°C for 30 seconds, at 60-64°C for 30 seconds, at 72°C for 30-90 seconds, followed by a final elongation at 72°C for 7 minutes. Amplification of full length *PAX5* fusion transcripts was accomplished either in one round or in two consecutive nested PCR reactions with Finnzymes Phusion™ Hot Start High-Fidelity DNA Polymerase (Biozym Scientific GmbH, Vienna, Austria). All primer sequences and the combinations used are provided in Supplementary Table 1. PCR products were either cut out from the gels and extracted with the PeqGOLD Gel Extraction Kit (Peqlab Biotechnology) or directly purified using the QiaQuick PCR Purification kit (Qiagen) and sequenced by Eurofins MWG Operon.

### Western blotting

Appropriate material for Western blot analysis was only available from one case with a *PAX5* rearrangement. The KIS-1 cell line served as *PAX5* wild-type positive control. Protein was extracted with standard lyses buffer in the presence of protease inhibitor (Roche). Total proteins were separated by SDS-PAGE on NuPAGE 4-12% Bis-Tris gels (Invitrogen) and transferred to nitrocellulose membrane using the XCell SureLock and the XCell II Blot module (Invitrogen) according to the manufacturer's instructions. After blocking with blocking reagent (Roche) membranes were incubated with an anti-N-terminal *PAX5* antibody (ab12000, Abcam, Cambridge, UK). Following incubation with a secondary antibody bands were visualized using the LI-COR Odyssey system (LI-COR Biosciences GmbH, Bad Homburg, Germany). Membranes were stripped with 1% SDS and 25 mM Glycine pH 2 and reincubated with anti-GAPDH antibody (6C5; Santa Cruz Biotechnology Inc., Santa Cruz, CA) and an appropriate secondary antibody.

### Gene and exon nomenclature

The gene nomenclature throughout this manuscript follows that approved by the human genome nomenclature committee HUGO (<http://www.genenames.org/>). Nucleotide reference sequences used for primer design and the description of the of the novel *PAX5* partner genes were the following: *PAX5*, NM\_016734; *HIPK1*, NM\_198268; *POM121*, NM\_172020 and OTTHUMT00000252020 POM121-001 (the reference sequence differs from the latter by lack of exon 4 described in Ensembl and the sequences have alternative 3' ends); *JAK2*, NM\_004972; *DACH1*, NM\_080759; *BRD1*, NM\_014577; *C20orf112*, NM\_080616; (National Center of Biotechnology Information [NCBI]).

## Results

### FISH screening for *PAX5* rearrangements

Interphase FISH analysis of 446 childhood ALL samples detected FISH patterns suggestive for *PAX5* rearrangements in 10 cases. *PAX5* rearrangements were exclusively found in B-cell precursor ALL (BCP-ALL) and, thus, the overall frequency in childhood ALL was 2.2% whereas the incidence in BCP-ALL was 2.6%.

In 7 cases (1.6%) the dual-color split-apart assay with *PAX5*-flanking BAC clones detected a separation of the signals suggesting the presence of a *PAX5* rearrangement. In 5 cases (1.1%) deletions of the 3' clone and in 15 (3.4%) of the 5' clone were observed. One single case displayed an additional 3' signal and further analysis confirmed a duplication encompassing the *PAX5* 3'-end and flanking sequences.

All aberrant cases were further analyzed using *PAX5* gene-specific cosmid, which proved the direct involvement of *PAX5* in all seven cases showing a split FISH pattern with the BAC clones. Out of the 15 cases with a 5' BAC clone deletion 8 were *ETV6-RUNX1* positive and were not further analyzed. One case was not analyzable, three displayed no *PAX5* aberration, and three a 5' deletion suggesting focal *PAX5* deletions.<sup>9</sup> In 2 out of the 5 cases with a 3' BAC clone deletion one entire copy of *PAX5* was absent, whereas in three cases a 3' internal deletion was confirmed indicating a *PAX5* fusion associated with a 3' deletion.

### Identification of *PAX5* fusion partners

In all 10 cases that displayed a FISH pattern suggestive for the presence of a *PAX5* fusion (Table 1) we attempted to identify the respective partner gene. In two of the cases, one each with a split FISH pattern and a *PAX5* 3' deletion we have previously identified *PML*<sup>13</sup> (case 1) and *ETV6*<sup>11</sup> (case 9) as fusion partners, respectively (Table 1). To determine whether in any of the cases one of the known *PAX5* partners was involved *PAX5* fusion gene-specific FISH and/or RT-PCR experiments were performed first, and as soon as we were able to unravel a novel fusion partner all cases were retrospectively analyzed.

### Identification of *PAX5* fusion partners in *PAX5*-rearranged leukemia

In cases 2 and 4, only a minor but significant percentage of the cells (20.8% and 19.3%) displayed a split FISH signal pattern (Table 1). Subsequent evaluation of metaphases clearly showed that the *PAX5*-flanking probes were separated and both located on chromosome 9p suggesting an inversion event (Figure 1A).

3' RACE using RNA isolated from the bone marrow obtained at relapse of case 4 resulted in an approximately 2 kb amplification product (data not shown) and sequence analysis

revealed fusion of *PAX5* exon 5 to *JAK2* exon 19 (Figure 1D). RT-PCR analysis of the diagnostic samples of both cases confirmed the presence of the same *PAX5-JAK2* transcripts (Figure 1B). Amplification of the reciprocal *JAK2-PAX5* fusion showed multiple splice variants that either included all respective *JAK2* exons or lacked exon 18 or exons 17 and 18 (Figure 1C,E). The splice variant containing all *JAK2* exons and that lacking exons 17 and 18 resulted in open reading frames. Using primers in the respective first and last coding exons, both *PAX5-JAK2* and *JAK2-PAX5* full length transcripts could be amplified, which apart from the splice variants described above did not lack any other exons (Figure 3A and B, and data not shown). Western blot analysis revealed expression of the predicted size mutant PAX5 protein as well as wild type PAX5 (Figure 3D).

The putative *PAX5-JAK2* chimeric protein contains the paired domain (PD) and the octapeptide (OP) domain of PAX5 and the JAK homology (JH) 1 kinase domain of JAK2. The full length hypothetical reciprocal *JAK2-PAX5* fusion protein consists of the JAK2 kinase domains JH2-JH7 fused to the PAX5 homeodomain (HD) and the transactivation (TA) and inhibitory (ID) domains (Figure 4B). The shorter *JAK2-PAX5* in-frame isoform would lack the JH2 domain.

In case 3, 3' RACE and direct sequencing of a PCR product revealed fusion of *PAX5* exon 5 to the noncoding region of *BRD1* exon 1. Subsequent fusion gene-specific RT-PCR verified the data obtained by RACE (Figure 2A). *PAX5* exon 5 was joined to 14 bp of the noncoding exon 1 of *BRD1* resulting in a putative chimeric protein consisting of the PAX5 PD and the octapeptide domain fused to 4 miscellaneous amino acids and the entire BRD1 protein, which contains highly conserved domains, such as an amino-terminal plant homeodomain (PHD) zinc finger and a bromodomain (Figure 4C). Insufficiency of material prevented amplification of the full length fusion transcript, whose coding region would have an estimated length of 3795 bp.

In case 5, FISH analysis clearly showed a *PAX5* rearrangement (Figure 2Bi-ii) but 3' RACE failed to identify the *PAX5* fusion partner. However, cloning and sequencing of 5' RACE products revealed that one clone encompassed *PAX5* exon 6 fused to the noncoding exon 4 of *POM121* (data not shown). These data prompted us to perform *PAX5-POM121*-specific RT-PCR experiments and indeed *PAX5-POM121* transcripts could be amplified (Figure 2Biii). Sequence analysis showed that *PAX5* exon 5 was fused to 112 bp of genomic DNA derived from chromosome 12 followed by *POM121* exon 5 (Figure 2B) suggesting a complex rearrangement between chromosomes 7, 9, and 12. Exons 1-4 of *POM121* are non-coding and the translational start codon is located in exon 5. Nevertheless the insertion of the 112 bp genomic DNA resulted in a complete open reading frame and a putative fusion protein consisting of the PD and the octapeptide domain of PAX5 joined to 88 amino acids neither homologous to PAX5 nor POM121, and the entire POM121 protein (Figure 4D). Owing to the

lack of appropriate material the full length coding transcript, which would have a calculated size of 3867 bp could not be amplified and, thus, it remains elusive whether all exons are retained or different splice variants of *PAX5-POM121* are expressed.

In case 6, FISH experiments showed that the 5'-end of *PAX5* was located on a der(9) chromosome whereas the 3'-end was translocated to 14q32 (data not shown). Further thorough FISH analysis confirmed the presence of complex rearrangements involving at least chromosomes 9, 3, 11, and 12 with insertion of chromosome 11p material into 9p (data not shown) indicating fusion of *PAX5* with a gene located on 11p. However, though 20 BAC clones, which encompassed 11p13-15 were hybridized none of them showed a co-localization with *PAX5* and, thus, this strategy failed to identify any candidate gene. Consequently, also in this case 3' and 5' RACE was performed but despite extensive efforts we were unable to identify the *PAX5* partner gene.

In case 7, FISH analysis showed a split signal for the *PAX5*-specific clones and 1-2 additional 5' signals (Figure 2Ci). Further FISH analysis again indicated complex aberrations involving several chromosomes, in particular 1p, which was translocated to 9p (data not shown). Cloning and sequencing of an approximately 1.8 kb 3' RACE product suggested involvement of the *HIPK1* gene. Fusion gene-specific RT-PCR experiments with primers located in exons 5 and exons 9/10 of *PAX5* and *HIPK1*, respectively, confirmed the RACE data (Figure 2Cii). Amplification of the fusion transcript with primers located in exons 1 and 5 of *PAX5* and at the junction of the last coding exons 15/16 of *HIPK1* showed that *PAX5* exons 1-5 were consistently present, but *HIPK1* C-terminal exons were alternatively spliced and, thus, several variants are expressed (data not shown). Reciprocal *HIPK1-PAX5* transcripts could not be detected.

The putative *PAX5-HIPK1* chimeric protein encoded by the notional full length transcript consists of the PD and the octapeptide domain of *PAX5* fused to a part of the homeodomain-interacting domain (ID), the Prolin-, Glutamic acid-, Serine-, Threonine-rich (PEST), and the tyrosine/histidine-rich (YH) domains of *HIPK1* (Figure 4E).

### Identification of *PAX5* fusion partners in cases with *PAX5* 3' deletions

In three out of the 446 childhood ALL patients FISH analysis with *PAX5*-specific cosmid clones displayed 3' deletions of *PAX5* also indicating the presence of *PAX5* rearrangements. In this respect, the dic(9;12)/*PAX5-ETV6* aberration results in loss of the *PAX5* 3'-end,<sup>11</sup> and the *PAX5* fusion partners *FOXP1*, *ZNF521*, *AUTS2*, and *C20orf112* were detected based on array CGH data that only permit the delineation of unbalanced genetic alterations.<sup>9,14</sup>

In case 8, fusion gene-specific FISH and RT-PCR assays for the known *PAX5* rearrangements revealed that in this case *PAX5* was fused to *C20orf112*<sup>14</sup> (Figure 2D). Sequence analysis of the *PAX5-C20orf112* transcripts showed an in-frame fusion of *PAX5*



exon 8 to *C20orf112* exon 12. Amplification of the full length coding chimeric transcript showed no alternative splicing of any of the exons (data not shown). At least in this case, the PAX5-C20orf112 fusion displays the most 3' breakpoint within PAX5 described so far, which joins almost the entire PAX5 protein including the PD, the octapeptide, the homeodomain (HD) and parts of the transactivation domain (TA) to the C-terminal end of C20orf112. Owing to the opposite transcriptional orientations of *PAX5* (centromere-telomere) and *C20orf112* (telomere-centromere), the generation of a functional fusion gene requires a complex genetic rearrangement or the formation of a dicentric chromosome.

In case 10, interphase FISH analysis showed deletion of the PAX5 3'-end (Figure 2Ei) and direct sequencing of one of several 3' RACE PCR products revealed an in-frame fusion of *PAX5* exon 5 to *DACH1* exon 5 (Figure 2Eii). Subsequent RT-PCR experiments using a forward primer located in exon 5 of *PAX5* and a set of reverse primers in exons 5, 8, 9, and 12 of *DACH1* showed the formerly described alternative splicing of *DACH1* skipping exons 4, 5, 6, or 7 or a combination thereof.<sup>17</sup> Fusion of *PAX5* to a *DACH1* isoform that was only detected in spleen could not be verified. Sequencing of RT-PCR products amplified with primers located in the first and last coding exon of the respective genes consistently showed the presence of *PAX5* exons 1-5 and confirmed splicing of *DACH1* (Figure 3C). Also in this case the centromere-telomere orientation of *PAX5* and the opposite telomere-centromere transcriptional direction of *DACH1* suggested a more complex rearrangement rather than a simple reciprocal translocation. The PAX5-DACH1 putative consensus fusion protein consisted of the PD and the octapeptide domain and the C-terminal conserved DD2 domain of DACH1 (Figure 4F).

## Discussion

Using a FISH approach for the detection of *PAX5* rearrangements, we performed a population-based screening of 446 consecutive childhood ALL cases and identified 10 (2.6%) BCP-ALL patients with a *PAX5* rearrangement. All *PAX5* fusion positive cases were negative for the most common genetic aberrations found in childhood ALL (*ETV6-RUNX1*, *BCR-ABL1*, *TCF3-PBX1*, *MLL-AF4*) and, thus, in contrast to *PAX5* deletions, they are most likely distinctive primary genetic events.

*PAX5* rearrangements were particularly associated with a common ALL phenotype. Except for the *PAX5-POM121* positive case, all patients showed a good response to prednisone according to the ALL-BFM 2000 or Interfant-99<sup>15</sup> protocol. Based on prednisone response and MRD risk stratification, all patients were treated with the respective therapy regimen and 9/10 patients are in first complete remission 6-84 months from diagnosis. Only one of the two *PAX5-JAK2* positive patients with a pre-B phenotype relapsed 2.5 years after initial diagnosis

but after recommencing therapy has achieved a second complete remission (Supplementary Table 2).

So far, the majority of *PAX5* rearrangements was detected by high-resolution single nucleotide polymorphism (SNP) array analysis,<sup>9,14</sup> a technology which, however, only allows for the detection of unbalanced aberrations and precludes the identification of balanced reciprocal translocations or inversions. Therefore, we took an alternative approach and developed a FISH screening assay that permits the unambiguous detection of all *PAX5* rearrangements independent of their balanced or unbalanced nature, including even those that would result in juxtaposition of *PAX5* under the regulatory elements of a partner gene as seen in the *PAX5-IGH@* translocation.<sup>7,8</sup> It is interesting to note that for the most *PAX5* rearrangements were found in cases with either normal or complex karyotypes, a fact that prevents detection by conventional cytogenetics and emphasizes their often cryptic nature. Further, at least in childhood ALL, we did not find any evidence for *PAX5* activating translocations.

Two of the ten *PAX5*-rearranged cases have been previously reported to harbor a *PAX5-ETV6*<sup>11</sup> and a *PAX5-PML*<sup>13</sup> aberration, and one showed the recently described *PAX5-C20orf112* fusion.<sup>14</sup> However, we identified five hitherto unknown *PAX5* fusion partners, namely *HIPK1*, *POM121*, *JAK2*, *DACH1*, and *BRD1* bringing the number of distinct *PAX5* chimera to at least twelve (Table 2). Similar to all previously described *PAX5* rearrangements, the majority of the fusion transcripts encode putative novel transcription factors, which consist of at least the amino-terminal paired DNA-binding domain and in most instances also the octapeptide of *PAX5*, and C-terminal regulatory sequences of a second transcription factor. However, involvement of *ELN* and *POM121* as structural proteins and the tyrosine kinase *JAK2* are remarkable as neither of these genes is directly implicated in transcriptional regulation.

The Janus kinase (JAK) family currently comprises four human members *JAK1*, *JAK2*, *JAK3*, and *TYK2*, which are receptor associated protein tyrosine kinases and are of critical importance for cytokine-mediated signal transduction.<sup>18,19</sup> Somatically acquired activating mutations in *JAK2* were recently reported to play a central role in the pathogenesis of myeloproliferative disorders.<sup>20</sup> Further, *JAK2* fusions with *ETV6*, *BCR*, *PCM1*, and *SSBP2* were described in a variety of hematopoietic malignancies.<sup>21,22</sup> The transforming potential of the previously described *JAK2* fusion proteins has been attributed to the cytokine-independent constitutive activation of *JAK2*, mediated by motifs of the partner gene that serve as dimerization/oligomerization interfaces.<sup>21</sup> For example, for the three distinct *ETV6-JAK2* fusions, which are potent activators of *STAT5*, transformation is strictly dependent on the *ETV6* pointed (PNT) self-association domain.<sup>23</sup> However, there is no evidence that the *PAX5* domains retained in the *PAX5-JAK2* protein are capable to mediate dimerization. In

contrast, both the DNA-binding domain and the nuclear localization signal (NLS) of PAX5<sup>24</sup> are retained in the PAX5-JAK2 fusion protein, which is suggestive of a nuclear localization, whereas JAK2-PAX5 may reside in the cytoplasm.

BRD1, BRPF1, MLLT6, and MLLT10 belong to a small evolutionary conserved family of putative nuclear transcription factors, which share a highly homologous cystein-rich region containing an amino-terminal PHD finger motif.<sup>25</sup> Two members of this family are involved in myeloid leukemia-associated rearrangements, namely *MLL-MLLT6* and *MLL-MLLT10*.<sup>26,27</sup> However, the respective chimeric proteins differ considerably from PAX5-BRD1 in that the conserved PHD domains of MLLT6 and MLLT10 are lost, whereas the entire BRD1 protein is fused to PAX5. Even though the actual function of BRD1 itself remains elusive, the presence of a PHD-bromodomain module, which is frequently found in chromatin-associated proteins, strongly indicates a role in chromatin remodelling and epigenetic regulation of gene transcription.<sup>28,29</sup> Considering that PAX5 has the capability to activate and suppress large sets of genes, this potential feature of BRD1 supports the notion of the PAX5-BRD1 chimera to modulate transcriptional activity.

HIPK1 belongs to the homeodomain-interacting protein kinase (HIPK) family, whose currently four members (HIPK1-4) are nuclear serine/threonine kinases that are primarily localized in the nucleus.<sup>30,31</sup> The HIPKs were originally identified as nuclear protein kinases that function as corepressors for various homeodomain-containing transcription factors but recently were also shown to interact with other proteins involved in apoptosis and signal transduction in a cellular localization-dependent manner. HIPK1 physically interacts with and promotes phosphorylation of e.g. TP53, DAXX, EP300, and RUNX1.<sup>32-34</sup> HIPK1 also regulates the nuclear export of DAXX and both proteins collaborate in transcriptional regulation,<sup>33</sup> a functional aspect of HIPK1, which is further substantiated by its modulation of TP53 activity.<sup>34</sup> On the other hand, in the cytoplasm HIPKs appear to transduce signals by death receptors and to induce MAP3K5 dependent apoptosis.<sup>35,36</sup> Owing to the multiple functions of HIPK1 it is intricate to ascribe any potential specific function to the PAX5-HIPK1 fusion protein, however, the most likely one is also transcriptional regulation.

*DACH1* is a human homologue of the *Drosophila dachshund (dac)* gene, which is a key regulator of cell fate determination during eye, leg, and brain development in the fly.<sup>37-39</sup> Members of the dachshund family of nuclear proteins encode highly conserved putative transcription factors, which contribute to the fundamental mechanisms of morphogenesis.<sup>40,41</sup> The DACH1 protein contains two domains (DD1, Dachbox N-domain and DD2, Dachbox C-domain or EYA domain), which are highly conserved from *Drosophila* to human.<sup>41</sup> DACH1 functions as a transcriptional repressor of TGF- $\beta$ -signaling in breast and ovarian cancer.<sup>42,43</sup> DACH1 is also a physiological regulator of endogenous *JUN* function, inhibiting *JUN* and *JUN* target gene expression, as well as a *CCND1* repressor.<sup>44</sup> Although target gene

repression by DACH1 requires the DD1 domain it is tempting to speculate that the PAX5-DACH1 chimeric protein, in spite of the fact that it lacks this conserved domain, may act as transcriptional repressor of *PAX5* activated target genes.

*PAX5* fusion partners, however, not only comprise transcription factors but also structural proteins such as ELN<sup>12</sup> and POM121. POM121 is one of the two integral pore membrane proteins that were identified as specific components of nuclear pore complexes of higher eukaryotes.<sup>45</sup> Both pore membrane proteins, NUP210<sup>46</sup> and POM121<sup>45</sup> have been proposed, although controversially discussed, to play important roles in nuclear pore complex (NPC) formation and anchoring the peripheral nucleoporins (NUPs) to the nuclear membrane.<sup>47,48</sup> The NPC is composed of multiple copies of about 30 different NUPs,<sup>49</sup> and so far, only two NUPs, namely NUP98<sup>50,51</sup> and NUP214,<sup>52-54</sup> were found involved in leukemia-associated translocations, which makes POM121 only the third component of the nuclear envelope implicated in leukemogenesis.

All *PAX5* fusion proteins contain the *PAX5* DNA-binding domain and, thus, are predicted to retain the ability to bind to *PAX5* transcriptional targets, but no longer provide normal transcriptional regulatory functions.<sup>55</sup> *PAX5-ETV6*, *PAX5-FOXP1*, and also *PAX5-ELN* indeed competitively inhibit the transcriptional activity of *PAX5* suggesting that *PAX5* fusions act as constitutive repressors to antagonize *PAX5* function provided by the second, wild-type *PAX5* allele.<sup>9,12,56</sup> Comprehensive studies are now required to elucidate whether all *PAX5* chimera in fact operate as aberrant transcription factors that impair the finely tuned *PAX5* target gene transcriptional network.

### *Acknowledgements*

This work was supported by a grant of the Austrian Ministry of Science and Research (GEN-AU II, GZ 200.136/1-VI/1/2005) (to S.S.) and the St. Anna Kinderkrebsforschung. We thank Meinrad Busslinger (IMP, Vienna, Austria) for kindly providing the *PAX5* cosmid probes and Tilman Johannes (MetaSystems, Altlußheim, Germany) for assistance with the Metafer4-Metacyte system. We would also like to thank all those people, who perform the routine diagnostic work-up and consistently provide the basis for our research. Further, we are indebted to Dasa Janousek for the efficient clinical data management and analysis.

## References

1. Busslinger M. Transcriptional control of early B cell development. *Annu Rev Immunol* 2004; **22**: 55-79.
2. Mikkola I, Heavey B, Horcher M, Busslinger M. Reversion of B cell commitment upon loss of Pax5 expression. *Science* 2002; **297**: 110-113.
3. Nutt SL, Eberhard D, Horcher M, Rolink AG, Busslinger M. Pax5 determines the identity of B cells from the beginning to the end of B-lymphopoiesis. *Int Rev Immunol* 2001; **20**: 65-82.
4. Nutt SL, Heavey B, Rolink AG, Busslinger M. Commitment to the B-lymphoid lineage depends on the transcription factor Pax5. *Nature* 1999; **401**: 556-562.
5. Delogu A, Schebesta A, Sun Q, Aschenbrenner K, Perlot T, Busslinger M. Gene repression by Pax5 in B cells is essential for blood cell homeostasis and is reversed in plasma cells. *Immunity* 2006; **24**: 269-281.
6. Schebesta M, Heavey B, Busslinger M. Transcriptional control of B-cell development. *Curr Opin Immunol* 2002; **14**: 216-223.
7. Busslinger M, Klix N, Pfeffer P, Graninger PG, Kozmik Z. Deregulation of PAX-5 by translocation of the Emu enhancer of the IgH locus adjacent to two alternative PAX-5 promoters in a diffuse large-cell lymphoma. *Proc Natl Acad Sci USA* 1996; **93**: 6129-6134.
8. Iida S, Rao PH, Nallasivam P, Hibshoosh H, Butler M, Louie DC *et al.* The t(9;14)(p13;q32) chromosomal translocation associated with lymphoplasmacytoid lymphoma involves the PAX-5 gene. *Blood* 1996; **88**: 4110-4117.
9. Mullighan CG, Goorha S, Radtke I, Miller CB, Coustan-Smith E, Dalton JD *et al.* Genome-wide analysis of genetic alterations in acute lymphoblastic leukaemia. *Nature* 2007; **446**: 758-764.
10. Cazzaniga G, Daniotti M, Tosi S, Giudici G, Aloisi A, Pogliani E *et al.* The paired box domain gene PAX5 is fused to ETV6/TEL in an acute lymphoblastic leukemia case. *Cancer Res* 2001; **61**: 4666-4670.
11. Strehl S, Konig M, Dworzak MN, Kalwak K, Haas OA. PAX5/ETV6 fusion defines cytogenetic entity dic(9;12)(p13;p13). *Leukemia* 2003; **17**: 1121-1123.
12. Bousquet M, Broccardo C, Quelen C, Meggetto F, Kuhlein E, Delsol G *et al.* A novel PAX5-ELN fusion protein identified in B-cell acute lymphoblastic leukemia acts as a dominant negative on wild-type PAX5. *Blood* 2007; **109**: 3417-3423.
13. Nebral K, Konig M, Harder L, Siebert R, Haas OA, Strehl S. Identification of PML as novel PAX5 fusion partner in childhood acute lymphoblastic leukaemia. *Br J Haematol* 2007; **139**: 269-274.
14. Kawamata N, Ogawa S, Zimmermann M, Sanada M, Hemminki K, Yamamoto G *et al.* Rearrangement and Deletion of the PAX5 Gene in Pediatric Acute B-Cell Lineage Lymphoblastic Leukemia. *ASH Annual Meeting Abstracts* 2007; **110**: 981.
15. Pieters R, Schrappe M, De Lorenzo P, Hann I, De Rossi G, Felice M *et al.* A treatment protocol for infants younger than 1 year with acute lymphoblastic leukaemia (Interfant-99): an observational study and a multicentre randomised trial. *Lancet* 2007; **370**: 240-250.
16. Konig M, Reichel M, Marschalek R, Haas OA, Strehl S. A highly specific and sensitive fluorescence in situ hybridization assay for the detection of t(4;11)(q21;q23) and concurrent submicroscopic deletions in acute leukaemias. *Br J Haematol* 2002; **116**: 758-764.
17. Ayres JA, Shum L, Akarsu AN, Dashner R, Takahashi K, Ikura T *et al.* DACH: genomic characterization, evaluation as a candidate for postaxial polydactyly type A2, and developmental expression pattern of the mouse homologue. *Genomics* 2001; **77**: 18-26.
18. Baker SJ, Rane SG, Reddy EP. Hematopoietic cytokine receptor signaling. *Oncogene* 2007; **26**: 6724-6737.
19. Murray PJ. The JAK-STAT signaling pathway: input and output integration. *J Immunol* 2007; **178**: 2623-2629.
20. Levine RL, Pardananani A, Tefferi A, Gilliland DG. Role of JAK2 in the pathogenesis and therapy of myeloproliferative disorders. *Nat Rev Cancer* 2007; **7**: 673-683.

21. Ihle JN, Gilliland DG. Jak2: normal function and role in hematopoietic disorders. *Curr Opin Genet Dev* 2007; **17**: 8-14.
22. Poitras JL, Cin PD, Aster JC, Deangelo DJ, Morton CC. Novel SSBP2-JAK2 fusion gene resulting from a t(5;9)(q14.1;p24.1) in pre-B acute lymphocytic leukemia. *Genes Chromosomes Cancer* 2008; **47**: 884-889.
23. Schwaller J, Frantsve J, Aster J, Williams IR, Tomasson MH, Ross TS *et al.* Transformation of hematopoietic cell lines to growth-factor independence and induction of a fatal myelo- and lymphoproliferative disease in mice by retrovirally transduced TEL/JAK2 fusion genes. *Embo J* 1998; **17**: 5321-5333.
24. Kovac CR, Emelyanov A, Singh M, Ashouian N, Birshtein BK. BSAP (Pax5)-importin alpha 1 (Rch1) interaction identifies a nuclear localization sequence. *J Biol Chem* 2000; **275**: 16752-16757.
25. McCullagh P, Chaplin T, Meerabux J, Grenzeliass D, Lillington D, Poulson R *et al.* The cloning, mapping and expression of a novel gene, BRL, related to the AF10 leukaemia gene. *Oncogene* 1999; **18**: 7442-7452.
26. Chaplin T, Bernard O, Beverloo HB, Saha V, Hagemeijer A, Berger R *et al.* The t(10;11) translocation in acute myeloid leukemia (M5) consistently fuses the leucine zipper motif of AF10 onto the HRX gene. *Blood* 1995; **86**: 2073-2076.
27. Prasad R, Leshkowitz D, Gu Y, Alder H, Nakamura T, Saito H *et al.* Leucine-zipper dimerization motif encoded by the AF17 gene fused to ALL-1 (MLL) in acute leukemia. *Proc Natl Acad Sci U S A* 1994; **91**: 8107-8111.
28. Ruthenburg AJ, Li H, Patel DJ, Allis CD. Multivalent engagement of chromatin modifications by linked binding modules. *Nat Rev Mol Cell Biol* 2007; **8**: 983-994.
29. Taverna SD, Li H, Ruthenburg AJ, Allis CD, Patel DJ. How chromatin-binding modules interpret histone modifications: lessons from professional pocket pickers. *Nat Struct Mol Biol* 2007; **14**: 1025-1040.
30. Arai S, Matsushita A, Du K, Yagi K, Okazaki Y, Kurokawa R. Novel homeodomain-interacting protein kinase family member, HIPK4, phosphorylates human p53 at serine 9. *FEBS Lett* 2007; **581**: 5649-5657.
31. Kim YH, Choi CY, Lee SJ, Conti MA, Kim Y. Homeodomain-interacting protein kinases, a novel family of co-repressors for homeodomain transcription factors. *J Biol Chem* 1998; **273**: 25875-25879.
32. Aikawa Y, Nguyen LA, Isono K, Takakura N, Tagata Y, Schmitz ML *et al.* Roles of HIPK1 and HIPK2 in AML1- and p300-dependent transcription, hematopoiesis and blood vessel formation. *Embo J* 2006; **25**: 3955-3965.
33. Ecsedy JA, Michaelson JS, Leder P. Homeodomain-interacting protein kinase 1 modulates Daxx localization, phosphorylation, and transcriptional activity. *Mol Cell Biol* 2003; **23**: 950-960.
34. Kondo S, Lu Y, Debbas M, Lin AW, Sarosi I, Itie A *et al.* Characterization of cells and gene-targeted mice deficient for the p53-binding kinase homeodomain-interacting protein kinase 1 (HIPK1). *Proc Natl Acad Sci U S A* 2003; **100**: 5431-5436.
35. Li X, Zhang R, Luo D, Park SJ, Wang Q, Kim Y *et al.* Tumor necrosis factor alpha-induced desumoylation and cytoplasmic translocation of homeodomain-interacting protein kinase 1 are critical for apoptosis signal-regulating kinase 1-JNK/p38 activation. *J Biol Chem* 2005; **280**: 15061-15070.
36. Rochat-Steiner V, Becker K, Micheau O, Schneider P, Burns K, Tschopp J. FIST/HIPK3: a Fas/FADD-interacting serine/threonine kinase that induces FADD phosphorylation and inhibits fas-mediated Jun NH(2)-terminal kinase activation. *J Exp Med* 2000; **192**: 1165-1174.
37. Chen R, Amoui M, Zhang Z, Mardon G. Dachshund and eyes absent proteins form a complex and function synergistically to induce ectopic eye development in *Drosophila*. *Cell* 1997; **91**: 893-903.
38. Davis RJ, Shen W, Heanue TA, Mardon G. Mouse Dach, a homologue of *Drosophila* dachshund, is expressed in the developing retina, brain and limbs. *Dev Genes Evol* 1999; **209**: 526-536.
39. Kozmik Z, Pfeiffer P, Kralova J, Paces J, Paces V, Kalousova A *et al.* Molecular cloning and expression of the human and mouse homologues of the *Drosophila* dachshund gene. *Dev Genes Evol* 1999; **209**: 537-545.

40. Wawersik S, Maas RL. Vertebrate eye development as modeled in *Drosophila*. *Hum Mol Genet* 2000; **9**: 917-925.
41. Hanson IM. Mammalian homologues of the *Drosophila* eye specification genes. *Semin Cell Dev Biol* 2001; **12**: 475-484.
42. Sunde JS, Donninger H, Wu K, Johnson ME, Pestell RG, Rose GS *et al*. Expression profiling identifies altered expression of genes that contribute to the inhibition of transforming growth factor-beta signaling in ovarian cancer. *Cancer Res* 2006; **66**: 8404-8412.
43. Wu K, Yang Y, Wang C, Davoli MA, D'Amico M, Li A *et al*. DACH1 inhibits transforming growth factor-beta signaling through binding Smad4. *J Biol Chem* 2003; **278**: 51673-51684.
44. Wu K, Liu M, Li A, Donninger H, Rao M, Jiao X *et al*. Cell fate determination factor DACH1 inhibits c-Jun-induced contact-independent growth. *Mol Biol Cell* 2007; **18**: 755-767.
45. Hallberg E, Wozniak RW, Blobel G. An integral membrane protein of the pore membrane domain of the nuclear envelope contains a nucleoporin-like region. *J Cell Biol* 1993; **122**: 513-521.
46. Gerace L, Ottaviano Y, Kondor-Koch C. Identification of a major polypeptide of the nuclear pore complex. *J Cell Biol* 1982; **95**: 826-837.
47. Antonin W, Franz C, Haselmann U, Antony C, Mattaj JW. The integral membrane nucleoporin pom121 functionally links nuclear pore complex assembly and nuclear envelope formation. *Mol Cell* 2005; **17**: 83-92.
48. Stavru F, Nautrup-Pedersen G, Cordes VC, Gorlich D. Nuclear pore complex assembly and maintenance in POM121- and gp210-deficient cells. *J Cell Biol* 2006; **173**: 477-483.
49. Lusk CP, Blobel G, King MC. Highway to the inner nuclear membrane: rules for the road. *Nat Rev Mol Cell Biol* 2007; **8**: 414-420.
50. Romana SP, Radford-Weiss I, Ben Abdelali R, Schluth C, Petit A, Dastugue N *et al*. NUP98 rearrangements in hematopoietic malignancies: a study of the Groupe Francophone de Cytogenetique Hematologique. *Leukemia* 2006; **20**: 696-706.
51. Slape C, Aplan PD. The role of NUP98 gene fusions in hematologic malignancy. *Leuk Lymphoma* 2004; **45**: 1341-1350.
52. Graux C, Cools J, Melotte C, Quentmeier H, Ferrando A, Levine R *et al*. Fusion of NUP214 to ABL1 on amplified episomes in T-cell acute lymphoblastic leukemia. *Nat Genet* 2004; **36**: 1084-1089.
53. Soekarman D, von Lindern M, Daenen S, de Jong B, Fonatsch C, Heinze B *et al*. The translocation (6;9) (p23;q34) shows consistent rearrangement of two genes and defines a myeloproliferative disorder with specific clinical features. *Blood* 1992; **79**: 2990-2997.
54. von Lindern M, Breems D, van Baal S, Adriaansen H, Grosveld G. Characterization of the translocation breakpoint sequences of two DEK-CAN fusion genes present in t(6;9) acute myeloid leukemia and a SET-CAN fusion gene found in a case of acute undifferentiated leukemia. *Genes Chromosomes Cancer* 1992; **5**: 227-234.
55. Cobaleda C, Schebesta A, Delogu A, Busslinger M. Pax5: the guardian of B cell identity and function. *Nat Immunol* 2007; **8**: 463-470.
56. Fazio G, Palmi C, Rolink A, Biondi A, Cazzaniga G. PAX5/TEL acts as a transcriptional repressor causing down-modulation of CD19, enhances migration to CXCL12, and confers survival advantage in pre-B1 cells. *Cancer Res* 2008; **68**: 181-189.

**Table 1. Summary of all *PAX5*-rearranged childhood ALL cases registered in the Austrian ALL-BFM 2000 and Interfant-99 studies between June 1999 and December 2007.**

<b>Case</b>	<b><i>PAX5</i> FISH pattern</b>	<b>% positive cells</b>	<b><i>PAX5</i> fusion</b>	<b>Reference</b>
1	split	49,1	<i>PAX5-PML</i>	Nebral et al <sup>13</sup>
2	split	20,8	<i>PAX5-JAK2</i>	this work
3	split	30,0	<i>PAX5-BRD1</i>	this work
4	split	19,3	<i>PAX5-JAK2</i>	this work
5	split	59,7	<i>PAX5-POM121</i>	this work
6	split	45,8	<i>PAX5-?</i>	this work
7	split	61,7	<i>PAX5-HIPK1</i>	this work
8	3' deletion	85,0	<i>PAX5-C20orf112</i>	this work
9	3' deletion	ND	<i>PAX5-ETV6</i>	Strehl et al <sup>11</sup>
10	3' deletion	78,2	<i>PAX5-DACH1</i>	this work

ND, not determined



**Table 2. PAX5 fusion partners in B-cell precursor ALL.**

Partner gene	Chr.	Localization/Function	Reference
HIPK1 homeodomain interacting protein kinase 1	1p13	nuclear (speckles) transcriptional regulation	this work
FOXP1 forkhead box P1	3p13	nuclear transcription factor	Mullighan et al <sup>9</sup>
POM121 POM121 membrane glycoprotein	7q11	nuclear pore membrane assembly of nuclear envelope	this work
ELN elastin	7q11	extracellular matrix, elastic fibers structural protein	Bousquet et al <sup>12</sup>
AUTS2 autism susceptibility candidate 2	7q11	intracellular unknown	Kawamata et al <sup>14</sup>
JAK2 Janus kinase 2	9p24	cytoplasmic tyrosine kinase, receptor signaling	this work
ETV6 ets variant gene 6 (TEL oncogene)	12p13	nuclear transcriptional repressor	Cazzaniga et al <sup>10</sup> Strehl et al <sup>11</sup>
DACH1 dachshund homolog 1	13q24	nuclear transcription factor	this work
PML promyelocytic leukemia	15q21	nuclear, PML bodies multiple functions	Nebral et al <sup>13</sup>
ZNF521 zinc finger protein 521	18q11	nuclear transcription factor	Mullighan et al <sup>9</sup>
C20orf112 chromosome 20 open reading frame 112	20q11	unknown unknown	Kawamata et al <sup>14</sup>
BRD1 bromodomain containing 1	22q13	nuclear putative transcription factor	this work

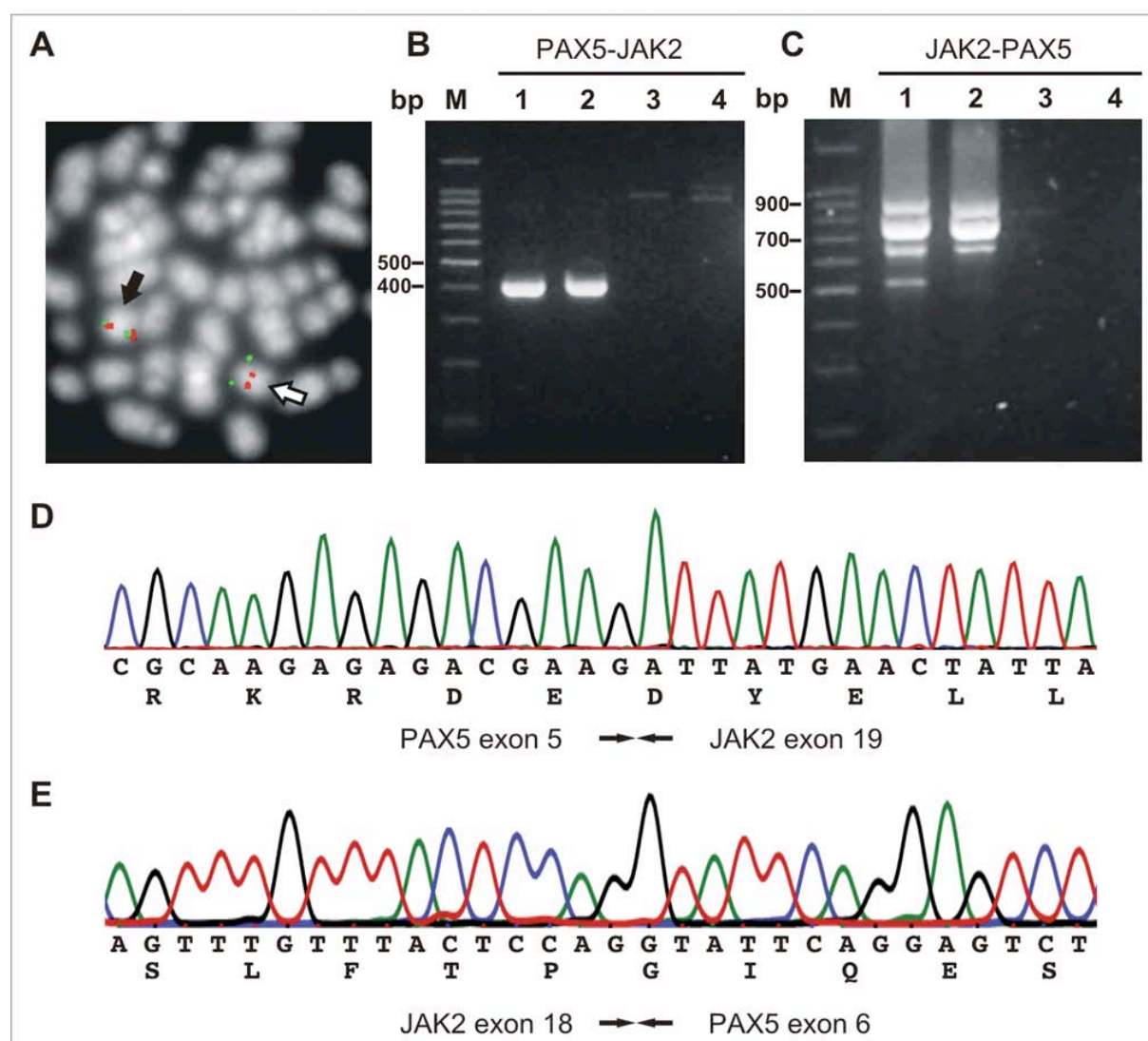


**Figure 1. *PAX5-JAK2* rearrangement.** (A) FISH with BAC clones RP11-220I1 (CY3) and RP11-12P15 (FITC) showing a split signal. Arrows indicate the normal chromosome 9 (black) and the derivative chromosome 9 (white). (B) RT-PCR analysis of the *PAX5-JAK2* fusion transcript. Lane 1, patient 4; lane 2, patient 2; lane 3, patient 6; lane 4, normal control. Case 6 was negative for the *PAX5-JAK2* fusion. (C) RT-PCR analysis of the *JAK2-PAX5* transcript showing multiple splice variants. Lane 1, patient 4; lane 2, patient 2; lane 3, normal control; lane 4, negative control. (D-E) Sequence chromatograms of *PAX5-JAK2* and *JAK2-PAX5* transcripts. (D) fusion of *PAX5* exon 5 to *JAK2* exon 19 and (E) *JAK2* exon 18 to *PAX5* exon 6. M, molecular weight marker, 100 bp ladder (Promega).

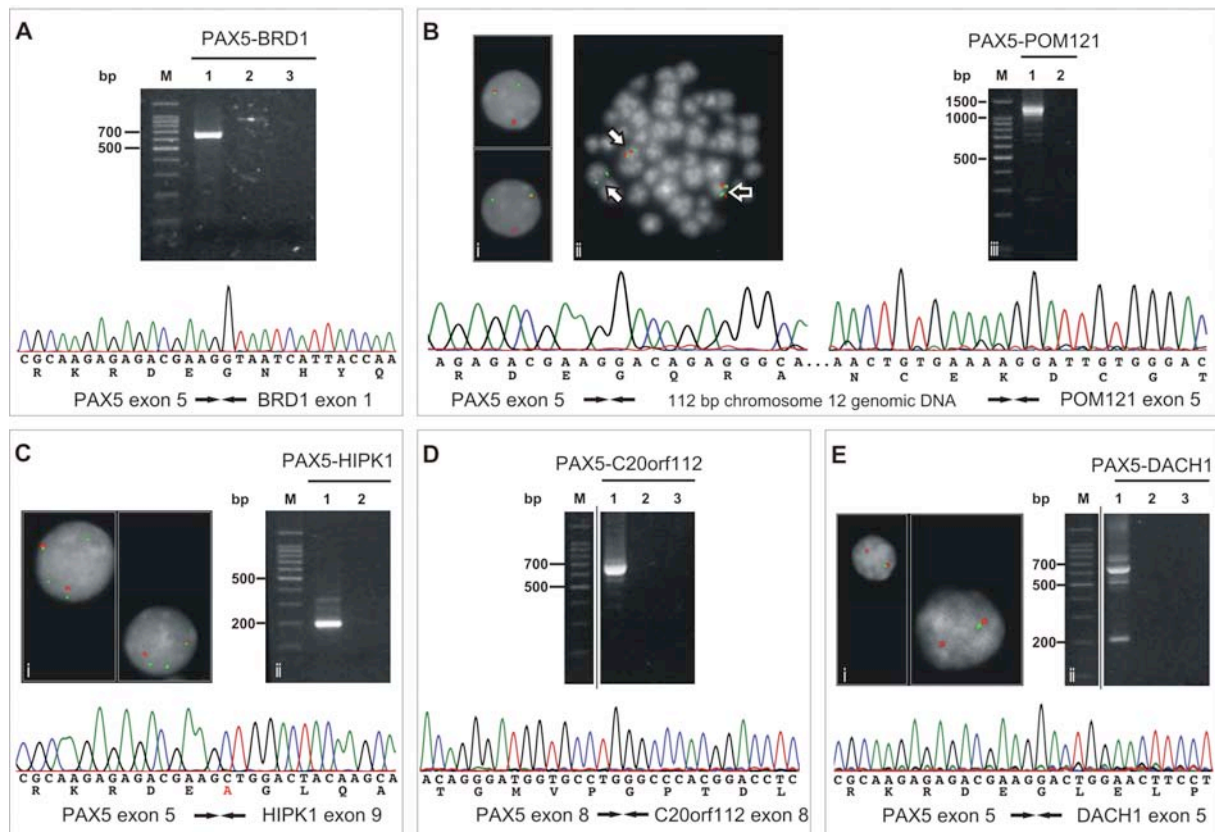


**Figure 2. FISH, RT-PCR, RACE, and sequence analyses of *PAX5*-rearranged patients.** (A) Case 3. RT-PCR and sequence analysis showing fusion of *PAX5* exon 5 to *BRD1* exon 1. Lane 1, patient 3; lane 2, normal control; lane 3, negative control. (B) Case 5. (Bi) Representative interphase nuclei displaying a *PAX5* split signal using RP11-22011 (CY3) and RP11-12P15 (FITC); (Bii) metaphase showing a *PAX5* split signal using RP11-465P6 (FITC) and RP11-84P7 located downstream of *PAX5* (CY3). Arrows indicate the normal chromosome 9 (black) and the derivative chromosomes (white). (Biii) RT-PCR showing the *PAX5-POM121* fusion transcript. Lane 1, patient 5; lane 2, negative control. Sequence chromatograms presenting fusion of *PAX5* exon 5 to 112 bp derived from chromosome 12 followed by *POM121* exon 5. (C) Case 7. (Ci) Representative aberrant interphase nuclei hybridized with RP11-22011 (CY3) and RP11-12P15 (FITC). (Cii) RT-PCR of *PAX5-HIPK1*. Lane 1, patient 7; lane 2, negative control, and sequence chromatogram showing fusion of *PAX5* exon 5 to *HIPK1* exon 9. (D) Case 8. RT-PCR and sequence chromatograms demonstrating fusion of *PAX5* exon 8 to *C20orf112* exon 8. Lane 1, patient 3; lane 2, normal control; lane 3, negative control. (E) Case 10. (Ei) Representative interphase nuclei hybridized with RP11-22011 (CY3) and RP11-12P15 (FITC) displaying a *PAX5* 3'-end deletion and (Eii) RT-PCR showing *PAX5-DACH1* transcripts. Lane 1, patient 10; lane 2, normal control; lane 3, negative control, and sequence chromatogram presenting fusion of *PAX5* exon 5 to *DACH1* exon 5. M, molecular weight marker, 100 bp ladder (Promega).

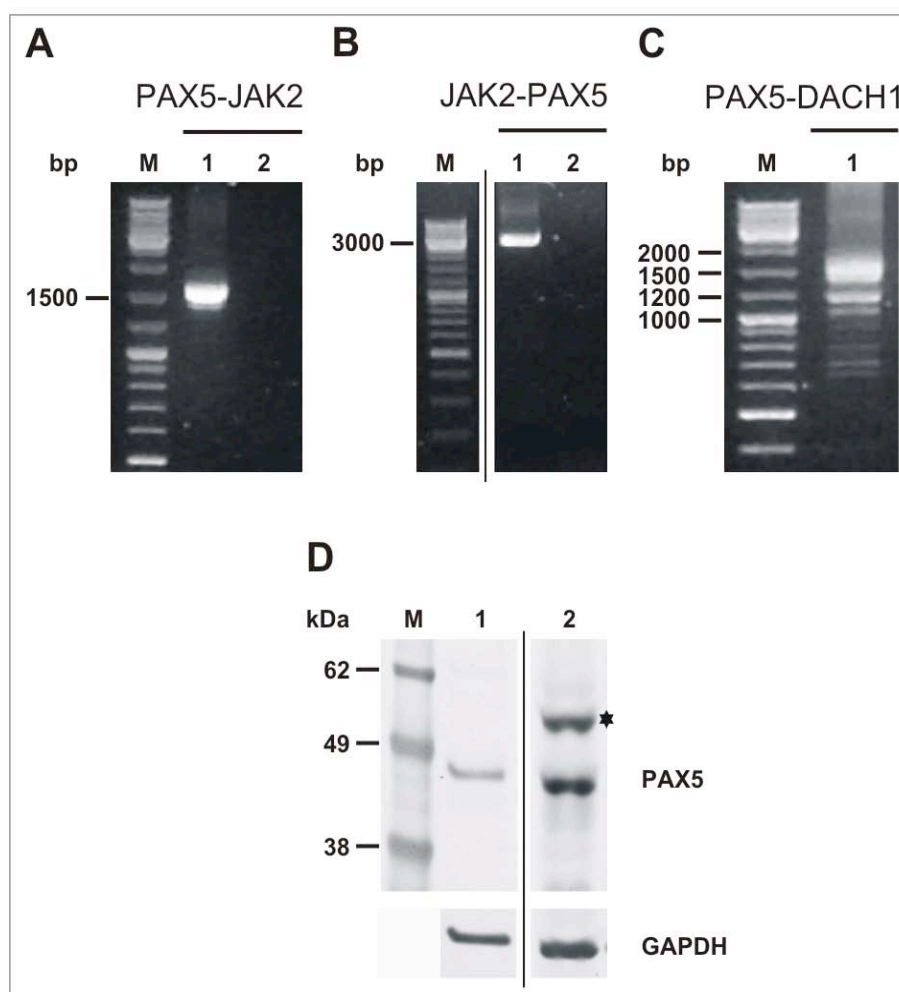


**Figure 3. Amplification of full length fusion transcripts and Western blot analysis.**

**(A-C)** Amplification of full length chimeric transcripts. **(A)** *PAX5-JAK2* and **(B)** reciprocal *JAK2-PAX5* transcripts of case 4. Lane 1, patient; lane 2, negative control. (Owing to the small size differences of the splice variants these are not distinguishable from the full length transcript.) **(C)** Case 10. *PAX5-DACH1* full length fusion transcript and several splice variants are expressed. M, peqGOLD Ladder-Mix (Peqlab Biotechnology). **(D)** Western blot of primary leukemic blasts of case 4 using an anti-N-terminal PAX5 antibody. Lane 1, KIS-1 cell line; lane 2, *PAX5-JAK2* positive case. Asterisk indicates the mutant *PAX5-JAK2* fusion protein. GAPDH served as loading control. M, SeeBlue® Plus2 Pre-Stained Standard (Invitrogen), sizes in kDa are indicated.

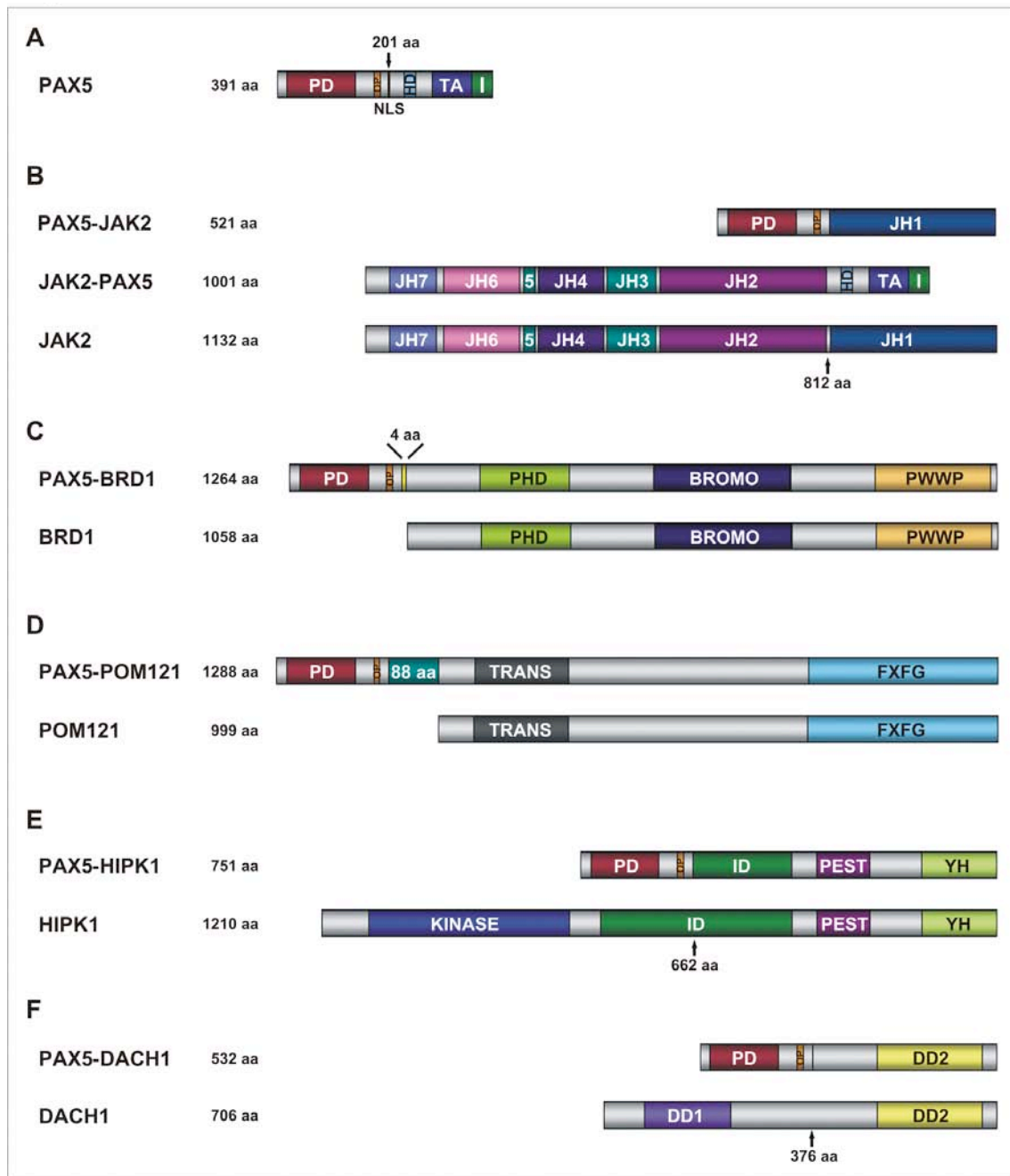


**Figure 4. Schematic representation of PAX5, partner wild-type and the putative chimeric PAX5 fusion proteins.**

Wild-type proteins are always depicted below the PAX5 chimera. **(A)** PAX5 wild-type protein. PD, paired domain; OP, octapeptide domain; HD, homeodomain; TA, transactivation domain; I, inhibitory domain; NLS, nuclear localization signal. **(B)** PAX5-JAK2 and the reciprocal full-length JAK2-PAX5 fusion proteins. JH1-7, JAK homology domains 1-7. **(C)** BRD1 wild-type and PAX5-BRD1 fusion protein with the insertion of 4 miscellaneous amino acids. PHD, plant homeodomain zinc finger domain; BROMO, bromodomain; PWWP, proline-tryptophan-tryptophan-proline motif. **(D)** POM121 wild-type and PAX5-POM121 fusion protein, insertion of the 88 novel amino acids encoded by the 112 bp of genomic DNA derived from chromosome 12 and the normally untranslated region of POM121 exon 5 is depicted. TRANS, potential transmembrane domain; FXFG, repetitive XFXFG pentapeptide motif; according to Ensembl POM121-001. **(E)** HIPK1 wild-type and PAX5-HIPK1 fusion protein. KINASE, protein kinase domain; ID, homeodomain-interacting domain; PEST, Prolin-, Glutamic acid-, Serine-, Threonine-rich sequence; YH, tyrosine/histidine-rich motif. **(F)** DACH1 wild-type and PAX5-DACH1 fusion protein. DD1, Dachbox N-domain; DD2, Dachbox C-domain.

**Supplementary Table 1. Oligonucleotide Primer Sequences**

Primer	Sequence	Direction	Gene/Exon
PAX5ex5-F1	TACTCCATCAGCGGCATCC	sense	PAX5/5
PAX5ex6-R2	CTGCTGCTGTGTGAACAAGTC	antisense	PAX5/6
PAX5ex7-R1	GGCCTTCATGTCGTCCAG	antisense	PAX5/7
PAX5ex10non-R1	AGTCCCTGGAGGAAGAGAGG	antisense	PAX5/10
P1-PAX5ex1-F1	ATGGATTTAGAGAAAAATTATCCGACT	sense	PAX5/1
P1-PAX5ex10-R1	TCAGTGACGGTCATAGGCAG	antisense	PAX5/10
JAK2ex3-F1	AAGACTCTGCATGGGAATGG	sense	JAK2/3
JAK2ex20-21-R1	TACGCCGACCAGCACTGTAG	antisense	JAK2/20-21
JAK2-forward	ACGGTCAACTGCATGAAACA	sense	JAK2/13
P1-JAK2ex3-F1	ATGGGAATGGCCTGCC	sense	JAK2/3
P1-JAK2ex25-R1	TCATCCAGCCATGTTATCCC	antisense	JAK2/25
BRD1ex1-R4	TCTCGAAGCGGTCCATCAG	antisense	BRD1/1
POM121ex13-R3	GCAGGCAGGGTAAAGGTAAATG	antisense	POM121/13
POM121-ex3-4-F1	GTCCAGCCCTTCACATCCTC	sense	POM121/3-4
HIPK1ex9-10-R1	CTTCCCTGCGTGAGAACTCC	antisense	HIPK1/9-10
HIPK1ex15-16-R1	TGCTGGTTCTGGCTAAGATTG	antisense	HIPK1/15-16
C20orf112ex8-R1	AGCAGGAAGGCAGCAGACTC	antisense	C20orf112/8
DACH1ex5-R1	GTGGTTCATCTGGCTCATTGC	antisense	DACH1/5
DACH1ex9-R1	GCCAACTGCTTCTCAAGTGTTTC	antisense	DACH1/9
P1-DACH1ex12-R1	TCAGTACATGACAGTAGTTTTCAAATACAG	antisense	DACH1/12

**Detection of Translocations by Reverse Transcription-PCR Analysis**

Fusion transcripts were amplified using the following primer combinations.

PAX5-JAK2: PAX5ex5-F1 and JAK2ex20-21-R1.

JAK2-PAX5: JAK2-forward and PAX5ex6-R2.

PAX5-BRD1: PAX5ex5-F1 and BRD1ex1-R4.

PAX5-POM121: PAX5ex5-F1 and POM121ex13-R3.

POM121-PAX5: POM121ex3-4-F1 and PAX5ex7-R1.

PAX5-HIPK1: PAX5ex5-F1 and HIPK1ex9-10-R1; PAX5ex5-F1 and HIPK1ex15-16-R1.

PAX5-C20orf112: PAX5ex5-F1 and C20orf112ex8-R1.

PAX5-DACH1: PAX5ex5-F1 and DACH1ex5-R1; PAX5ex5-F1 and DACH1ex9-R1.

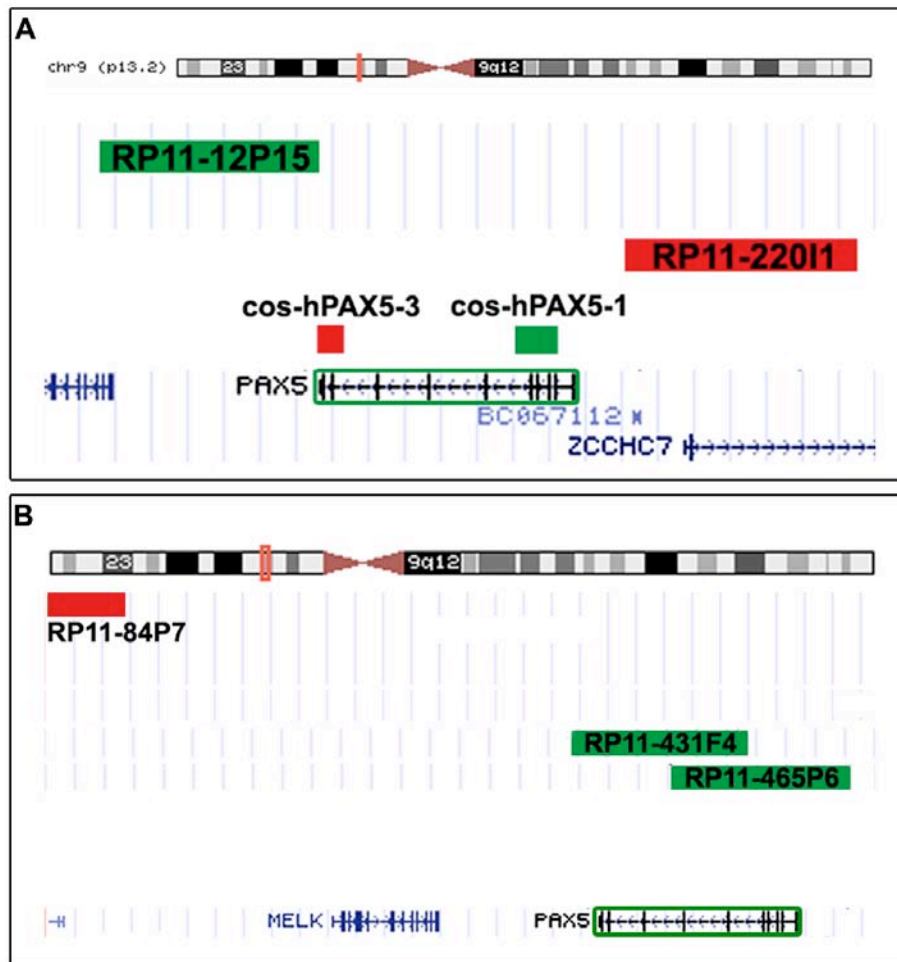
**Detection of full length fusion transcripts by Reverse Transcription-PCR Analysis**

PAX5-DACH1: P1-PAX5ex1-F1 and P1-DACH1ex12-R1

PAX5-JAK2: P1-PAX5ex1-F1 and P1-JAK2ex25-R1

JAK2-PAX5: JAK2ex3-F1 and PAX5ex10non-R1; P1-JAK2ex3-F1 and P1-PAX5ex10-R1  
(nested PCR reaction)

## Supplementary Figure S1.



**(A) PAX5 FISH screening assay.** Adapted screenshot from the UCSC Genome Browser on Human March 2006 Assembly ([www.genome.ucsc.edu](http://www.genome.ucsc.edu)), which displays the localization of the used PAX5 BAC clones RP11-12P15 and RP11-220I1, and the cosmid clones cosh-PAX5-1 and coshPAX5-3.

**(B) FISH clones - PAX5 locus.** Adapted screenshot from the UCSC Genome Browser on Human March 2006 Assembly ([www.genome.ucsc.edu](http://www.genome.ucsc.edu)) showing approximately 800 kb of chromosomal region at 9p13.2. The utilized FISH clones RP11-84P7, RP11-431F4 and RP11-465P6 are depicted.



**Supplementary Table 2.****Clinical and immunophenotypic characteristics of the *PAX5*-rearranged cases.**

Case	Age (yrs)/ Sex	Phenotype	Clinical status	Prednisone response <sup>#</sup>	MRD risk
1	0.8/F	cALL	CR 84 mo +	good	ND*
2	6.9/F	cALL	CR 65 mo +	good	IR
3	2.2/M	cALL	CR 44 mo +	good	SR
4	9.6/M	pre-B ALL	1 <sup>st</sup> CR 29 mo 2 <sup>nd</sup> CR 10 mo +	good -	IR
5	2.0/M	pre-B ALL	CR 20 mo +	poor	HR
6	3.4/M	cALL	CR 11 mo +	good	IR
7	3.4/M	cALL	CR 6 mo +	good	IR
8	1.8/M	cALL, CD117 <sup>+</sup>	CR 71 mo +	good	IR
9	12.0/F	cALL	CR 71 mo +	good	IR
10	4.8/M	cALL, My <sup>+</sup>	CR 23 mo +	good	IR

\* Interfant-99, standard risk

<sup>#</sup> Good prednisone response: less than 1000/μl peripheral blasts after a 7-day prephase with prednisone and one intrathecal dose of methotrexate on day 1 according to the ALL-BFM 2000 or Interfant-99 protocol.

CR, complete remission

HR, high risk

IR, intermediate risk

mo, months

MRD, minimal residual disease

ND, not done

SR, standard risk

yrs, years

## **CHAPTER 4**

### **MONOALLELIC LOSS AND FREQUENT MUTATION OF THE SECOND ALLELE OF *PAX5* IN DIC(9;20) CHILDHOOD ACUTE LYMPHOBLASTIC LEUKEMIA**

Daniela Krehan, Karin Nebral, Margit König, Dagmar Denk, Sabine Strehl

in preparation

CCRI, Children's Cancer Research Institute, St. Anna Kinderkrebsforschung, Vienna, Austria

## Abstract

The presence of a dic(9;20) is a characteristic abnormality found in roughly 1.5% of childhood B-cell precursor acute lymphoblastic leukemia (BCP-ALL). Although in about 40% of the cases this is the sole structural rearrangement and, thus, considered as the primary leukemogenic event little is known about the underlying molecular genetic lesions. In order to determine whether *PAX5* is implicated in the leukemogenesis of this genetically poorly characterized leukemia subtype, several cases were analyzed for their *PAX5* status. Our studies show that dic(9;20) leukemia is consistently associated with deletion of one copy of *PAX5* and frequent concomitant mutation of the retained allele.

## Introduction

Approximately 1,5% of childhood B-cell precursor acute lymphoblastic leukemia (BCP-ALL) is associated with the presence of a dic(9;20)(p13;q11).<sup>1,2</sup> In roughly 40% of the cases the dic(9;20) is the sole karyotypic change suggesting that this alteration is the primary leukemogenic event.<sup>1,2</sup> However, so far all efforts to delineate the gene(s) involved in this specific rearrangement have failed. This is mainly due to the heterogeneity of the breakpoints and, thus, neither a single affected gene on either chromosome nor the generation of a fusion gene has been observed.<sup>3,4</sup> Owing to the fact that the dic(9;20) aberration consistently results in partial monosomy 9p but not always 20q<sup>1,3</sup> the crucial gene(s) are more likely located at 9p. Accordingly, a dic(9;20) is frequently associated with hetero- or homozygous deletion of *CDKN2A*.<sup>1,3</sup>

The transcription factor PAX5, located at 9p13, encodes the B-cell lineage specific activator protein (BSAP) and is a master regulator of B-cell development.<sup>5,6</sup> Recently, it was shown that hypodiploid ALL has one null *PAX5* allele and a significant proportion of cases harbor point mutations in the second allele.<sup>7</sup>

Here we show that dic(9;20), leukemia in general accompanied by hypodiploidy,<sup>8</sup> which, however, can be masked by nonrandom gains of chromosomes<sup>1</sup> is associated with consistent loss of one *PAX5* copy and frequent mutation of the retained allele.

## Patients, Material and Methods

### Patients

Seven cases with *de novo* ALL were selected based on cytogenetic evidence of a dic(9;20)<sup>2</sup> (Table 1). Written informed consent that surplus material not required for diagnostic purposes may be used for research purposes was obtained from the patients' parents or their legal guardians.

### FISH analysis

Samples were hybridized with: centromere-specific probes for chromosomes 9 (D9Z5; Oncor/Qbiogene, Heidelberg, Germany) and 20 (D20Z1; M. Rocchi, Department of Cytogenetics, University of Bari, Italy); *PAX5* flanking BAC clones RP11-12P15 and RP11-22011 (Pieter de Jong, BACPAC Resources, Children's Hospital and Research Center Oakland, CA, USA); *PAX5* exon-specific cosmids cos-hPAX5-1 (exons 2-5) and cos-hPAX5-3 (exons 9-10);<sup>9</sup> Vysis LSI p16 (9p21) SpectrumOrange/CEP9 Spectrum Green (Abbott Molecular, Vienna Austria). FISH was performed as described.<sup>10</sup>

### **PAX5 mutation analysis**

Mutations in all coding exons and flanking intronic sequences of *PAX5* were identified by direct sequencing (Eurofins MWG Operon, Ebersberg, Germany) of PCR amplified genomic DNA. Primer sequences and PCR conditions are available upon request.

### **Identification of PAX5 splice variants**

*PAX5* isoforms were amplified using primers located in (i) exons 1A and 10 (PAX5ex1A-F2 5'-CCCTGTCCATTCCATCAAGTCC-3', PAX5ex10-R1 5'-TCACCCTCAATAGGTGCCA TCAG-3'), (ii) exons 1A and 6 (PAX5ex1A-F2, PAX5ex6-R1 5'-CTCCCCGCATCTGCTT CC-3'), (iii) exons 5 and 10 (PAX5ex5-F2 5'-CGGCATCCTGGGCATCAC-3', PAX5ex10-R2 5'-CGGTCTCATGGGCTCTCTGG-3'). RT-PCR reactions were carried out using Hot Start Taq (Qiagen, Vienna, Austria); cycling conditions: 95°C for 14 min; 35-40 cycles at 95°C for 30 sec, at 66°C for 30 sec, at 72°C for 2 min; 72°C for 7 min.

## **Results and Discussion**

### **PAX5 and CDKN2A status in dic(9;20) leukemia**

FISH analysis confirmed the presence of a dic(9;20) in all 7 cases (Figure 1A) and showed that one *PAX5* allele was consistently deleted (Figure 1B). Sequencing of all coding exons of the retained allele revealed mutations in *PAX5* in 4/7 (57%) of the cases (Figure 1D, Table 1). These mutations affected amongst PAX genes highly conserved residues<sup>11,12</sup> and substituted either threonines with alanines (T75A, exon 3; T311A, exon 8) or proline with arginine (P80R, exon 3). The T75A and the P80R mutations affect the *PAX5* paired DNA-binding domain, and the P80R mutation was reported to have a significant impact on protein structure.<sup>7</sup> The novel T311A substitution is located in the transactivation domain of *PAX5* in proximity to a P321 frame-shift mutation described earlier.<sup>7,11</sup>

Evaluation of the expression patterns of *PAX5* isoforms showed that in one of the non-mutated cases (case 7) no full-length transcript was present (Figure 1Ei and 1Eiii; lanes 7). All other cases expressed full-length *PAX5* and different splice variants in variable patterns and levels (Figure 1E). Direct sequencing of several transcripts revealed that these corresponded mainly to the known *PAX5* splice variants *PAX5* $\Delta$ 8, *PAX5* $\Delta$ 9, *PAX5* $\Delta$ 7/8, and *PAX5* $\Delta$ 7/8/9.<sup>13,14</sup> Of note, in the case that harbored the T311A exon 8 mutation, the transcript lacking exon 8 was predominantly expressed (Figure 1Ei and 1Eiii; lanes 4). Further, a novel *PAX5* splice variant skipping exon 2 (Figure Eii; lane 5), which so far was only described for murine *Pax5*<sup>15,16</sup> was identified.

While multiple *PAX5* isoforms were observed in B-cells of normal healthy donors<sup>14</sup> also a possible association with childhood leukemia was reported.<sup>13</sup> Further studies are required to

resolve whether the differential expression of *PAX5* alternatively spliced transcripts is leukemia-associated or reflects physiological stages of B-cell development.

FISH showed either a heterozygous (n=3), a homozygous (n=2), or a mixed pattern of homo- and heterozygous deletion (n=1) of *CDKN2A* (Figure 1Ci; Table 1). However, one sample (case 3) had two *CDKN2A* copies (Figure 1Cii). *CDKN2A* was lost from the dic(9;20) and the second signal was located on a marker chromosome (data not shown) suggesting a more complex rearrangements that results in a slightly different dic(9;20), nevertheless indicating that loss of *CDKN2A* is not a consistent feature of cytogenetically defined dic(9;20) leukemia. In conclusion, we show that dic(9;20) childhood BCP-ALL or at least a subtype of this purely cytogenetically defined entity is consistently associated with deletion of one *PAX5* allele and frequent mutation of the second allele. A certain impairment of *PAX5* function in combination with loss or mutation of other genes such as *CDKN2A* may play a crucial role in the development of this leukemia.

### Acknowledgements

This work was supported by a grant of the Austrian National Bank (Project No. 12547) (to S.S.) and the St. Anna Kinderkrebsforschung. We thank Meinrad Busslinger (IMP, Vienna, Austria) for kindly providing the *PAX5* cosmid probes and Maximilian-Otto Kauer for his help with statistical analysis.

### Authorship

D.K., K.N., and M.K. performed the experiments; D.D. analyzed data; S.S. designed and supervised the project and wrote the manuscript.

Conflict-of-interest disclosure: The authors declare no competing financial interests.

## References

1. Forestier E, Gauffin F, Andersen MK, et al. Clinical and cytogenetic features of pediatric dic(9;20)(p13.2;q11.2)-positive B-cell precursor acute lymphoblastic leukemias: a Nordic series of 24 cases and review of the literature. *Genes Chromosomes Cancer*. 2008;47:149-158.
2. Clark R, Byatt SA, Bennett CF, et al. Monosomy 20 as a pointer to dicentric (9;20) in acute lymphoblastic leukemia. *Leukemia*. 2000;14:241-246.
3. Schoumans J, Johansson B, Corcoran M, et al. Characterisation of dic(9;20)(p11-13;q11) in childhood B-cell precursor acute lymphoblastic leukaemia by tiling resolution array-based comparative genomic hybridisation reveals clustered breakpoints at 9p13.2 and 20q11.2. *Br J Haematol*. 2006;135:492-499.
4. Strefford JC, Worley H, Barber K, et al. Genome complexity in acute lymphoblastic leukemia is revealed by array-based comparative genomic hybridization. *Oncogene*. 2007;26:4306-4318.
5. Cobaleda C, Schebesta A, Delogu A, Busslinger M. Pax5: the guardian of B cell identity and function. *Nat Immunol*. 2007;8:463-470.
6. Busslinger M. Transcriptional control of early B cell development. *Annu Rev Immunol*. 2004;22:55-79.
7. Mullighan CG, Goorha S, Radtke I, et al. Genome-wide analysis of genetic alterations in acute lymphoblastic leukaemia. *Nature*. 2007;446:758-764.
8. Raimondi SC, Zhou Y, Mathew S, et al. Reassessment of the prognostic significance of hypodiploidy in pediatric patients with acute lymphoblastic leukemia. *Cancer*. 2003;98:2715-2722.
9. Busslinger M, Klix N, Pfeffer P, Graninger PG, Kozmik Z. Deregulation of PAX-5 by translocation of the Emu enhancer of the IgH locus adjacent to two alternative PAX-5 promoters in a diffuse large-cell lymphoma. *Proc Natl Acad Sci USA*. 1996;93:6129-6134.
10. Konig M, Reichel M, Marschalek R, Haas OA, Strehl S. A highly specific and sensitive fluorescence in situ hybridization assay for the detection of t(4;11)(q21;q23) and concurrent submicroscopic deletions in acute leukaemias. *Br J Haematol*. 2002;116:758-764.
11. Dorfler P, Busslinger M. C-terminal activating and inhibitory domains determine the transactivation potential of BSAP (Pax-5), Pax-2 and Pax-8. *Embo J*. 1996;15:1971-1982.
12. Bouchard M, Schleifer A, Eisenhaber F, Busslinger M. Evolution and function of Pax Genes. In: Cooper DN, ed. *Encyclopedia of the Human Genome*. Vol. 4: Nature Publishing Group; 2003:527-534.
13. Sadakane Y, Zaitzu M, Nishi M, et al. Expression and production of aberrant PAX5 with deletion of exon 8 in B-lineage acute lymphoblastic leukaemia of children. *Br J Haematol*. 2007;136:297-300.
14. Robichaud GA, Nardini M, Laflamme M, Cuperlovic-Culf M, Ouellette RJ. Human Pax-5 C-terminal isoforms possess distinct transactivation properties and are differentially modulated in normal and malignant B cells. *J Biol Chem*. 2004;279:49956-49963.
15. Lowen M, Scott G, Zwollo P. Functional analyses of two alternative isoforms of the transcription factor Pax-5. *J Biol Chem*. 2001;276:42565-42574.
16. Zwollo P, Arrieta H, Ede K, Molinder K, Desiderio S, Pollock R. The Pax-5 gene is alternatively spliced during B-cell development. *J Biol Chem*. 1997;272:10160-10168.

**Table 1. Cytogenetics, FISH and mutation analysis of dic(9;20) leukemia.**

Case	Age (yrs)/ Sex	Phenotype	Cytogenetics	PAX5 mutation	<i>CDKN2A</i> deletion
1	1.6/F	pre-B ALL	47,XX,dic(9;20)(p11-13;q11),+10,+21[8]/48,idem,+X[6]/49,idem,+del(X)(q23),+8?[2]	WT	23% hetero
2	9.9/F	pro-B ALL	46,XX,dic(9;20)(p13;q11),+21[17]/46,idem,del(2)(p23?) [3]	p.P80R	40% hetero/50% homo
3	9.6/M	pre-B ALL	46~47,XY,+7[4],der(9)dic(9;20)(p11;q11),add(12)(q24),-20[7],+21,add(22)(q13)[cp12]	p.T311A	normal
4	4.0/F	pre-B ALL	45,XX,dic(9;20)(p11;q11),-20[15]/45,idem,del(12)(p12)[9]	WT	90% hetero
5	2.5/F	pre-B ALL	45,XX,dic(9;20)(p11-13;q11)[7]	p.T75A	42% hetero
6	4.4/F	cALL	45,XX,del(1)(q32),t(1;17)(q32;q25),add(2)(p25),-20[10]	WT	60% homo
7	14.7/F	cALL	46,XX,del(9)(p21)[11]/45,idem,-20[5]	p.P80R	74% hetero

cALL, common ALL

WT, wild-type

hetero, heterozygous

homo, homozygous



Figure 1.

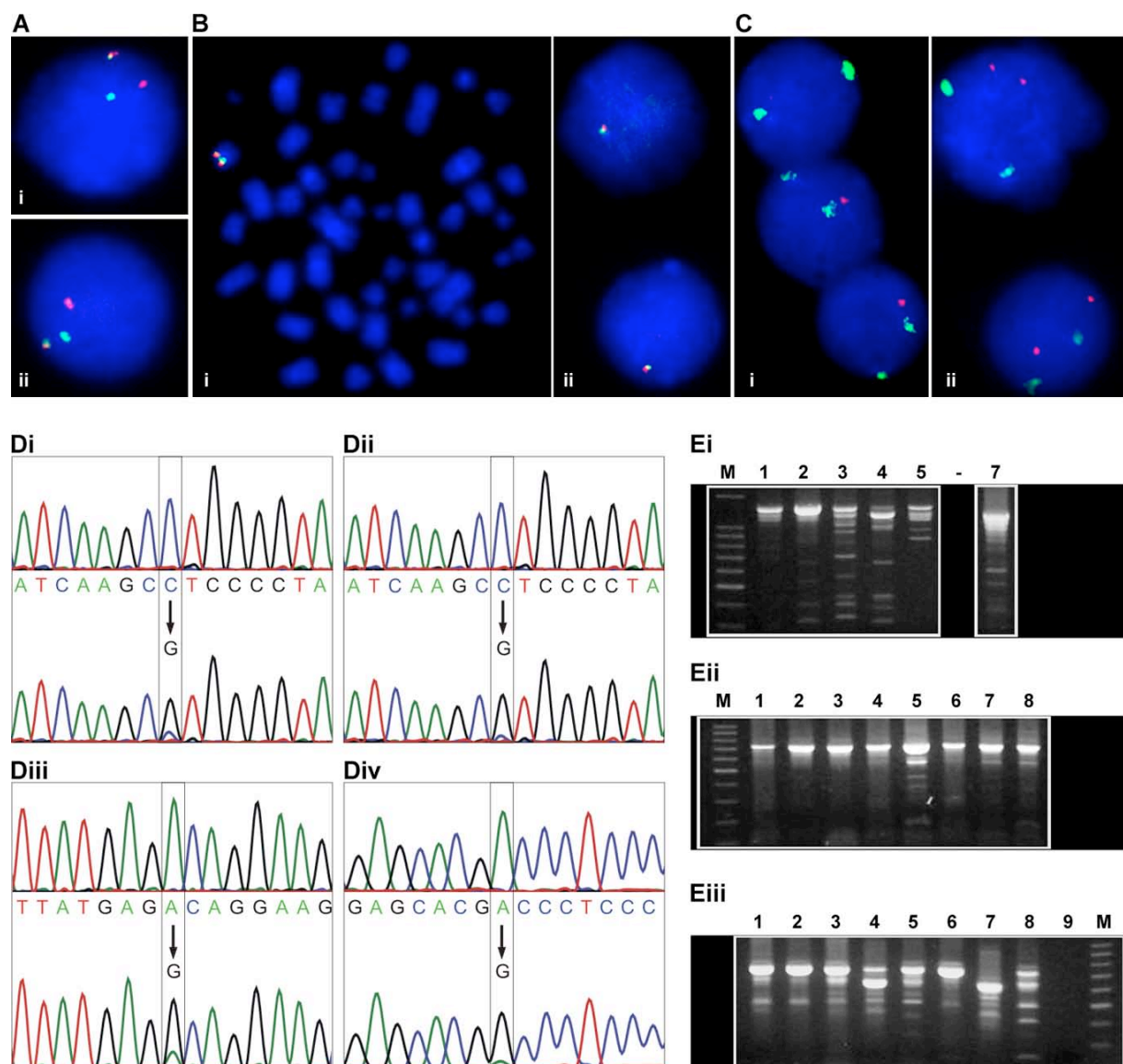


**Figure 1. Analysis of dic(9;20) leukemia.**

**(A-C)** FISH analysis. Images were taken using an Axioplan fluorescent microscope (Zeiss, Göttingen, Germany) equipped with the appropriate filter sets for DAPI, FITC, and Cy3, fitted with a Plan-Neofluar 100x/1.3 oil immersion objective and a CCD camera (CH250, Photometrix LTD, Tucson, AZ) using the IPLabs software (Vysis, Inc., Stuttgart, Germany). **(A)** Hybridization with chromosome 9 (Cy3) and 20 (FITC) centromere-specific probes showing colocalization of the signals confirming the presence of a dic(9;20); (Ai) case 3 and (Aii) case 5. **(B)** Hybridization with *PAX5* exon-specific cosmid clones cos-hPAX5-1 (FITC) and cos-hPAX5-3 (Cy3). (Bi) Metaphase of case 7 and (Bii) representative interphase nuclei of case 4 both displaying deletion of one *PAX5* copy. **(C)** (Ci-ii) Hybridization with *CDKN2A*-specific probe LSI p16 (9p21) (SpectrumOrange)/CEP9 (Spectrum Green) showing the mixed pattern of hetero- and homozygous loss of *CDKN2A* in case 2 (Ci) and the normal FISH pattern observed in case 3 (Cii). **(D)** Mutation analysis of leukemic blast (bottom chromatograms) and corresponding remission samples (top chromatograms). (Di-iii) Exon 3 (encoding the C-terminal portion of the *PAX5* paired DNA-binding domain) mutations, (Di-ii) C>G P80R and (Diii) A>G T75A. (Div) A>G T311A exon 8 (encoding part of the *PAX5* transactivation domain) mutation. **(E)** Expression of *PAX5* splice variants. (Ei) Amplification of full-length *PAX5* using primers located in exons 1A and 10. Lane 1, REH cell line; lane 2, case 1; lane 3, case 2; lane 4, case 3; lane 5, case 4; lane 7, case 6. (Eii) N-terminal isoforms amplified with primers located in exons 1A and 6. Lane 1, REH cell line; lane 2, case 1; lane 3, case 2; lane 4, case 3; lane 5, case 4; lane 6, case 5; lane 7, case 6; lane 8, case 7. (Eiii) C-terminal isoforms amplified with primers located in exons 5 and 10. Lane 1, REH cell line; lane 2, case 1; lane 3, case 2; lane 4, case 3; lane 5, case 4; lane 6, case 5; lane 7, case 6; lane 8, case 7; lane 9, negative control. M, molecular weight marker, 100 bp ladder (Promega, Mannheim, Germany).

## CHAPTER 5

### 5. ADDITIONAL METHODS AND RESULTS

#### 5.1. Establishment and validation of automated FISH screening

FISH screening of large numbers of samples requires highly standardized approaches including reliable and robust FISH protocols, and evaluation and data management procedures. For automated FISH analysis, FISH signals have to be highly specific and homogenous, and high hybridization efficiencies have to be achieved. Thus, both the FISH probe and the slide preparation were adjusted to the requirements of automated analysis.

##### *TempliPhi™ DNA amplification*

For preparation of large-scale FISH probes the TempliPhi™ 100 Amplification Kit (GE Healthcare, Vienna, Austria) was utilized, which produces microgram quantities of DNA from nanogram amounts of starting material. The TempliPhi™ DNA Amplification Kit uses rolling circle amplification (RCA) catalyzed by bacteriophage Phi29 DNA polymerase.

One  $\mu\text{l}$  (10ng/ $\mu\text{l}$ ; quantified using the Hoefer DyNA Quant™ 200 fluorometer (GE Healthcare)) of highly purified BAC DNA was transferred to 50 $\mu\text{l}$  of TempliPhi sample buffer, followed by denaturation at 93°C for 3min. Then 50 $\mu\text{l}$  of TempliPhi premix consisting of 50 $\mu\text{l}$  reaction buffer complemented with 2 $\mu\text{l}$  of enzyme mix were added to each denatured sample. Following incubation at 30°C for about 20hrs, the Phi29 DNA polymerase was heat-inactivated at 65°C for 10min and the amplification products were stored at 4°C or -20°C until further usage. Amplification of cosmid DNA was essentially performed as for BAC DNA, but only 1/10 of the reaction volume was required and the incubation time was reduced to 12-18hrs. However, in some instances the reaction volume was scaled-up to obtain higher amounts of DNA.

The amplified DNA was precipitated with 3 volumes of 95% ethanol (VWR International GmbH, Vienna, Austria) and 3M Na-Acetate (VWR International GmbH), washed with 500 $\mu\text{l}$  of 70% ethanol (VWR International GmbH) and resuspended in 25-50 $\mu\text{l}$  of sterile water. After DNA amplification the quality of the BAC and cosmid DNA was checked on 2% agarose gels by gel electrophoreses and the DNA concentration was quantified by UV spectrophotometry. In general, from approximately 10ng of DNA between 3-15 $\mu\text{g}$  BAC or cosmid DNA was obtained. The amount of input material was a critical factor for the successful amplification of high-quality DNA.

### *Probe preparation*

In order to standardize probe preparation always 1 µg of BAC or cosmid DNA was labeled by incorporation of digoxigenin-11-dUTP or biotin-16-dUTP (Roche Diagnostics, Vienna, Austria) nucleotides in a nick-translation reaction.

The labeled DNA was ethanol (VWR International GmbH) precipitated together with COT-1 and SSP DNA (Invitrogen GesmbH, Lofer, Austria), afterwards resuspended in hybridization solution [60% Formamide (VWR International GmbH), 1% Triton-X (VWR International GmbH), 2xSSC] and dissolved by incubation in a thermomixer at 45°C shaking at 500rpm for about one hour. These FISH probes were then denatured and pre-annealed to avoid cross-hybridization with repetitive sequences and were stored at -20°C, ready for use.

### *Sample and slide preparation*

Methanol/acetic acid fixed cell suspensions of patient samples originally used for cytogenetic analysis were dropped on test slides to control the cell density. To allow for automated FISH scanning of a slide within a reasonable time-frame (10hrs - 14hrs) and to ensure appropriate hybridization efficiency, the cell density had to be relatively high but individual cells clearly separated. To achieve equal cell densities for all patient samples each sample was fixed with a freshly prepared appropriate amount of cold fixative [methanol (VWR International GmbH):acetic acid (VWR International GmbH) = 3:1]. Three µl of the fixed cell suspensions were dropped on frozen 3-well slides, each sample on one individual well, and incubated in Nonidet P40 (Sigma-Aldrich, Vienna, Austria) 0.4% / 2xSSC at 37°C for 1hr. After dehydration through an ascending ethanol series followed by 3min of pepsin digestion FISH was essentially performed as previously described (Konig *et al*, 2002).

### *Automated fluorescence in situ hybridization - Metafer4-Metacyte (Metasystems)*

For high-throughput analysis and the objective evaluation of FISH patterns a standardized automated spot counting system including 3-dimensional distance measurements between the signals captured in different color channels was used. In particular, when split-apart FISH probes on the genomic level are separated by a larger distance (*PAX5* clones RP11-22011 and RP11-12P15 are separated by approximately 250kb), it is difficult to distinguish a separation of the probes from a mere slightly larger gap between signals (false-positives) dependent on the genomic distance by manual scoring (for details see 5.1.1.).

The Metafer4-Metacyte (MetaSystems, Altlußheim, Germany) slide scanning system is based on a motorized Zeiss Axioplan 2 Imaging fluorescence microscope (Zeiss, Göttingen, Germany) equipped with a motorized slide scanning stage and a Zeiss AxioCam MRm CCD camera. Both the microscope and the scanning stage are controlled by the special Metafer software package.

The system automatically scans up to 8 slides, takes images in different focal planes and enumerates the numbers of signals per cells (Fig. 9). Further analysis is conducted on the acquired digital images according to preset software parameters. These parameters have to be defined and saved in a so-called classifier. As the system allows to define a broad spectrum of different parameters, it is highly flexible and can be utilized for an almost unlimited number of assays. However, to obtain optimal results, the system has to be trained and adjusted to the individual requirements of each FISH assay.

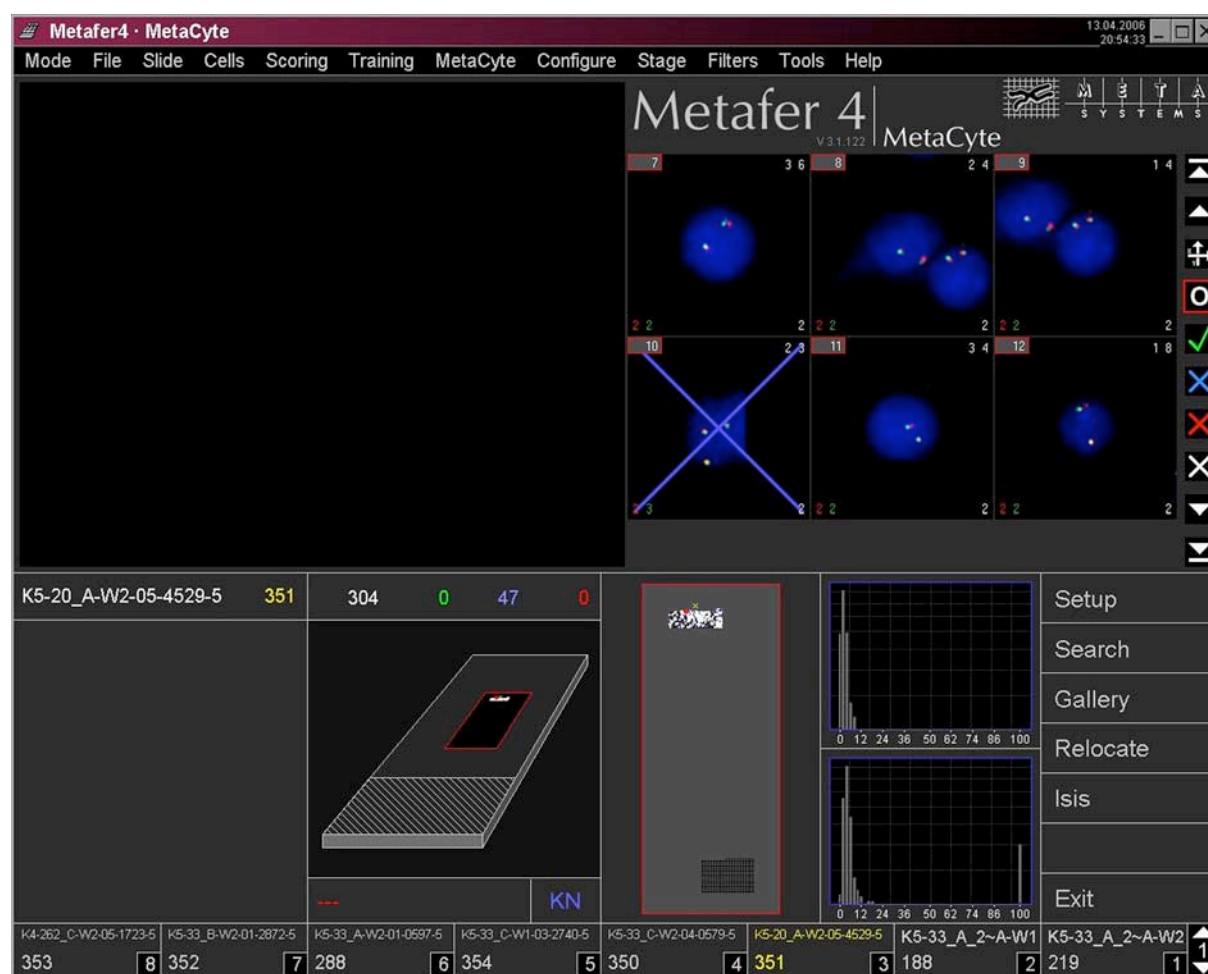


**Figure 9. Metafer4-Metacyte user interface.** Screenshot of the Metafer4-Metacyte user interface, which consists of a menu bar for selection of the operation mode (top), an image area for live image display (upper left), the gallery (upper right) showing the acquired interphase nuclei, and command buttons with quick links to the most important functions (lower right). Further, current slide data including the scanned area and feature diagrams (lower part) as well as slide-specific data of one whole scan (bottom) are displayed.

The classifier parameters depend on the objective lense, the cell type and the fluorochromes used for the detection of the FISH probe. Parameters how the system captures the image fields in the different color channels are set in 'Capture', e.g. an automatic exposure mode with a maximum integration time for ~2s and 2.9s for channels CY3 and FITC, respectively,

were defined, and the number and the distance of focus planes were set at 5 and 0.75 $\mu\text{m}$ , respectively (Fig. 10). Further, parameters for an automatic exposure mask and for image processing operations were adjusted. In the classifier group 'Cell Selection' the parameters define how the system selects the interphase cells to be analyzed. These parameters strongly depend on the cell type and have to be optimized by training. For example, values for minimum and maximum nucleus area were 35 $\mu\text{m}^2$  and 500 $\mu\text{m}^2$ , respectively, and for the maximum aspect ratio 1.7 was used. This setting defines the ratio of the nucleus diameters along the long and short principle axis to discriminate round objects from more elongated ones. If a cell is accepted by the cell selection procedure, a sub-image of the cell from the captured field image is created, which is the basis for further processing and measurements, and therefore parameters for image processing operations were sparingly defined.

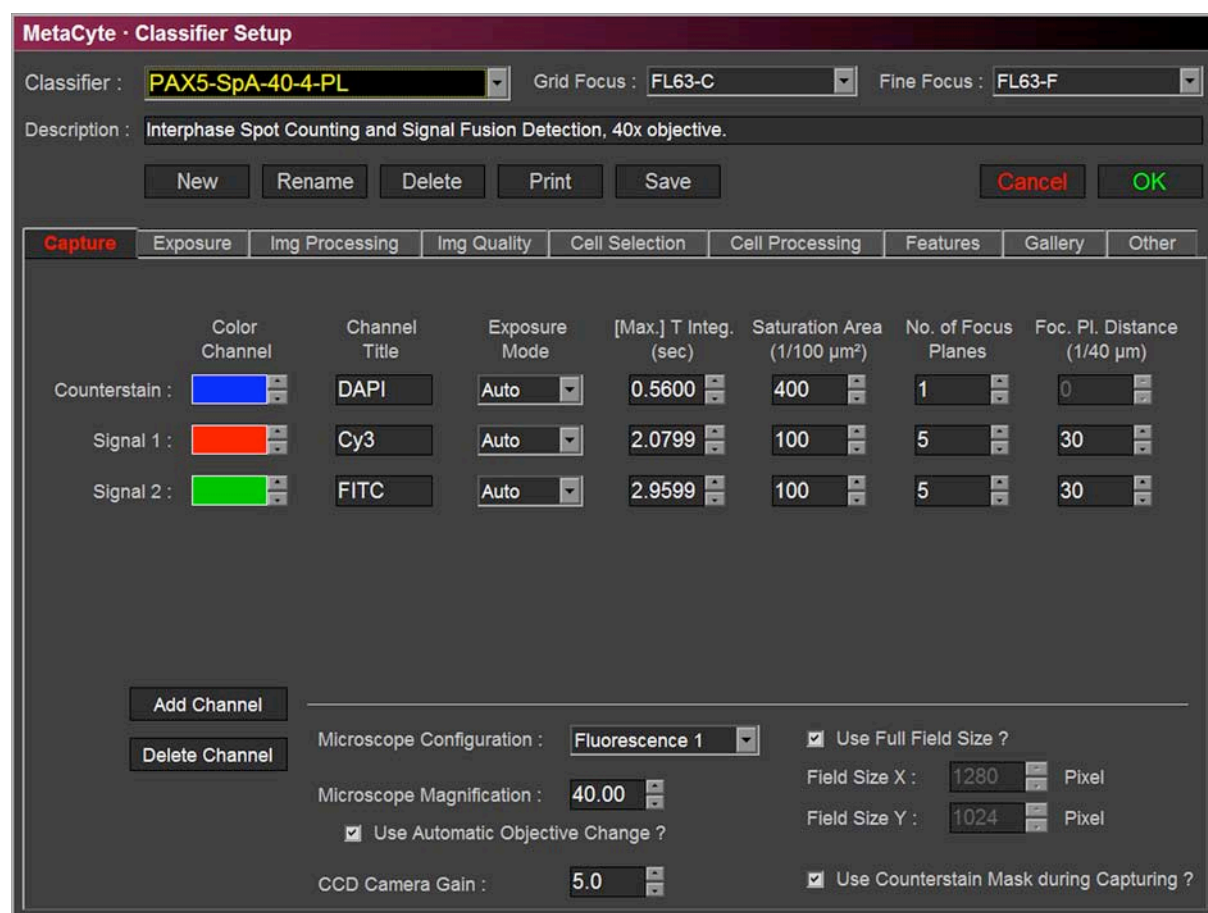


**Figure 10. Metafer4-Metacyte Classifier Setup.** Screenshot of the 'Capture' submenu of the classifier is shown as an example. The parameters, which have to be defined within this group are displayed.

Some of the most important parameters in our assay were set in the 'Features', in which the definitions for the measurements and the spot counting applied to the cell images during scanning are adjusted.

The system measures the 3-dimensional distances between spots of different colors and defines the 1<sup>st</sup> and the 2<sup>nd</sup> smallest distance between them (Fig. 11). The parameter for 'Spot Fusion Count' was set at  $\leq 10$  Pixel meaning that 2 signals of different colors are counted as fusion signal if the distance is  $\leq 10$  Pixel (about  $1.6\mu\text{m}$ ). In cells lacking a value for the 2<sup>nd</sup> smallest distance, for example due to a deletion event, the value for the 2<sup>nd</sup> smallest distance was arbitrarily set at 100 Pixel (for details see 5.1.1.).

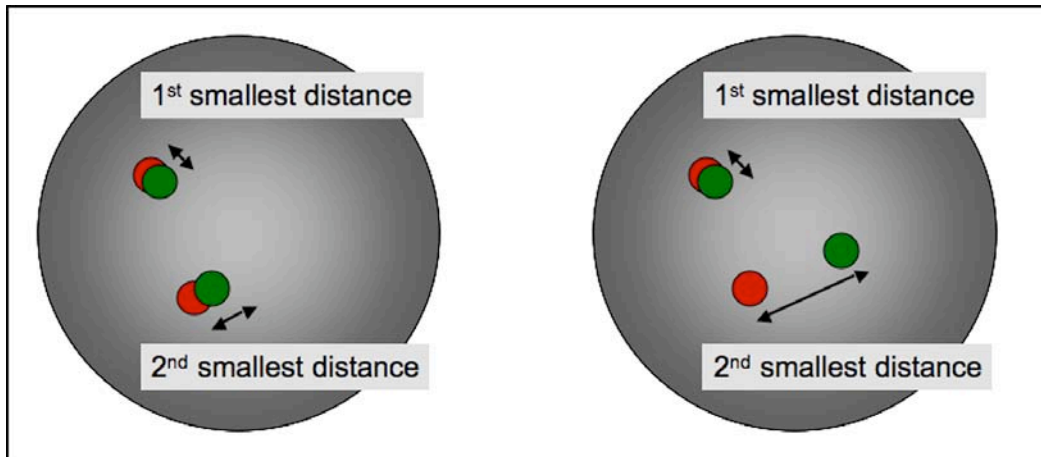


**Figure 11. Distance Measurement.** Schematic representation of a normal FISH pattern (left) showing a normal 2<sup>nd</sup> smallest distance and an abnormal FISH pattern (right) with a larger 2<sup>nd</sup> smallest distance.

The spot counting parameters also included an absolute spot area, which was set at  $0.15\mu\text{m}^2$ , a minimum spot distance ( $1.4\mu\text{m}$ ) and a relative minimum spot intensity (30%) within one color channel. The parameters were the same in both channels, CY3 and FITC. Additionally, a relative maximum spot area compared to the whole nucleus was set at 80/1000 units and the size of the area, which should be scanned during the search process was defined by the number of search fields around a certain coordinate (18x18 in the *PAX5* classifier).



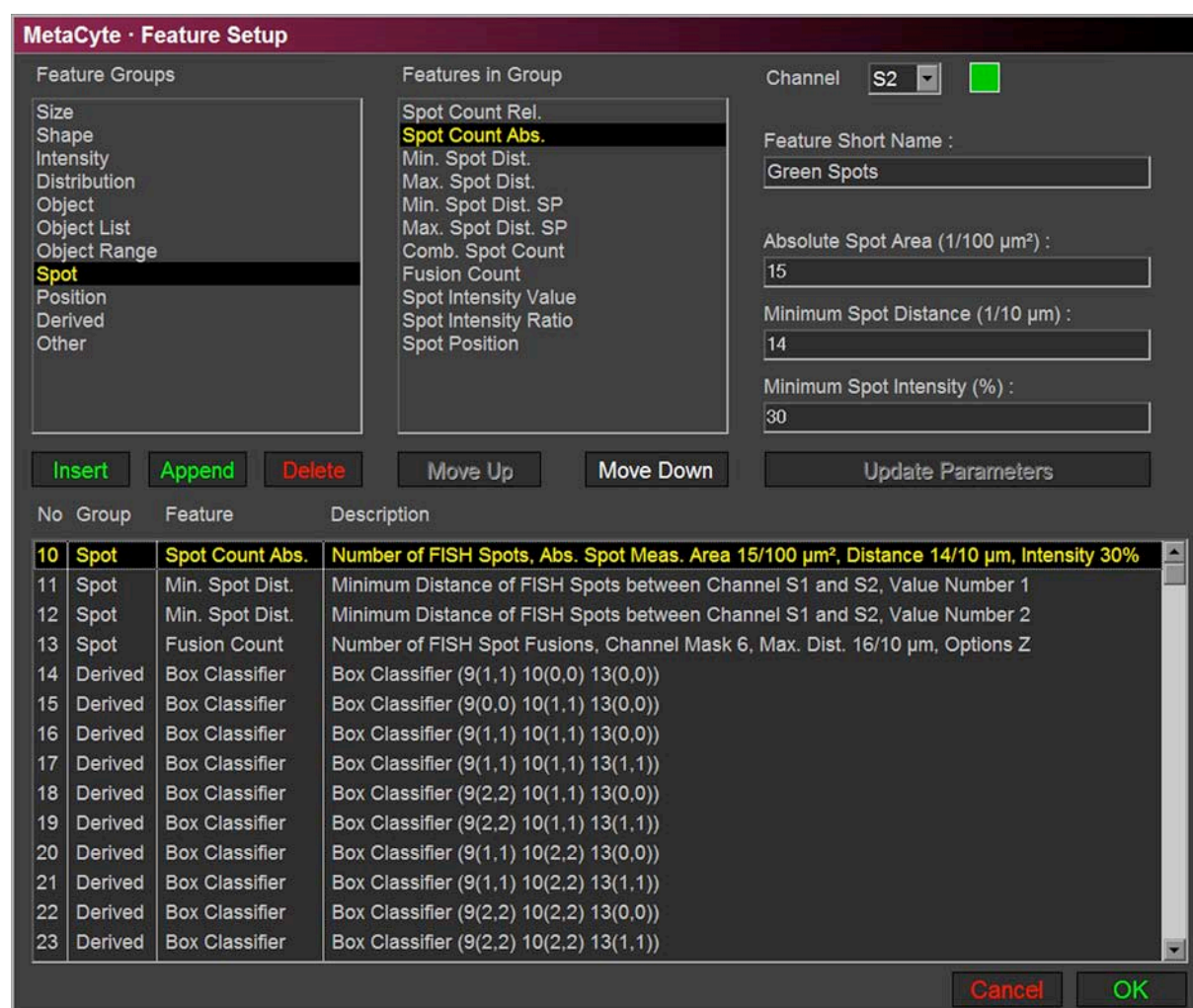


**Figure 12. Metafer4-Metacyte Features Setup.** As an example, the feature list of channel 2 (FITC) of the submenu 'Features' is displayed with the spot counting parameters highlighted.

Several parameters for the 'Gallery', and finally the output form were defined. A special 'MetaCyte Report', which included for example information fields in terms of the analyzed sample and the hybridization procedure was created. Moreover, in this report histograms of the first and second smallest distances and display fields for a selection of the processed cells were displayed.

All parameters defined in the PAX5 'Metafer4 Metacyte Classifier' are listed in the Appendix.

### Evaluation

All patient samples were automatically analyzed followed by manual evaluation of each individual cell captured and displayed in the cell gallery. Evaluation is facilitated by options such as cell sorting according to different parameters, changing of signal thresholds, and relocation of individual cells for visual inspection. This procedure, was in particular required to reject false-positive cells and to correct erroneous spot counts.



### 5.1.1. Analysis of control samples

The classifier for the *PAX5* split-apart FISH assay was established using mononuclear cells isolated from peripheral blood of 3 healthy controls and blast cells of 2 different leukemic bone marrow samples that showed a normal karyotyp and a normal *PAX5* status.

Representative mononuclear cells of a control hybridized with the *PAX5* split-apart FISH assay are shown in Figure 13A. These examples illustrate the difficulty to unambiguously distinguish a fusion signal from a split signal pattern by visual observation. In Figure 13B typical histograms of the 1<sup>st</sup> and 2<sup>nd</sup> smallest distances found in normal controls are shown. In 8 different hybridization experiments of 3 control samples second smallest distances between 0 and 28 Pixel were observed with a mean of 4,8 Pixel and a standard deviation of 0,56. Moreover, in at least 96% of cells the 2<sup>nd</sup> smallest distances were  $\leq 10$  Pixel, thus, the spot fusion count parameter was set accordingly in the *PAX5* classifier.

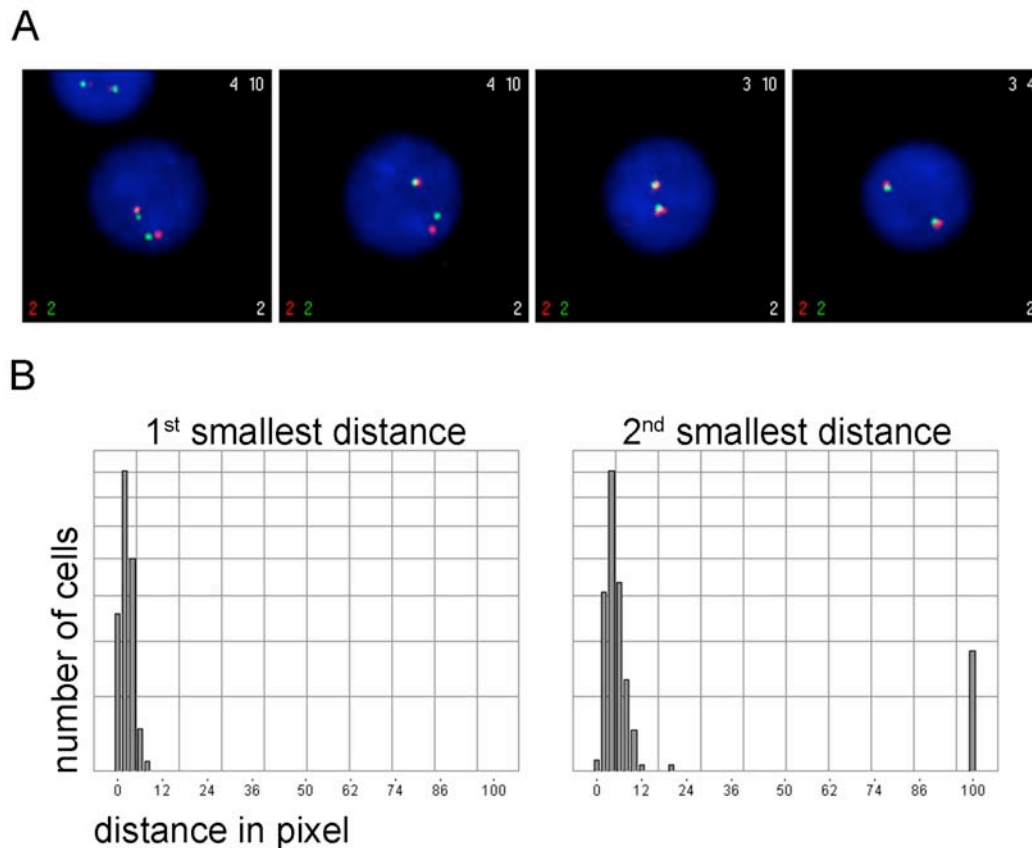


**Figure 13. Distance measurements Metafer4-Metacyte (Metasystems).** (A) Representative interphase nuclei of a normal control hybridized with *PAX5*-flanking BAC clones RP11-22011 (5'-end-specific; red) and RP11-12P15 (3'-end-specific; green) showing a normal FISH pattern (left lower corner of each picture: total number of red and green signals; right lower corner: number of fusion signals) and different 1<sup>st</sup> and 2<sup>nd</sup> smallest distances (shown in the upper right corner of each picture). Interphase pictures were taken from the Metafer4-Metacyte cell gallery. (B) Representative histograms that illustrate the distribution of the 1<sup>st</sup> and 2<sup>nd</sup> smallest distances in a normal control.

The data obtained by the automated FISH analysis were summarized in a "MetaCyte Report" and as an example one of a normal control is shown in Figure 14.

**MetaCyte Report**

**Surname:**  
**Name:**

**Case Name:** Normalkontrolle

**Slide:** K4-115\_B-W2-05-0641-1

**Slide Comment:** PAX5-5'bio-3'dig. K4-112-Mix

**Classifier:** PAX5-SpA-40-4

**Search Date:** 30.12.05

**User:** ADM

**Directory:** D:\MSData\

**Result:** PAX5-5'bio-3'dig. K4-112-Mix; PSI-Prep, TempliPhi, Hyb.mix (60% FA, 1% Triton-X, 2xSSC). 1h NP40 + 3min Pepsin

**Analyzed Cells:** 305      **Marked Cells:** 15  
**Rejected Cells:** 29      **Undefined Cells:** 261

**Statistics:**

Class (R/G/F)	No. of Cells	%	Class (R/G/F)	No. of Cells	%	Class (R/G/F)	No. of Cells	%
1/0/0	0	0.0	3/3/0	0	0.0	4/4/0	0	0.0
0/1/0	0	0.0	3/3/1	0	0.0	4/4/1	0	0.0
1/1/0	0	0.0	3/3/2	1	0.4	4/4/2	0	0.0
1/1/1	11	4.0	3/3/3	0	0.0	4/4/3	0	0.0
2/1/0	0	0.0	1/3/0	0	0.0	4/4/4	0	0.0
2/1/1	9	3.3	1/3/1	3	1.1	1/4/0	0	0.0
1/2/0	0	0.0	2/3/0	0	0.0	1/4/1	0	0.0
1/2/1	5	1.8	2/3/1	3	1.1	2/4/0	0	0.0
2/2/0	0	0.0	2/3/2	17	6.2	2/4/1	0	0.0
2/2/1	3	1.1	4/1/0	0	0.0	2/4/2	2	0.7
2/2/2	198	71.7	4/1/1	0	0.0	3/4/0	0	0.0
2/0/0	0	0.0	4/2/0	0	0.0	3/4/1	0	0.0
0/2/0	0	0.0	4/2/1	0	0.0	3/4/2	0	0.0
3/1/0	0	0.0	4/2/2	3	1.1	3/4/3	0	0.0
3/1/1	0	0.0	4/3/0	0	0.0			
3/2/0	0	0.0	4/3/1	0	0.0	<b>Total</b>	276	100.0
3/2/1	1	0.4	4/3/2	0	0.0	<b>Rest</b>	0	0.0
3/2/2	20	7.2	4/3/3	0	0.0			

**Figure 14. MetaCyte Report of a normal control.** Summary of the results obtained by hybridization with PAX5-flanking BAC clones RP11-22011 (5'-end-specific; red) and RP11-12P15 (3'-end-specific; green) to a control sample. The different classes of FISH patterns and the number of enumerated cells are shown: 305 interphase nuclei were captured, 29 of them were rejected upon evaluation, and 276 were finally analyzed. R, red; G, green; F, fusion signal.

### 5.1.2. Validation of the FISH assay in *PAX5*-rearranged samples

As positive controls the KIS-1 cell line and a patient previously identified as *PAX5*-rearranged were used to validate the FISH assay.

The KIS-1 cell line harbors a  $t(9;14)(p13;q32)/PAX5-IGH@$  translocation and the breakpoint is located upstream of *PAX5* exon 1A. Cytogenetic analysis revealed further aberrations and a very complex karyotype with additional marker chromosomes, which is in concordance with published data (George *et al*, 2005). Representative interphase nuclei of the KIS-1 cell line showing a separation of the *PAX5* FISH probes and 3-5 additional *PAX5* 3'-end-specific signals are depicted in Figure 15A. Examples of interphase nuclei of the *PAX5*-rearranged patient that also display a separation of the *PAX5* FISH probes are shown in Figure 16A. The histograms of the positive controls illustrate the broader distribution of the 2<sup>nd</sup> smallest distances, which correspond to the separated *PAX5* FISH probes (Fig 15B and 16B).

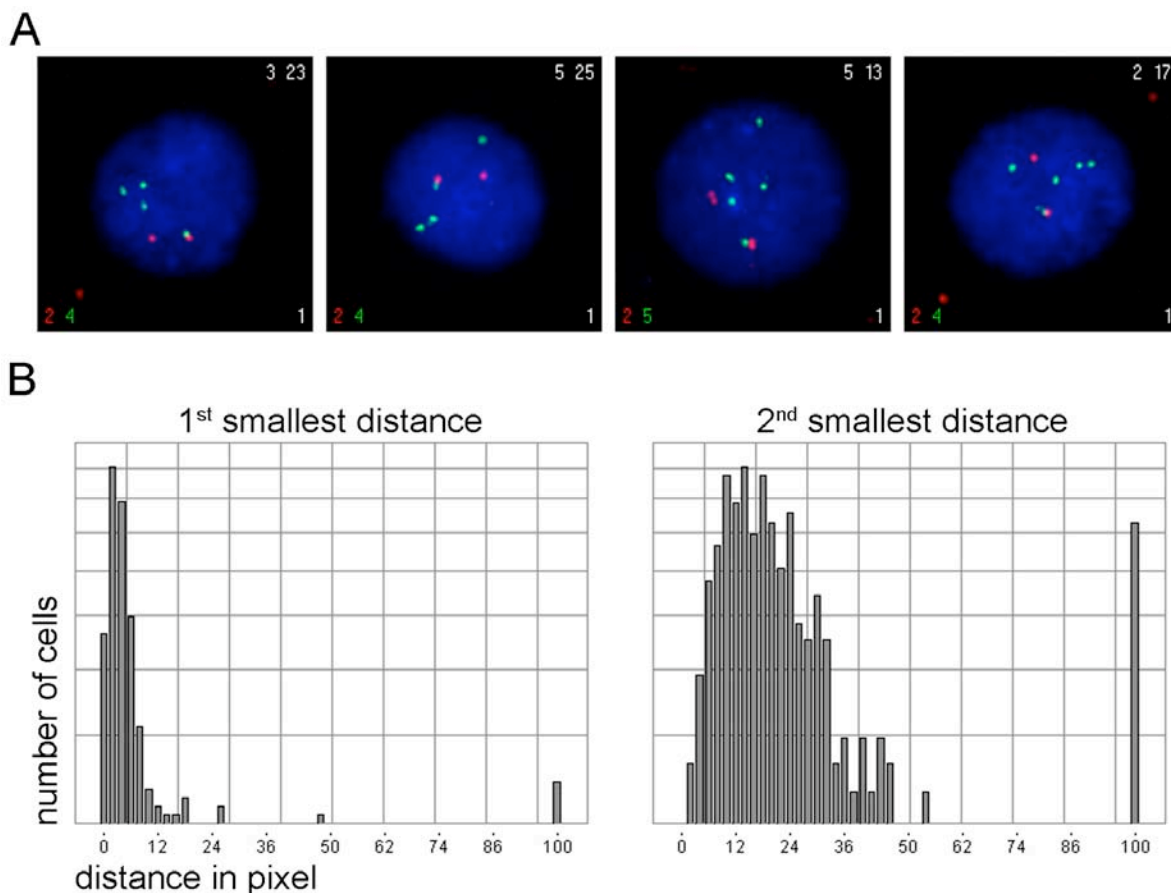


**Figure 15. KIS-1 cell line as positive control for the Metafer4-Metacyte automated FISH analysis and distance measurements. (A)** Representative interphase nuclei of the KIS-1 cell line hybridized with *PAX5*-flanking BAC clones RP11-22011 (5'-end-specific; red) and RP11-12P15 (3'-end-specific; green); (left lower corner of each picture: total number of red and green signals; right lower corner: number of fusion signals) with different 1<sup>st</sup> and 2<sup>nd</sup> smallest distances (shown in the upper right corner of each picture). Images of interphase nuclei were taken from the Metafer4-Metacyte cell gallery. **(B)** Histograms that show the distribution of the distances between the FISH signals.

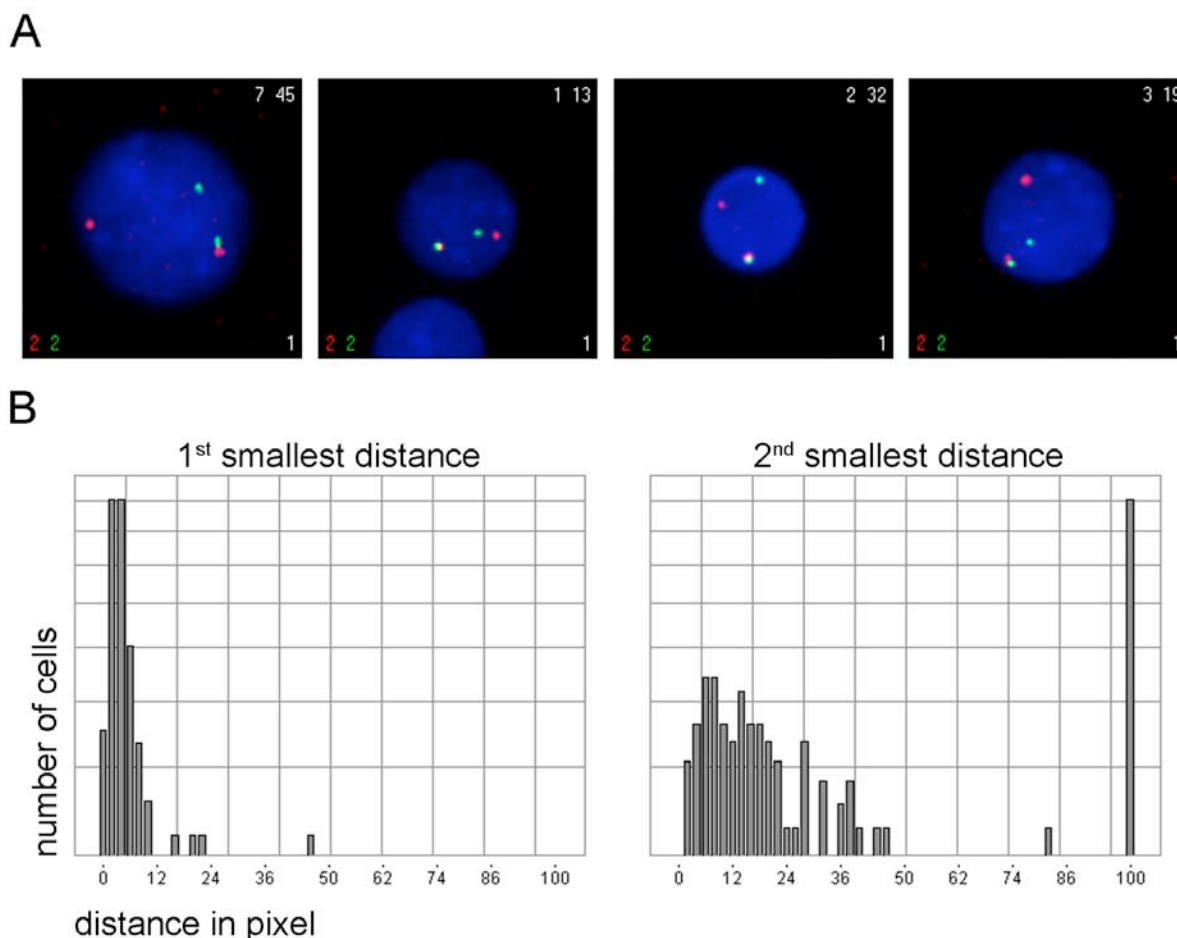


**Figure 16. A *PAX5* rearranged patient used as positive control for the Metafer4-Metacyte automated FISH analysis and distance measurements. (A)** Aberrant interphase nuclei hybridized with *PAX5*-flanking BAC clones RP11-22011 (5'-end-specific; red) and RP11-12P15 (3'-end-specific; green); (left lower corner of each picture: total number of red and green signals; right lower corner: number of fusion signals) with different 1<sup>st</sup> and 2<sup>nd</sup> smallest distances (shown in the upper right corner of each picture). Images of interphase nuclei were taken from the Metafer4-Metacyte cell gallery. **(B)** Histograms that show the distribution of the distances between the FISH signals.

### 5.1.3. Novel *PAX5* positive cases - Metafer 4 Metacyte analysis

Ten patients showed a FISH pattern suggestive for a *PAX5* rearrangement. As an example, the Metafer4-Metacyte Report of a representative case is shown in Figure 17. In this case, 350 interphase nuclei were captured, 92 of these were rejected, thus, 258 were included in the statistical analysis, and a separation of the *PAX5* FISH probes was found in 59,7% of cells. The corresponding distribution of the 2<sup>nd</sup> smallest distances between the FISH signals is also illustrated in the 'MetaCyte Report'.

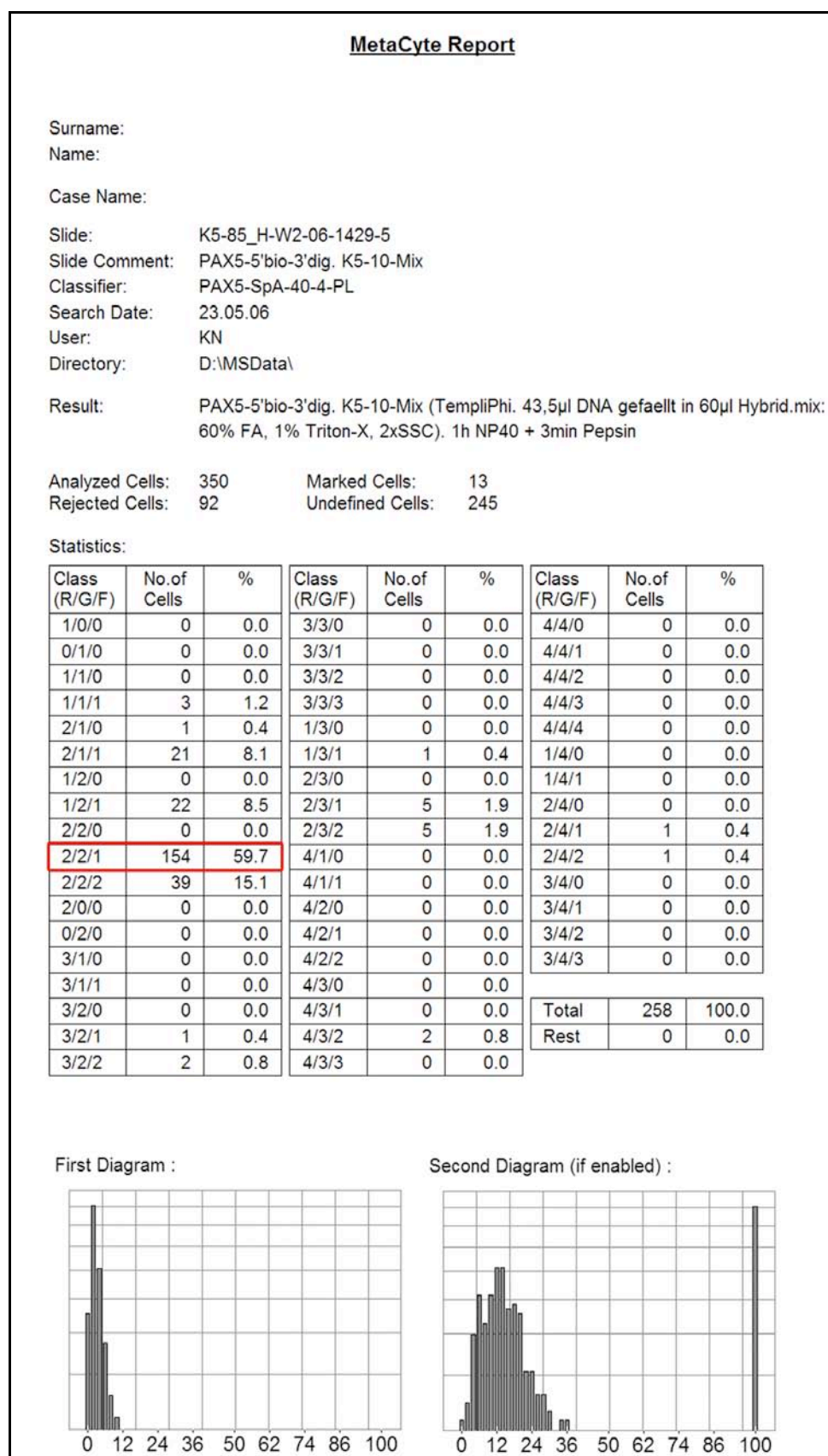


**Figure 17. Representative MetaCyte Report.** The results of the automated FISH analysis using *PAX5*-flanking BAC clones RP11-22011 (5'-end-specific; red) and RP11-12P15 (3'-end-specific; green) of a *PAX5*-rearranged case are shown. The significant aberrant FISH pattern is boxed in red. The histograms of the 1<sup>st</sup> (first diagram) and 2<sup>nd</sup> smallest (second diagram) distances are depicted at the bottom. R, red; G, green; F, fusion signal.

### *Distances between FISH signals in PAX5 positive patients*

In all positive patients that showed a separation of the *PAX5* FISH probes the distributions of 2<sup>nd</sup> smallest distances of the FISH signals were analyzed in detail (Table 1). All cells, in which the 2<sup>nd</sup> smallest distance was set to 100, e.g. cells with a deletion event, were excluded from this analysis. The percentage of cells that showed 2<sup>nd</sup> smallest distances >10 Pixel representing cells with an aberrant pattern ranged from about 24-71%. The differences between the 2<sup>nd</sup> smallest distances of all positive patients as compared to those of normal controls were highly significant (p-values  $10^{-10}$  -  $10^{-58}$  by Student's T-test).

**Table 1. FISH signal distances in *PAX5* positive cases**

Case No*	2 <sup>nd</sup> smallest distance (mean)	2 <sup>nd</sup> smallest distance (standard deviation)	Distance values (min. - max.)	% of cells with distance >10 Px	No of cells
2	8,33	4,14	1-23	23,60	212
3	10,46	7,93	1-41	36,40	228
4	8,11	6,86	1-46	25,10	219
5	14,17	6,57	1-36	70,50	210
6	12,98	8,44	2-50	53,80	182
7	13,10	6,45	1-33	66,30	270

\*For case descriptions see Nebral *et al*, in press.

## 5.2. Detailed analysis of selected cases

*PAX5* rearrangements were observed either in cases with normal or complex karyotypes. In order to further characterize these aberrations, additional *PAX5* gene-specific probes and clones located adjacent to *PAX5* were hybridized in various combinations to metaphase and/or interphase nuclei (Fig. 18). Several whole chromosome painting probes, and sets of probes hybridizing to the potentially affected chromosome regions in the individual cases were also applied.

Further, particularly, in cases with focal/partial *PAX5* deletions FISH clones located in proximity to the *PAX5* locus were used to elucidate the extent of these deletions (Fig. 18). The additional FISH clones are listed in Table 1 in the Appendix.

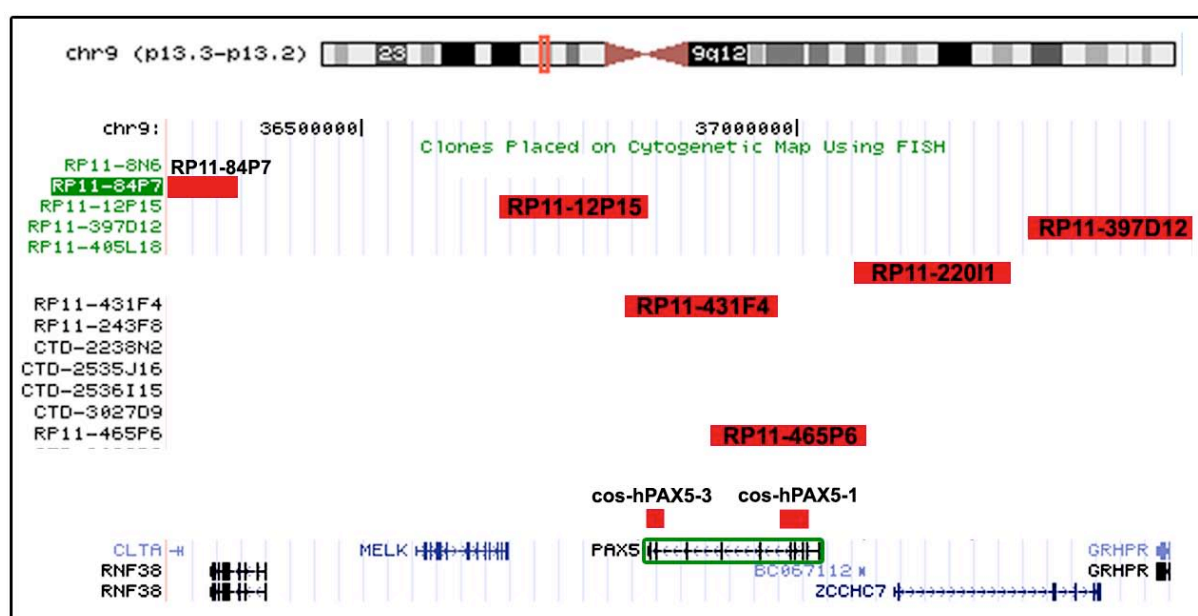


**Figure 18. FISH clones located at 9p13.** Adapted screenshot from the UCSC Genome Browser on Human March 2006 Assembly ([www.genome.ucsc.edu](http://www.genome.ucsc.edu)) with the utilized FISH clones depicted in red. The *PAX5* gene is transcribed from centromere to telomere (5' - 3').



### 5.2.1. *PAX5* rearranged cases

Selected *PAX5* positive cases were analyzed in further detail. The case numbers correspond to those in Chapter 3: "Incidence and diversity of *PAX5* fusion genes in childhood acute lymphoblastic leukemia", Nebral *et al*, page 39.

#### Case 5

In this case, cytogenetic analysis showed a 46,XY,del(7)(q22q33)?,del(9)(q22?),del(12)(p11)[8] karyotype suggesting complex rearrangements with involvement of chromosomes 7, 9, and 12, but 9p13 was not affected. Thus, conventional chromosome banding did not provide any evidence for involvement of *PAX5*. However, FISH analysis indicated a *PAX5* rearrangement and on the molecular level *PAX5* exon 5 was fused to *POM121* exon 5 with insertion of genomic material from chromosome 12 at the breakpoint.

Subsequent hybridization of *PAX5*-aberrant metaphases with whole chromosome painting probes for chromosomes 7 and 9 confirmed involvement of these chromosomes in a complex at least 3-way translocation (Fig. 19B). Moreover, this analysis revealed that the 3'-end of *PAX5* was located on a der(7;9) chromosome, whereas the 5'-end was translocated to a der(7), most probably harboring the *PAX5-POM121* fusion (Fig. 19).

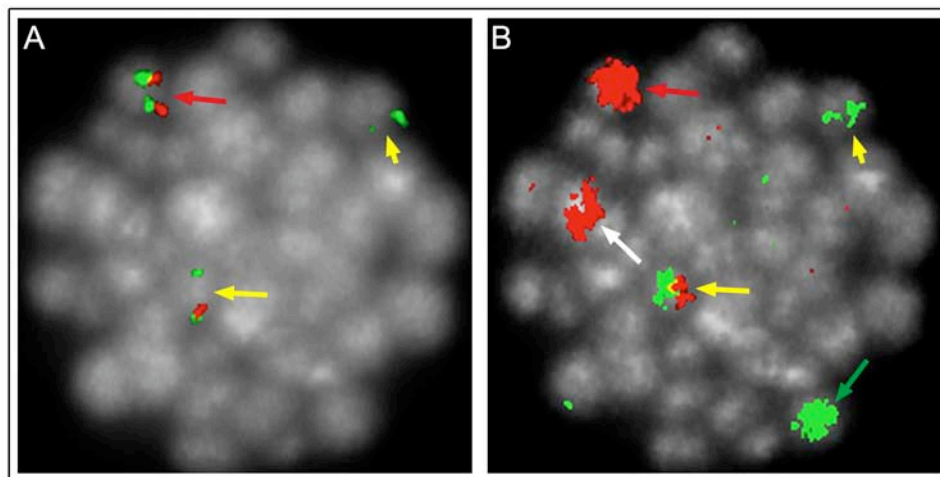


**Figure 19. FISH analysis of case 5. (A)** Metaphase hybridized with the *PAX5* 5'-end encompassing clone RP11-456P6 (green) and RP11-84P7 (red), located telomeric (3') of *PAX5*, showing a split signal pattern. **(B)** The same metaphase was analyzed with whole chromosome painting probes for chromosomes 9 (red) and 7 (green). Arrows indicate the normal chromosomes 9 (red) and 7 (green), the der(9) (white) and der(7) (short yellow), and the der(7;9) (yellow).



## Case 6

In case 6, about 46% of interphase nuclei showed a separation of the *PAX5*-flanking BAC clones and rearrangement of *PAX5* was confirmed by hybridization with the *PAX5*-specific cosmid clones. Subsequent fusion gene-specific RT-PCR and/or FISH analysis for all known *PAX5* partner genes did not detect any specific chimeric transcript and no abnormal FISH pattern (Fig. 20) was observed. All Oligonucleotide primer sequences and the FISH clones used for these analyses are listed in Table 2 and Table 1, respectively, in the Appendix.

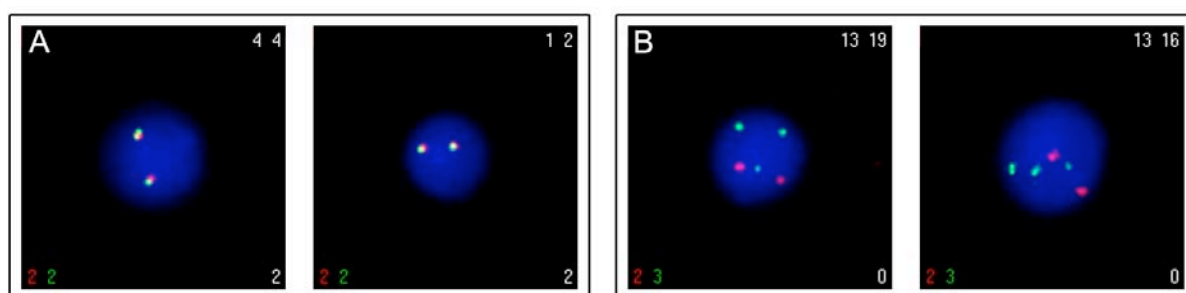


**Figure 20. Examples of the fusion gene-specific FISH analysis of case 6. (A)** Interphase nuclei hybridized with *ELN* 5'-end RP11-148M21 (red) and *ELN* 3'-end RP11-349P21 (green) specific clones displaying a normal FISH signal pattern. **(B)** Analysis of interphase nuclei with *PAX5*-spanning clones RP11-465P6 and RP11-431F4 (green) in combination with *AUTS2*-spanning clones RP11-243F5 and RP11-88H22 (red) which showed a *PAX5* split signal and two normal signals for *AUTS2*.

Hybridization of metaphases with whole chromosome painting probes for chromosomes 9 and 14 showed that the *PAX5* 5'-end was located on a der(9) chromosome whereas the 3'-end was translocated to 14q32 (Fig. 21A). Participation of *IGH@* and *BCL11B* located at 14q32 was excluded by FISH analysis. Yet, 24-color FISH suggested involvement of chromosomes 3, 9, 11, and 12 in complex rearrangements and further FISH analysis revealed translocation of chromosome 9 material to 3q (Fig. 21Aii) and 3q material to 9q (Fig. 21B and data not shown), as well as insertion of 11p material into both 9p and 14q (Fig. 21C). Based on these data we suspected that a novel *PAX5* fusion partner was located at 11p and in order to narrow down the potential breakpoint between *LMO1* and *WT1*, 20 BAC clones (see Appendix, Table 1 and Fig. 22), which encompassed 11p13-15 were hybridized to metaphases in combination with *PAX5*-specific probes. However, although all clones were properly either observed on the der(9) or the der(14) chromosomes (examples are shown in Fig 23) neither of them showed a co-localization with *PAX5* in interphase nuclei. Finally, one single BAC clone, RP11-52H5, located at the 5'-end of the *BDNF* gene, was deleted. This gene consists of only 2 exons but RT-PCR experiments using primers PAX5ex5-F1 and BDNFex2-R1 or BDNFex2-R2 did not detect any specific fusion transcripts.

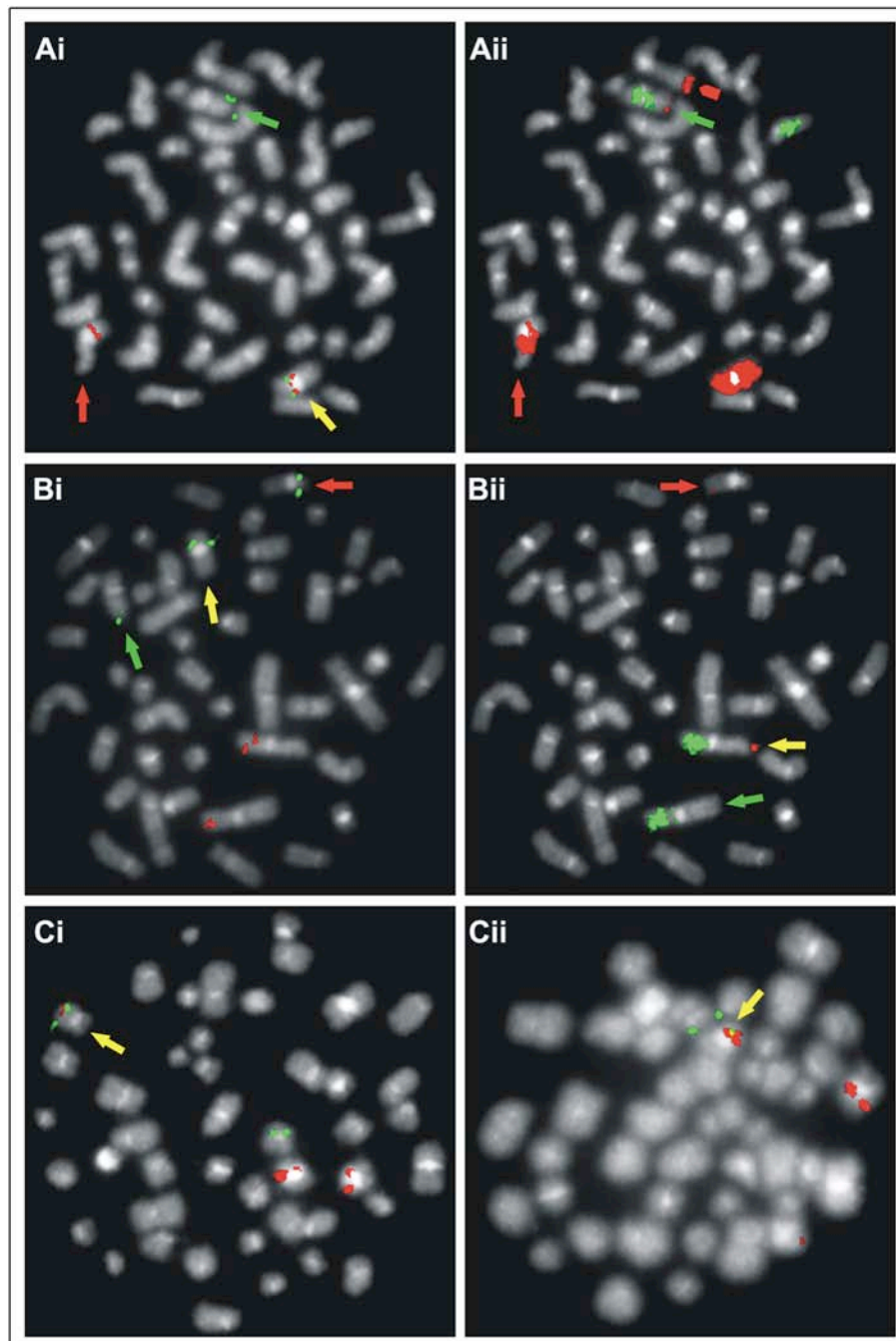


**Figure 21. FISH analysis of case 6.** (A) Metaphase hybridized with the *PAX5* locus-specific BAC clones RP11-220I1 (red) and RP11-12P15 (green) (Ai) and with whole chromosome painting probes for chromosome 9 (red) and 14 (green) (Aii). Arrows indicate the normal chromosome 9 (yellow), the der(9) (red) and the der(14) (green). Red arrowhead points to the der(3). (Bi) Metaphase that shows a *PAX5* split signal pattern using *PAX5*-spanning clones RP11-465P6 and RP11-431F4 (green) and two normal *TOP2B*-specific (3p24) signals with clone RP11-659P16 (red). Arrows denote the normal chromosome 9 (yellow), the der(9) (red) and the der(14) (green). (Bii) Same metaphase as in (Bi) displaying a translocation of the 3q-subtelomere region using clone 196F4 (red) and normal signals for 3p with 3p-arm-specific painting probe (green). Arrows point to the der(9) (red) and the der(3) (green) chromosomes and the normal chromosome 3 (yellow). (Ci) Hybridization of a metaphase with *PAX5*-spanning clones RP11-465P6 and RP11-431F4 (red) and the *WT1*-specific (11p13) clone RP11-74J1 (green) shows a disruption of *PAX5*. Arrow denotes the der(14). (Cii) Metaphase displaying a split signal with *PAX5*-spanning clones RP11-465P6 and RP11-431F4 (red) and signals for *LMO1* (11p15) using RP11-379P15 clone (green). Arrow indicates the der(9).

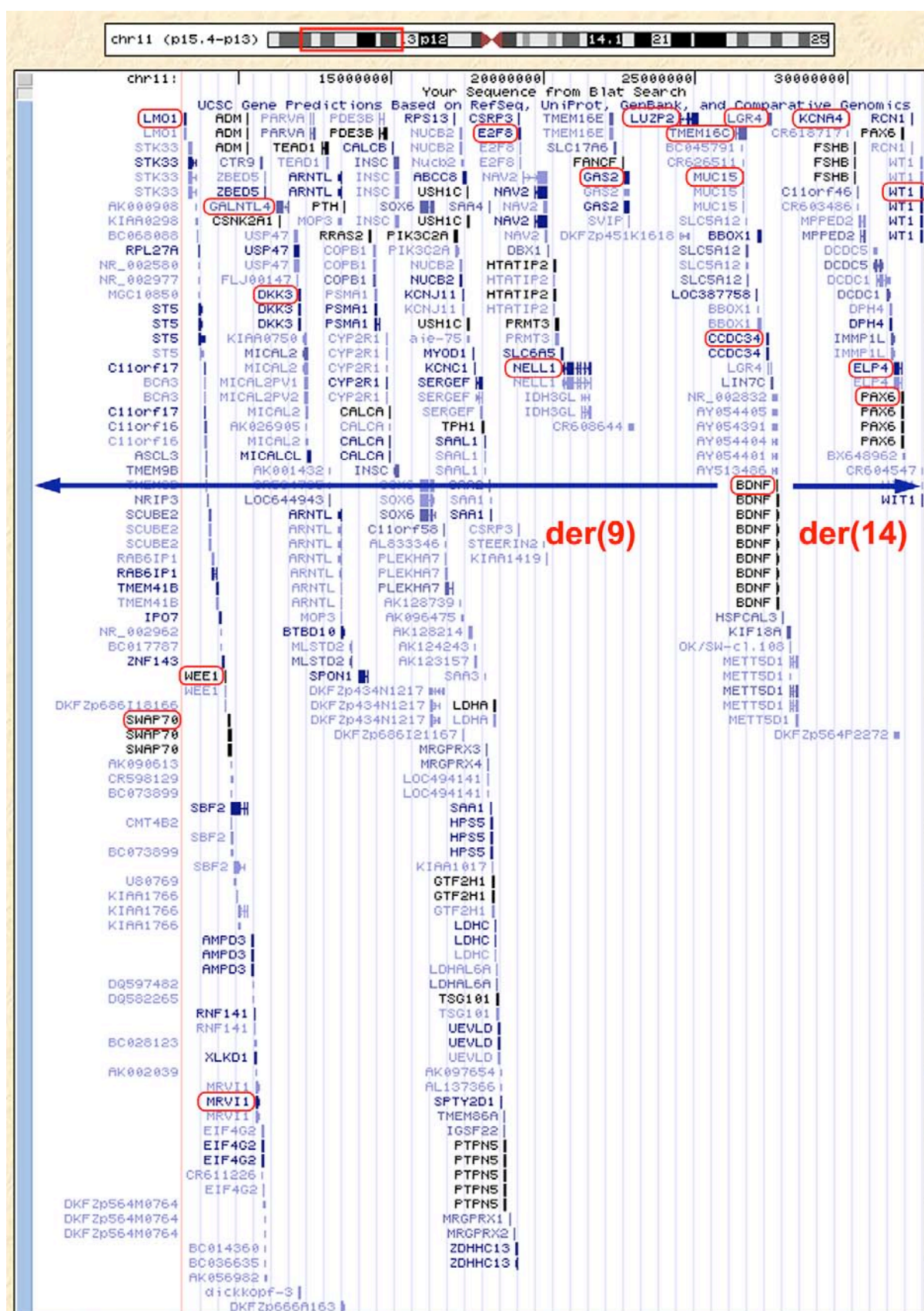


**Figure 22. Predicted breakpoint region at chromosome 11p15.4-p13.** Adapted screenshot from the UCSC Genome Browser on Human March 2006 Assembly ([www.genome.ucsc.edu](http://www.genome.ucsc.edu)) displaying all genes located within this region. Genes detected by locus-specific FISH clones (see Appendix, Table 1) are encircled and the localization of the signals on the respective derivative chromosomes is indicated by the arrows.



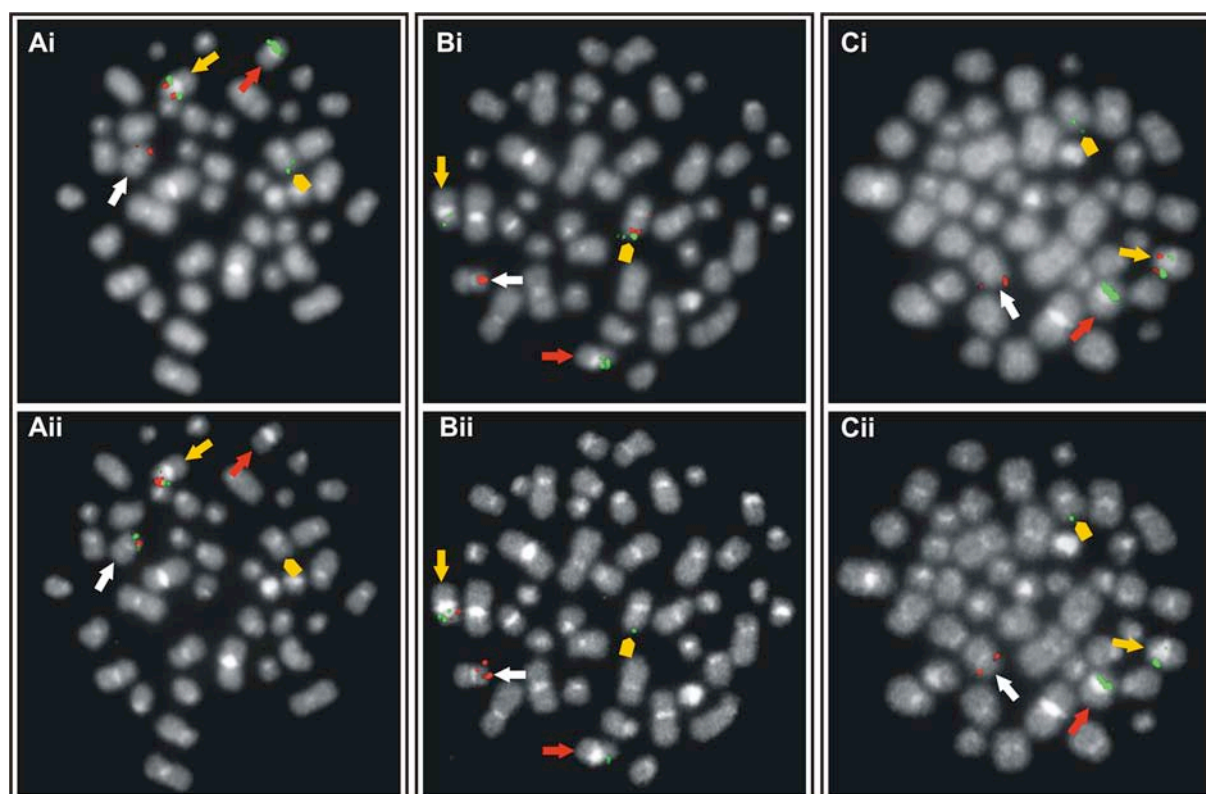


**Figure 23. Analysis of case 6 with FISH probes located at 11p.** *PAX5*-spanning clones RP11-465P6 and RP11-431F4 (green) were applied to metaphases in combination with 11p-specific clones. In all metaphases shown the arrows indicate the der(9) (yellow), the normal chromosomes 9 (red) and 11 (white), and the yellow arrowhead the der(14). **(Ai)** Hybridization with *PAX5*-spanning clones (green) in combination with *MRVI*-specific clone RP11-58H20 (red). **(Aii)** *NELL1*-specific clones RP11-3E17 and RP11-116O9 (red) in combination with *E2F8*-specific clone RP11-428C19 (green). All these 11p-specific clones were localized on the der(9). **(B)** The *ELP4* 5'-end specific clone RP5-1137O17 (red) was observed on the der(14) **(Bi)**, whereas the *LGR4* 3'-end-specific clone RP11-426P16 (red) was located on the der(9) **(Bii)**. **(C)** Metaphase hybridized with *LUZP2* 5'-end RP11-372B5 (red) **(Ci)** and *BDNF* 5'-end-specific clone RP11-52H5 (red) **(Cii)** shows the localization of *LUZP2* 5'-end on der(9) and deletion of the *BDNF* 5'-end encompassing clone.

As the FISH strategy was unsuccessful to delineate the *PAX5* partner gene, rapid amplification of cDNA ends (RACE) was performed, but also all RACE experiments using various primer combinations and PCR conditions, which should permit amplification of any fusion product resulting from every possible breakpoint within *PAX5* (Fig. 24 and Table 2 of Appendix) failed to identify the fusion partner.

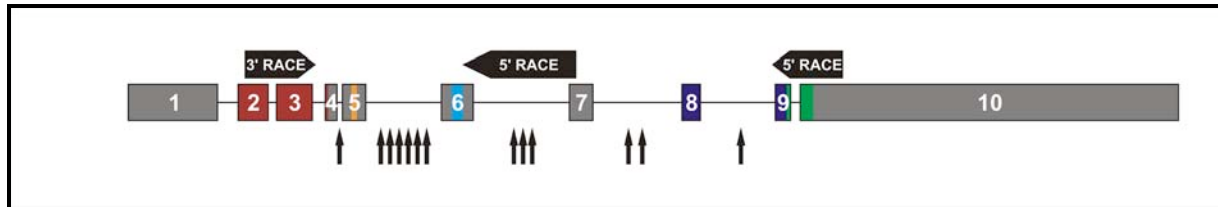


**Figure 24. *PAX5* RACE assay.** A schematic structure of the *PAX5* gene is depicted and all known breakpoints of *PAX5* fusions are indicated (arrows). Localizations of the different gene-specific RACE primers used in the first round of amplification are shown (arrowheads).

### Case 7

Case 7 showed a *PAX5*-split signal in about 62% of cells with additional 1-2 *PAX5* 5'-end signals. Cytogenetics revealed a particularly complex karyotype: 46,XY,add(1)(q44)[3],der(1)t(1;?)(p31;?)add(1)(q44)[3],-5,-8,del(9)(p13),del(11)(q23),+2mar[6cp]/46,XY[14].

Analysis of aberrant metaphases by FISH showed that the genes *ABL1* (9q34) (Fig. 25A) and *RCSD1* (1q24) (Fig. 25C) were located on a derivative chromosome, which carried the *PAX5* 5'-end signal strongly suggesting the presence of a dic(1;9)(p?;p13) (Fig. 25). Moreover, additional derivative chromosomes with *PAX5* signals were observed but not further analyzed. In concordance with the data obtained by FISH, RACE identified *HIPK1* located at 1p13 as novel *PAX5* fusion partner. Owing to the opposite transcriptional orientation of *PAX5* (centromere-telomere) and *HIPK1* (telomere-centromere) the formation of a dic(1;9)(p13;p13) as seen in this case or a complex rearrangement is required to generate a functional fusion gene.

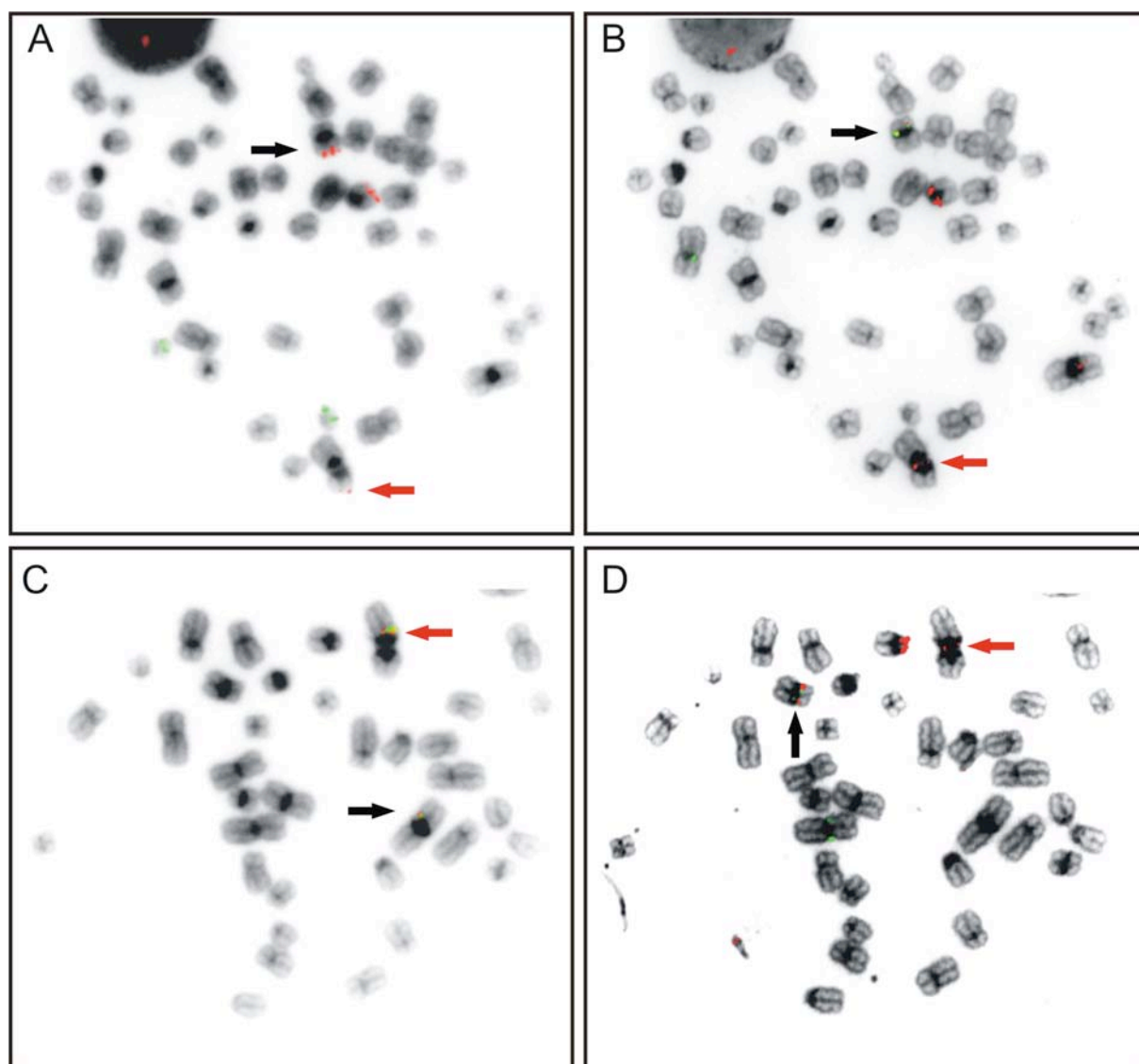


**Figure 25. FISH analysis of case 7.** (A) Metaphase hybridized with probes specific for the *BCR* (green) and *ABL1* (red) genes located at 22q11 and 9q34, respectively. (B) Same metaphase as in A hybridized with *PAX5* flanking clones RP11-22011 (red) and RP11-12P15 (green) clones. Arrows indicate the normal chromosome 9 (black) and the der(9) (red). (C) Metaphase hybridized with *RCSD1* 5'-end (red) and 3'-end-specific (green) probes located at 1q24. Arrows point to the normal chromosome 1 (black) and the dic(1;9). (D) Same metaphase as in C hybridized with *PAX5* 5'-end RP11-22011 (red) and *PAX5* 3'-end RP11-12P15 (green) specific clones. Arrows denote the normal chromosome 9 (black) and the dic(1;9) (red).

### 5.2.2. *PAX5* deletions

Recently, it was shown that apart from *PAX5* rearrangements, *PAX5* is also a target of other somatic mutations in particular monoallelic deletions, which in a significant proportion of the cases are focal and just affecting a few exons (Mullighan *et al*, 2007a). Although our *PAX5* FISH assay was not specifically designed for the detection of *PAX5* deletions *per se*, nevertheless a high percentage of the cases (about 10%) displayed monoallelic loss of the gene. Moreover, in approximately 4% of the non-rearranged cases focal deletions of the *PAX5* locus affecting either the 5' or the 3' region were detected. These cases were further analyzed using a panel of FISH probes, whose signal patterns reflected the size and the extent of the deletions. Examples of the most frequent patterns are described in the following.

### Pattern No. 1

In some cases hybridization with the *PAX5*-flanking BAC clones revealed a deletion of the 3'-clone RP11-12P15 in a significant proportion of the interphase nuclei (Fig. 26Ai), whereas after hybridization with the *PAX5*-specific cosmid a deletion of one entire copy of *PAX5* was observed (Fig. 26Aii). Further FISH analysis using *PAX5*-spanning probes RP11-465P6 and RP11-431F in combination with RP11-84P7 showed that the deletion encompassed also the region telomeric of *PAX5* (Fig. 26B). Moreover, a small second signal of the *PAX5*-spanning clones was observed, probably reflecting partial retention of the 5'-end clone RP11-465P6. This clone extends beyond the 5'-end of *PAX5* suggesting that the deletion starts in *PAX5* exon 1 or just upstream of exon 1 encompassing at least clone RP11-84P7 (Fig. 26).

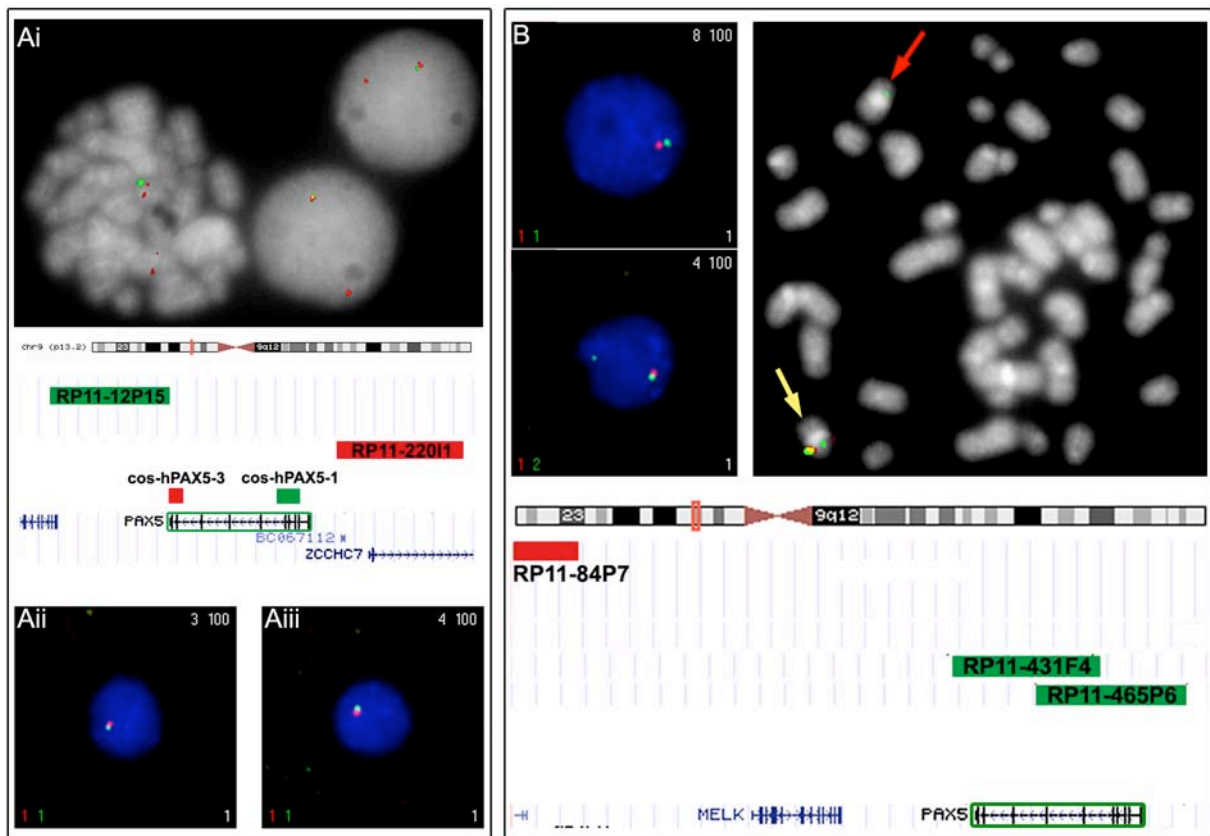


**Figure 26. *PAX5* deletion pattern no. 1.** (Ai) Metaphase and interphase nuclei hybridized with FISH probes RP11-220I1 (red) and RP11-12P15 (green) displaying deletion of one signal of RP11-12P15. (Aii) Hybridization of interphase nuclei with cos-hPAX5-1 (green) and cos-hPAX5-3 (red) that shows a deletion of one entire copy of *PAX5*. (B) Interphase and metaphase analysis with *PAX5*-spanning clones RP11-465P6 and RP11-431F4 (green) in combination with RP11-84P7 (red) demonstrate deletion of the region telomeric of *PAX5*. Arrows indicate the normal chromosome 9 (yellow) and the chromosome 9 with the interstitial deletion (red) showing a smaller signal resulting from partial retention of clone RP11-465P6. The schematic maps show the utilized FISH clones.



## Pattern No. 2

Some cases showed a deletion of the *PAX5*-flanking clone RP11-22011 (Fig. 27A), whereas hybridization of the *PAX5*-specific cosmid probes detected two normal copies of *PAX5* (Fig. 27B). Moreover, FISH analysis using the clone RP11-397D12 together with *PAX5*-spanning probes demonstrated two normal signals (Fig. 27D) suggesting the presence of a focal deletion encompassing only the region, which is spanned by RP11-22011 (Fig. 27). Of note, this pattern was also observed in *ETV6-RUNX1* positive cases.

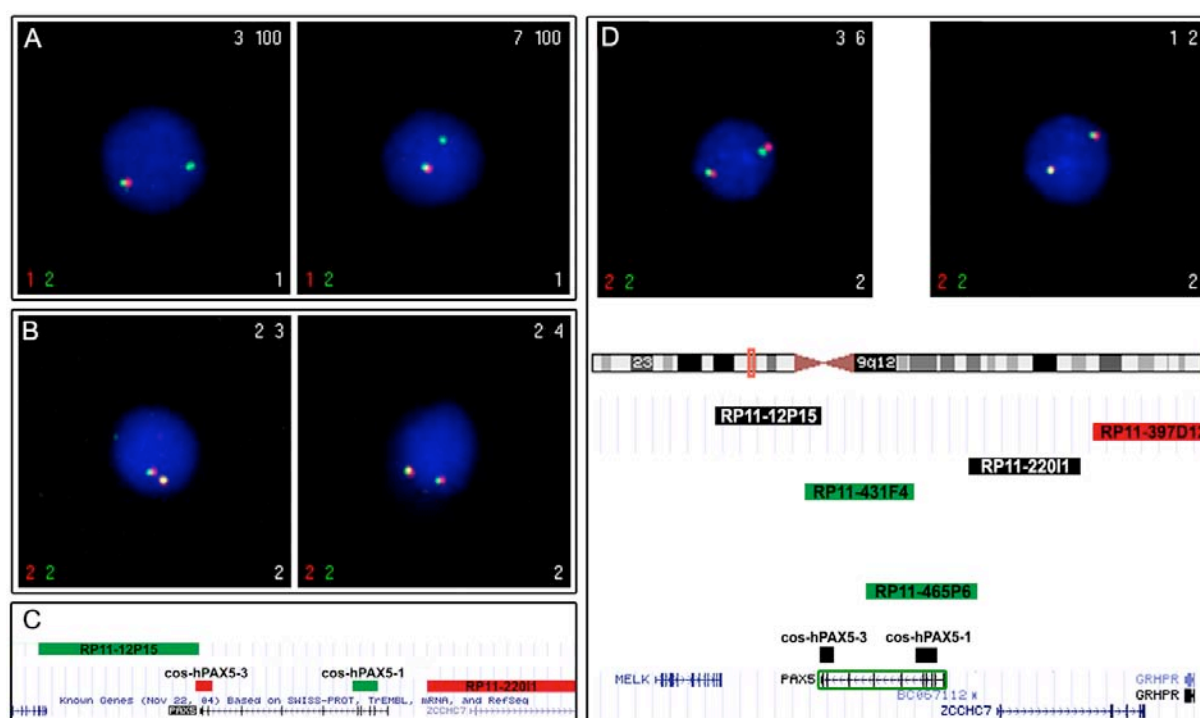


**Figure 27. *PAX5* deletion pattern no. 2.** Interphase nuclei hybridized with (A) *PAX5*-flanking clones RP11-22011 (red) and RP11-12P15 (green) displaying a deletion of RP11-22011 and (B) *PAX5*-specific probes cos-hPAX-1 (green) and cos-hPAX5-3 (red) showing a normal pattern. (D) Hybridization of interphase nuclei with *PAX5* probes RP11-465P6 and RP11-431F4 (green) in combination with RP11-397D12 (red), which demonstrates normal signals. Schematic representation of the localization of the utilized FISH clones are shown in the lower panels.

**Pattern No. 3**

A third different pattern was also observed in both *ETV6-RUNX1* positive and negative cases. FISH analysis with *PAX5* BAC clones RP11-220I1 and RP11-12P12 showed a deletion of the 5'-end flanking clone RP11-220I1 (Fig. 28Ai and Aii) and also a deletion of the *PAX5* 5'-specific probe cos-hPAX5-1 (Fig. 28Aiii). In the example shown, hybridization was done on *ETV6-RUNX1* positive metaphases to ensure analysis of aberrant cells and to verify that the *PAX5* deletion concurs in the same leukemic clone (Fig. 28A and B).

FISH was also performed using the *PAX5*-spanning clones in combination with RP11-397D12, which showed either complete loss of the clone or a smaller but clearly visible second signal suggesting a partial deletion of the clone (Fig. 28C). This pattern may on the one hand depend on the hybridization efficiency or indicate the presence of two different subclones. Of note, the remaining 3'-part of *PAX5* could not be detected with the *PAX5*-spanning clones, which possible results from a weaker hybridization efficiency of clone RP11-431F4. Together, this type of deletion encompasses only the 5'-end of *PAX5* and extends at least beyond the *ZCCHC7* gene (Fig. 28C).

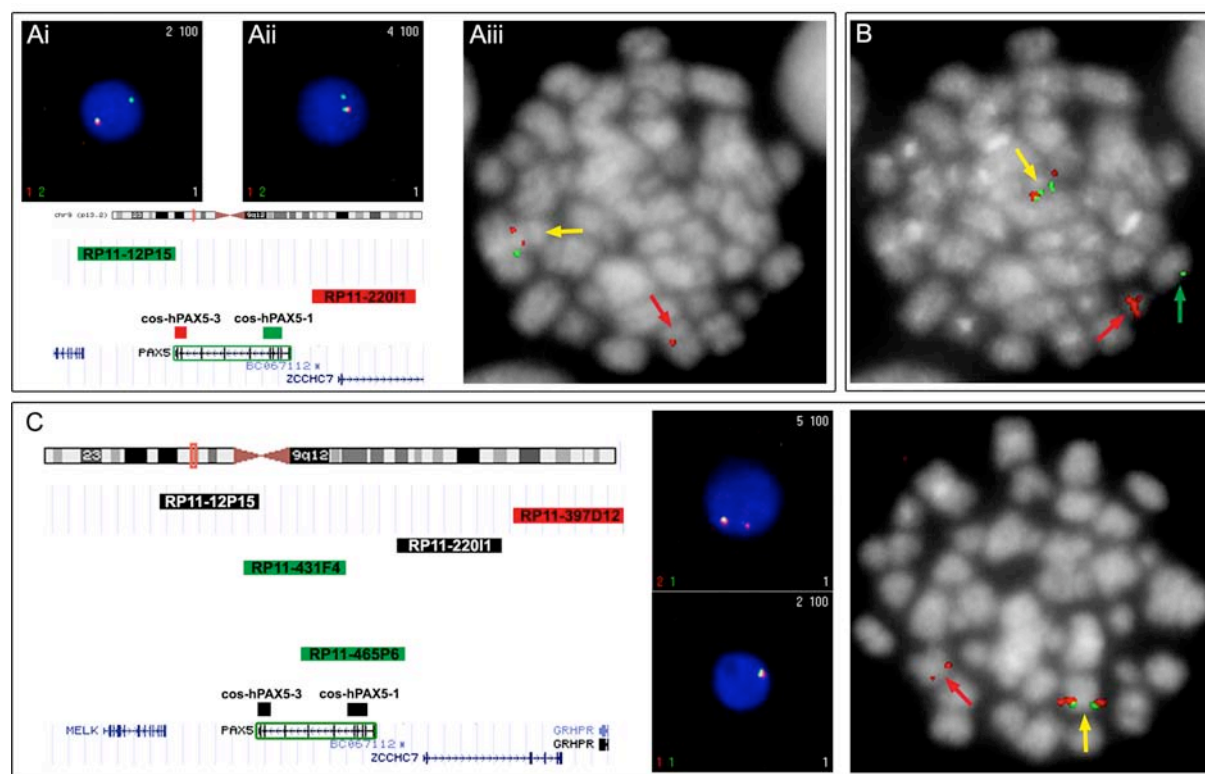


**Figure 28. FISH analysis of *PAX5* deletion pattern 3.** (Ai-ii) Hybridization of interphase nuclei with *PAX5* RP11-220I1 (red) and RP11-12P15 (green) showing a deletion of the 5'-end flanking clone RP11-220I1. (Aiii) Metaphase hybridized with *PAX5* cos-hPAX5-1 (green) and cos-hPAX5-3 (red) that display a *PAX5* 5'-end deletion. (B) The LSI TEL (green)-AML1 (red) ES Dual Color Translocation probe (Abbott Molecular) was applied on the same metaphase as in (A). Arrows point to the der(12), which harbors the *ETV6-RUNX1* (*TEL-AML1*) fusion (yellow), and to the normal chromosomes 12 (green) and 21 (red). (C) Metaphase and interphase nuclei analysis with the *PAX5*-spanning probes RP11-465P6 and RP11-431F4 (green) in combination with RP11-397D12 (red) that revealed either no, a partial or a complete deletion of clone RP11-397D12. (A and C) Arrows indicate the normal (yellow) and the derivative chromosomes 9 (red). Schematic maps depict the applied FISH clones.

**Pattern No. 4**

The most frequently observed deletion pattern was a complete deletion of *PAX5* that occurred in approximately 10% of the analyzed patients and in nearly all cases was associated with a cytogenetically detectable deletion of 9p. These cases were only analyzed with the *PAX5*-flanking clones RP11-220I1 and RP11-12P15.

In Figure 29 an example is shown that displays a deletion of one entire copy of *PAX5*.

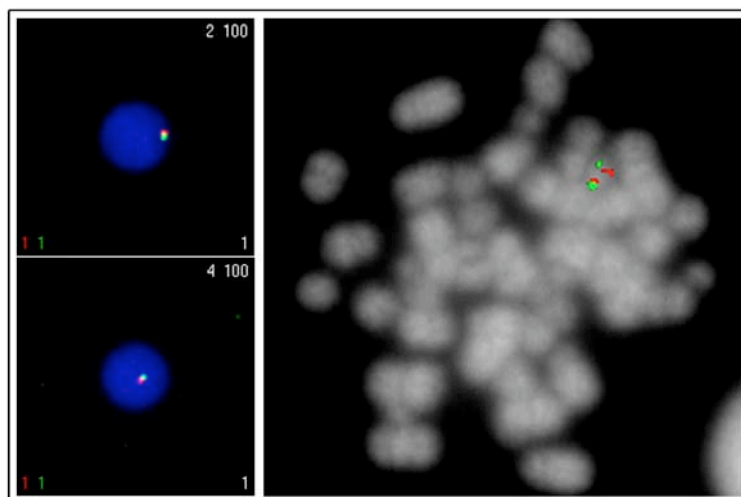


**Figure 29. FISH analysis of *PAX5* deletion pattern 4.** Interphase and metaphase nuclei hybridized with *PAX5*-flanking probes RP11-220I1 (red) and RP11-12P15 (green), which display a deletion of one copy of *PAX5*.

### A unique case

In one single patient cytogenetic analysis showed del(9)(p22) suggesting a deletion telomeric of *PAX5*. However, 54% of the interphase nuclei displayed only one signal for the *PAX5* 3'-flanking BAC clone and no other signals were observed (Fig. 30A). Hybridization with the *PAX5* cosmid probes demonstrated deletion of one entire copy of *PAX5* and one apparently intact allele (Fig. 30B). Therefore, FISH analysis indicated loss of one *PAX5* allele accompanied by a deletion of the region upstream of *PAX5* encompassing *ZCCHC7* on the second chromosome.

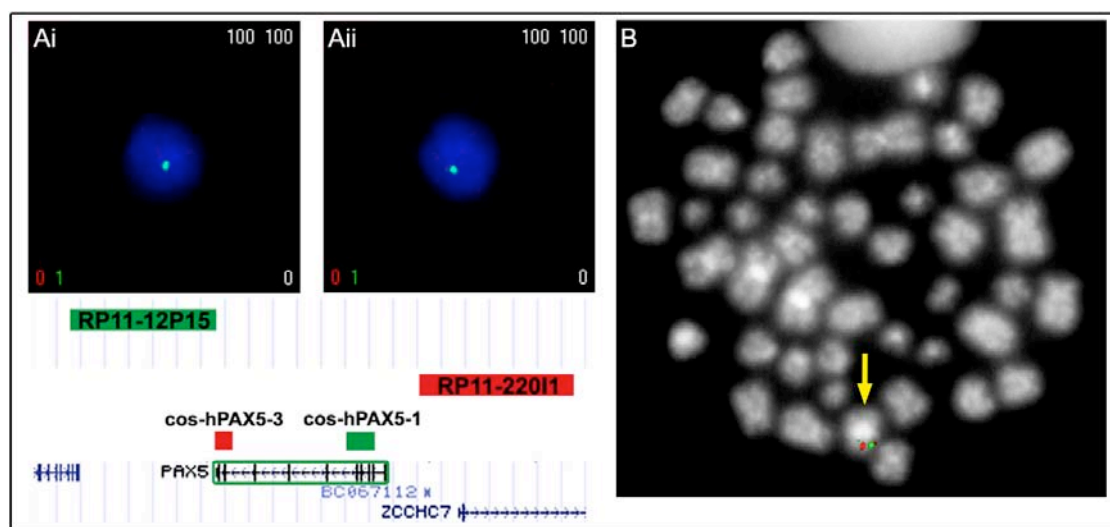


**Figure 30. A special deletion pattern.** (Ai-ii) Examples of interphase nuclei hybridized with RP11-12P15 (green) and RP11-220I1 (red) that show only one *PAX5* 3'-end RP11-12P15 signal. (B) Metaphase analyzed with *PAX5* cos-hPAX5-1 (green) and cos-hPAX5-3 (red) displaying a deletion of one *PAX5* allele. Arrow points to the "normal" chromosome 9. The schematic map at the bottom shows of the localization of the applied FISH clones.

## CHAPTER 6

### 6. DISCUSSION

#### The discovery of the *PAX5* fusion genes

The aim of the presented research project was to determine the overall incidence of *PAX5* rearrangements and the whole spectrum of fusion partners in childhood ALL in a population-based survey. At the time this study was initiated only the *PAX5-IGH@* activating translocation (Busslinger *et al*, 1996; Iida *et al*, 1996) and one single *PAX5* fusion gene, namely *PAX5-ETV6* were known (Cazzaniga *et al*, 2001; Strehl *et al*, 2003).

During the time this study was still ongoing, genome-wide analysis using high-resolution SNP arrays revealed chromosomal imbalances resulting in *PAX5* fusions in 2.1% (Mullighan *et al*, 2007a) and 2% (Kawamata *et al*, 2008) of childhood B-cell precursor ALL (BCP-ALL). However, our study still represents the first population-based study using a FISH assay, which allows for the detection of all possible *PAX5* rearrangements irrespective of chromosomal imbalances. Our data corroborate the finding that *PAX5* fusions occur exclusively in BCP-ALL and at an incidence of about 2.5%.

Intriguingly, *PAX5* can fuse to a multitude of different partner genes encoding transcription factors, structural proteins, a tyrosine kinase, and some proteins of still unknown function. All breakpoints within *PAX5* occur in intron 5 or downstream (except for the *PAX5-ETV6* rearrangement) (Fig. 31) fusing at least the *PAX5* DNA-binding paired domain to the C-terminal region or even the entire protein encoded by the partner gene (Bousquet *et al*, 2007; Mullighan *et al*, 2007a; Nebral *et al*, 2007; Kawamata *et al*, 2008; Nebral *et al*, in press). Therefore, all *PAX5* chimeric proteins are predicted to retain the ability to bind to *PAX5* target genes, but would no longer provide normal transcriptional regulatory functions.

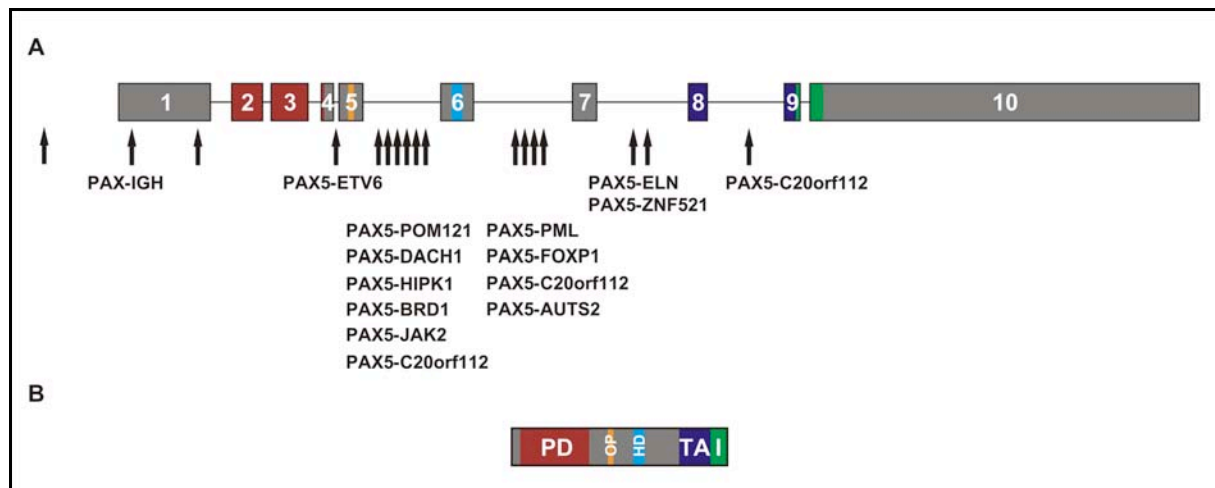


**Figure 31. *PAX5* breakpoints.** (A) Schematic representation of the *PAX5* gene structure. Arrows indicate the breakpoints in the respective introns of all known *PAX5* translocations (intron sizes are not in scale). (B) *PAX5* protein showing the corresponding protein domains. PD, paired domain; OP, octapeptide domain; HD, homeodomain; TA, transactivation domain; I, inhibitory domain.

### The relevance of *PAX5* deletions

The second major finding of the SNP array studies was the frequent deletion of regulators of B-cell development, amongst which *PAX5* was affected in approximately 30% of BCP-ALL (Kuiper *et al*, 2007; Mullighan *et al*, 2007a). Intriguingly, *PAX5* deletions were also detected in *ETV6-RUNX1* positive BCP-ALL (Mullighan *et al*, 2007a; Parker *et al*, 2008) and may, thus, belong to the cooperating mutations required to complete leukemogenesis. Yet, *PAX5* deletions occur only in about 30% of the cases and to some extent coincide with other genetic lesions such as deletions of the second *ETV6* allele or *CDKN2A* (S. Strehl, K. Nebral, M. König *et al.*, *unpublished observation*). Thus, whether *PAX5* deletions indeed belong to those secondary genetic lesions required to convert an *ETV6-RUNX1* positive preleukemic clone to overt leukemia remains to be proven.

Monoallelic loss of *PAX5* is proposed to lead to haploinsufficiency of the BSAP protein contributing to the differentiation arrest seen in BCP-ALL (Kuiper *et al*, 2007; Mullighan *et al*, 2007a). This assumption is based on the initial observation that only a single *Pax5* allele is transcribed during the earliest phase of B-cell commitment and that B-cell differentiation relies on the switch to biallelic expression (Nutt *et al*, 1999b). Consequently, loss of a wild-type allele would eliminate the ability to switch on biallelic transcription. However, recent investigations clearly show biallelic expression of *Pax5* at all stages of B-cell development (Fuxa & Busslinger, 2007). The hypothesis that haploinsufficiency of *PAX5* may contribute to a differentiation block (Kuiper *et al*, 2007; Mullighan *et al*, 2007a) is further challenged by the fact that in heterozygous *Pax5*<sup>+/-</sup> mice B-cell development is normal (Urbanek *et al*, 1994; Nutt *et al*, 1999b). Moreover, inactivation of one *Pax5* allele in mature B-cells in

heterozygous *Cd19-cre Pax5<sup>fl/+</sup>* mice in the absence of other oncogenic lesions is not sufficient to induce tumor development. On the other hand, complete loss of *Pax5* in late B-cells results in the development of aggressive progenitor cell lymphoma (Cobaleda *et al*, 2007a). Although some of the deletions in BCP-ALL are confined to *PAX5*, in several cases even to a few exons (focal deletions), many of them are broader and encompass a number of genes, whose concomitant deletion/haploinsufficiency may as well promote leukemogenesis.

### Hypomorphic alleles and splice variants

Alternative splicing of pre-mRNA is a fundamental process that increases proteomic diversity and contributes to genetic variability. Increasing evidence substantiates that splicing defects (e.g. caused by inherited or somatic mutations in regulatory elements) not only account for inherited diseases susceptibility but also increase proteome complexity in cancer cells, and that alternative splicing may well be one of the basic causes for cancerogenesis (Kalnina *et al*, 2005; Venables, 2006; Skotheim & Nees, 2007). In this regard, also for several members of the *PAX* gene family a cancer-specific expression of certain isoforms has been observed (reviewed by (Barr, 1997; Robson *et al*, 2006; Lang *et al*, 2007; Wang *et al*, 2008)).

Several human *PAX5* isoforms have been described that result either from transcription of two alternative promoters leading to expression of exon 1A or 1B containing transcripts (Busslinger *et al*, 1996), or from alternative splicing of exons that encode the C-terminal transactivation and inhibitory domains (Robichaud *et al*, 2004; Sekine *et al*, 2007). Expression of different *PAX5* isoforms was observed in B-cells of normal healthy donors (Robichaud *et al*, 2004) but also a possible association with childhood leukemia was reported (Sadakane *et al*, 2007). In this respect, we have identified a novel human *PAX5* isoform that skips exon 2, and which may specifically occur in BCP-ALL (Krehan *et al*, in preparation).

Therefore, in-depth studies are required to elucidate whether the differential expression of *PAX5* alternatively spliced transcripts is of any pathological relevance or reflects physiological stages of B-cell development. In particular, imbalances in the expression of *PAX5* isoforms may result in modulatory effects on downstream genes.

Deletions within the *PAX5* gene, which are confined to a subset of internal exons result in the expression of so-called hypomorphic alleles, which resemble potential splice variants. However, such splice variants have so far not been detected in normal B-lymphocytes suggesting that they are specifically generated by the intragenic deletion events. Recently, similar focal deletions of *IKZF1* (Mullighan *et al*, 2008) and *ERG* (Mullighan *et al*, 2007b) in *BCR-ABL1* positive ALL and a novel BCP-ALL subtype with a unique gene expression profile, respectively, were identified. Thus, focal mono-allelic intragenetic deletions may represent a distinct mechanism to generate tumor-specific isoforms.



### The potential oncogenic function of PAX5 mutants

Several lines of evidence suggest that the various *PAX5* aberrations found in BCP-ALL result in an impairment of *PAX5* activity rather than a complete loss of function.

One of the defining features of BCP-ALL blast cells is the expression of the cell surface antigens CD19 and/or CD79A and/or CD22, which were readily expressed in both the *PAX5*-rearranged cases and those with monoallelic *PAX5* deletions. Even concomitant mutations of the second allele did not abolish expression of the CD19 and CD79A proteins. In leukemic blast cells, also on the transcriptional level no correlation between *PAX5* mutation status and *CD19* and *CD79A* expression was observed (Mullighan *et al*, 2007a; Kawamata *et al*, 2008). While the lack of *CD19* responsiveness, whose expression is strictly *PAX5*-dependent, to *PAX5* mutation remains elusive, transcription of *CD79A* is also initiated by EBF1 and its expression can be activated independently of *PAX5* (Hagman & Lukin, 2005; Pongubala *et al*, 2008). Although gene expression profiling identified a differential gene expression signature between *PAX5*-deleted and *PAX5* wild-type *ETV6-RUNX1* BCP-ALL (Mullighan *et al*, 2007a), the differentially expressed genes included only a small subset of those regulated by *PAX5*.

*In vitro*, using a *luc*-CD19 reporter gene assay *PAX5* mutants showed reduced transcriptional activity as compared to wild-type *PAX5* (Bousquet *et al*, 2007; Mullighan *et al*, 2007a; Kawamata *et al*, 2008), and mutations that affect the *PAX5* DNA-binding paired domain had a lower binding capacity to *CD19* promoter sequences (Mullighan *et al*, 2007a). In contrast to *PAX5* DNA-binding and internal deletion mutants, which have only a weak competitive activity (Mullighan *et al*, 2007a), *PAX5* fusion genes, appear to act in a dominant-negative manner over wild-type *PAX5* (Bousquet *et al*, 2007; Mullighan *et al*, 2007a; Fazio *et al*, 2008; Kawamata *et al*, 2008). Thus, *PAX5* chimera are considered to function as aberrant transcription factors that antagonize *PAX5* activity provided by the second, wild-type allele (Cobaleda *et al*, 2007b).

Recent data obtained by *in vitro* transfection experiments with the *PAX5-C20orf112* fusion also suggest that the antagonizing function of the chimeric protein is confined to a subset of *PAX5* target genes (Kawamata *et al*, 2008). This observation raises the question whether the various *PAX5* chimera deregulate a common, or dependent on the moieties provided by the partner protein, distinct sets of target genes.

While *in vitro* studies are certainly required to determine the functional consequences of *PAX5* mutants, only validation of the data in primary leukemic blast cells will prove their true impact. In this respect, transfection of the post-germinal-center B-cell line DG75 with *PAX5-ELN* resulted in downregulation of the *PAX5* target genes *BLNK*, *LEF1*, and *CD79A*, but in leukemic pre-B cells these genes were not affected (Bousquet *et al*, 2007). These data suggest a cellular context-dependent impact of the *PAX5* fusion proteins, and that the results

obtained by *in vitro* transfection experiments - in particular using lymphoma cells, which are derived from later stages of B-cell development - may not faithfully reflect their effect in the context of B-cell precursor leukemia.

The B-cell developmental stage-dependent function of *Pax5* provides a possible explanation for this observation. While during the early stages of B-cell development *Pax5* expression is required for B-cell development, its downregulation is pivotal for terminal plasma cell differentiation. Thus, reliant on the developmental stage of the B-cell both loss-of-function and gain-of-function mutation of PAX5 may disrupt B-cell homeostasis.

Indeed, in B-cell lymphoma derived from later stages of B-cell development ectopic expression of *PAX5* suggests a gain-of-function mutation (Thomas-Tikhonenko & Cozma, 2008). In these tumors, which mostly arise from germinal-center B-cells with a functional BCR, enforced *PAX5* expression results in ligand-independent BCR signaling (Cozma *et al*, 2007). Thus, increased expression of *PAX5* in post-germinal center B-cells promotes tumor growth by perturbing the *PAX5*-dependent B-cell gene expression program or a block in terminal differentiation into plasma cells by failed *PAX5* repression (Shaffer *et al*, 2002; Cobaleda *et al*, 2007b). In this cellular context, *PAX5* most likely exerts its oncogenic effects via the functional BCR (Cozma *et al*, 2007; Thomas-Tikhonenko & Cozma, 2008). Loss of *Pax5* in the context of strong BCR signaling results in forward differentiation of mature B-cells to plasma cells, whereas *Pax5* inactivation in the absence of BCR signaling initiates the reversal of differentiation to uncommitted progenitors (Cobaleda *et al*, 2007a).

In contrast, in BCP-ALL, which is derived from immature pro- or pre-B-cells *PAX5* mutants are without exception loss-of-function mutations, which impair but not abolish *PAX5* function. However, the impact of the *PAX5* mutants on the finely tuned B-cell transcription network has yet to be elucidated *in vitro* and more importantly, *in vivo*.

### Concluding remarks

Although the fundamental role of *PAX5* for B-cell development was recognized almost two decades ago, until very recently its possible involvement in B-cell malignancy has been essentially neglected. Only now *PAX5* also emerges as a major player in leukemogenesis and it will probably take at least another two decades before the potential oncogenic role of *PAX5* mutation will be finally elucidated. Dissecting the impact of these peculiar mutants on the complex B-cell development regulatory transcriptional network with its multiple combinatorial inputs and feedback loops will be a challenging task.

## CHAPTER 7

### 7. References

- Adolfsson, J., Mansson, R., Buza-Vidas, N., Hultquist, A., Liuba, K., Jensen, C.T., Bryder, D., Yang, L., Borge, O.J., Thoren, L.A., Anderson, K., Sitnicka, E., Sasaki, Y., Sigvardsson, M. & Jacobsen, S.E. (2005) Identification of Flt3+ lympho-myeloid stem cells lacking erythro-megakaryocytic potential a revised road map for adult blood lineage commitment. *Cell*, **121**, 295-306.
- Aifantis, I., Raetz, E. & Buonamici, S. (2008) Molecular pathogenesis of T-cell leukaemia and lymphoma. *Nat Rev Immunol*, **8**, 380-390.
- Akashi, K., Traver, D., Miyamoto, T. & Weissman, I.L. (2000) A clonogenic common myeloid progenitor that gives rise to all myeloid lineages. *Nature*, **404**, 193-197.
- Armstrong, S.A. & Look, A.T. (2005) Molecular genetics of acute lymphoblastic leukemia. *J Clin Oncol*, **23**, 6306-6315.
- Attarbaschi, A., Mann, G., Konig, M., Steiner, M., Strehl, S., Schreiberhuber, A., Schneider, B., Meyer, C., Marschalek, R., Borkhardt, A., Pickl, W.F., Lion, T., Gadner, H., Haas, O.A. & Dworzak, M.N. (2006) Mixed lineage leukemia-rearranged childhood pro-B and CD10-negative pre-B acute lymphoblastic leukemia constitute a distinct clinical entity. *Clin Cancer Res*, **12**, 2988-2994.
- Barr, F.G. (1997) Chromosomal translocations involving paired box transcription factors in human cancer. *Int J Biochem Cell Biol*, **29**, 1449-1461.
- Barr, F.G. (2001) Gene fusions involving PAX and FOX family members in alveolar rhabdomyosarcoma. *Oncogene*, **20**, 5736-5746.
- Barr, F.G., Fitzgerald, J.C., Ginsberg, J.P., Vanella, M.L., Davis, R.J. & Bennicelli, J.L. (1999) Predominant expression of alternative PAX3 and PAX7 forms in myogenic and neural tumor cell lines. *Cancer Res*, **59**, 5443-5448.
- Baumann Kubetzko, F.B., Di Paolo, C., Maag, C., Meier, R., Schafer, B.W., Betts, D.R., Stahel, R.A. & Himmelfmann, A. (2004) The PAX5 oncogene is expressed in N-type neuroblastoma cells and increases tumorigenicity of a S-type cell line. *Carcinogenesis*, **25**, 1839-1846.
- Bernardin, F., Yang, Y., Cleaves, R., Zahurak, M., Cheng, L., Civin, C.I. & Friedman, A.D. (2002) TEL-AML1, expressed from t(12;21) in human acute lymphocytic leukemia, induces acute leukemia in mice. *Cancer Res*, **62**, 3904-3908.
- Bertrand, P., Bastard, C., Maingonnat, C., Jardin, F., Maisonneuve, C., Courel, M.N., Ruminy, P., Picquenot, J.M. & Tilly, H. (2007) Mapping of MYC breakpoints in 8q24 rearrangements involving non-immunoglobulin partners in B-cell lymphomas. *Leukemia*, **21**, 515-523.
- Bouchard, M., Schleifer, A., Eisenhaber, F. & Busslinger, M. (2003) Evolution and function of Pax Genes. *Encyclopedia of the human Genome*.
- Bousquet, M., Broccardo, C., Quelen, C., Meggetto, F., Kuhlein, E., Delsol, G., Dastugue, N. & Brousset, P. (2007) A novel PAX5-ELN fusion protein identified in B-cell acute lymphoblastic leukemia acts as a dominant negative on wild-type PAX5. *Blood*, **109**, 3417-3423.
- Busslinger, M., Klix, N., Pfeffer, P., Graninger, P.G. & Kozmik, Z. (1996) Deregulation of PAX-5 by translocation of the Emu enhancer of the IgH locus adjacent to two alternative PAX-5 promoters in a diffuse large-cell lymphoma. *Proc Natl Acad Sci U S A*, **93**, 6129-6134.
- Cazzaniga, G., Daniotti, M., Tosi, S., Giudici, G., Aloisi, A., Pogliani, E., Kearney, L. & Biondi, A. (2001) The paired box domain gene PAX5 is fused to ETV6/TEL in an acute lymphoblastic leukemia case. *Cancer Res*, **61**, 4666-4670.
- Cobaleda, C., Jochum, W. & Busslinger, M. (2007a) Conversion of mature B cells into T cells by dedifferentiation to uncommitted progenitors. *Nature*, **449**, 473-477.
- Cobaleda, C., Schebesta, A., Delogu, A. & Busslinger, M. (2007b) Pax5: the guardian of B cell identity and function. *Nat Immunol*, **8**, 463-470.
- Cozma, D., Yu, D., Hodawadekar, S., Azvolinsky, A., Grande, S., Tobias, J.W., Metzgar, M.H., Paterson, J., Erikson, J., Marafioti, T., Monroe, J.G., Atchison, M.L. & Thomas-Tikhonenko, A. (2007)

- B cell activator PAX5 promotes lymphomagenesis through stimulation of B cell receptor signaling. *J Clin Invest*, **117**, 2602-2610.
- Czerny, T., Schaffner, G. & Busslinger, M. (1993) DNA sequence recognition by Pax proteins: bipartite structure of the paired domain and its binding site. *Genes Dev*, **7**, 2048-2061.
- Davis, R.J., D'Cruz, C.M., Lovell, M.A., Biegel, J.A. & Barr, F.G. (1994) Fusion of PAX7 to FKHR by the variant t(1;13)(p36;q14) translocation in alveolar rhabdomyosarcoma. *Cancer Res*, **54**, 2869-2872.
- Delogu, A., Schebesta, A., Sun, Q., Aschenbrenner, K., Perlot, T. & Busslinger, M. (2006) Gene repression by Pax5 in B cells is essential for blood cell homeostasis and is reversed in plasma cells. *Immunity*, **24**, 269-281.
- Einsiedel, H.G., von Stackelberg, A., Hartmann, R., Fengler, R., Schrappe, M., Janka-Schaub, G., Mann, G., Hahlen, K., Gobel, U., Klingebiel, T., Ludwig, W.D. & Henze, G. (2005) Long-term outcome in children with relapsed ALL by risk-stratified salvage therapy: results of trial acute lymphoblastic leukemia-relapse study of the Berlin-Frankfurt-Munster Group 87. *J Clin Oncol*, **23**, 7942-7950.
- Fasching, K., Panzer, S., Haas, O.A., Marschalek, R., Gadner, H. & Panzer-Grumayer, E.R. (2000) Presence of clone-specific antigen receptor gene rearrangements at birth indicates an in utero origin of diverse types of early childhood acute lymphoblastic leukemia. *Blood*, **95**, 2722-2724.
- Fazio, G., Palmi, C., Rolink, A., Biondi, A. & Cazzaniga, G. (2008) PAX5/TEL acts as a transcriptional repressor causing down-modulation of CD19, enhances migration to CXCL12, and confers survival advantage in pre-B1 cells. *Cancer Res*, **68**, 181-189.
- Fischer, S., Mann, G., Konrad, M., Metzler, M., Ebetsberger, G., Jones, N., Nadel, B., Bodamer, O., Haas, O.A., Schmitt, K. & Panzer-Grumayer, E.R. (2007) Screening for leukemia- and clone-specific markers at birth in children with T-cell precursor ALL suggests a predominantly postnatal origin. *Blood*, **110**, 3036-3038.
- Fitzsimmons, D., Hodsdon, W., Wheat, W., Maira, S.M., Wasylyk, B. & Hagman, J. (1996) Pax-5 (BSAP) recruits Ets proto-oncogene family proteins to form functional ternary complexes on a B-cell-specific promoter. *Genes Dev*, **10**, 2198-2211.
- Forestier, E., Gauffin, F., Andersen, M.K., Autio, K., Borgstrom, G., Golovleva, I., Gustafsson, B., Heim, S., Heinonen, K., Heyman, M., Hovland, R., Johannsson, J.H., Kerndrup, G., Rosenquist, R., Schoumans, J., Swolin, B., Johannsson, B. & Nordgren, A. (2008) Clinical and cytogenetic features of pediatric dic(9;20)(p13.2;q11.2)-positive B-cell precursor acute lymphoblastic leukemias: a Nordic series of 24 cases and review of the literature. *Genes Chromosomes Cancer*, **47**, 149-158.
- Fuxa, M. & Busslinger, M. (2007) Reporter gene insertions reveal a strictly B lymphoid-specific expression pattern of Pax5 in support of its B cell identity function. *J Immunol*, **178**, 8222-8228.
- Fuxa, M., Skok, J., Souabni, A., Salvagiotto, G., Roldan, E. & Busslinger, M. (2004) Pax5 induces V-to-DJ rearrangements and locus contraction of the immunoglobulin heavy-chain gene. *Genes Dev*, **18**, 411-422.
- Galili, N., Davis, R.J., Fredericks, W.J., Mukhopadhyay, S., Rauscher, F.J., 3rd, Emanuel, B.S., Rovera, G. & Barr, F.G. (1993) Fusion of a fork head domain gene to PAX3 in the solid tumour alveolar rhabdomyosarcoma. *Nat Genet*, **5**, 230-235.
- Garvie, C.W., Hagman, J. & Wolberger, C. (2001) Structural studies of Ets-1/Pax5 complex formation on DNA. *Mol Cell*, **8**, 1267-1276.
- George, T.I., Wrede, J.E., Bangs, C.D., Cherry, A.M., Warnke, R.A. & Arber, D.A. (2005) Low-grade B-Cell lymphomas with plasmacytic differentiation lack PAX5 gene rearrangements. *J Mol Diagn*, **7**, 346-351.
- Goldberg, J.M., Silverman, L.B., Levy, D.E., Dalton, V.K., Gelber, R.D., Lehmann, L., Cohen, H.J., Sallan, S.E. & Asselin, B.L. (2003) Childhood T-cell acute lymphoblastic leukemia: the Dana-Farber Cancer Institute acute lymphoblastic leukemia consortium experience. *J Clin Oncol*, **21**, 3616-3622.
- Greaves, M.F. & Wiemels, J. (2003) Origins of chromosome translocations in childhood leukaemia. *Nat Rev Cancer*, **3**, 639-649.
- Hagman, J. & Lukin, K. (2005) Early B-cell factor 'pioneers' the way for B-cell development. *Trends Immunol*, **26**, 455-461.

- Harris, R.G., White, E., Phillips, E.S. & Lillycrop, K.A. (2002) The expression of the developmentally regulated proto-oncogene Pax-3 is modulated by N-Myc. *J Biol Chem*, **277**, 34815-34825.
- Hong, D., Gupta, R., Ancliff, P., Atzberger, A., Brown, J., Soneji, S., Green, J., Colman, S., Piacibello, W., Buckle, V., Tsuzuki, S., Greaves, M. & Enver, T. (2008) Initiating and cancer-propagating cells in TEL-AML1-associated childhood leukemia. *Science*, **319**, 336-339.
- Horcher, M., Souabni, A. & Busslinger, M. (2001) Pax5/BSAP maintains the identity of B cells in late B lymphopoiesis. *Immunity*, **14**, 779-790.
- Husson, H., Carideo, E.G., Neuberg, D., Schultze, J., Munoz, O., Marks, P.W., Donovan, J.W., Chillemi, A.C., O'Connell, P. & Freedman, A.S. (2002) Gene expression profiling of follicular lymphoma and normal germinal center B cells using cDNA arrays. *Blood*, **99**, 282-289.
- Hystad, M.E., Myklebust, J.H., Bo, T.H., Sivertsen, E.A., Rian, E., Forfang, L., Munthe, E., Rosenwald, A., Chiorazzi, M., Jonassen, I., Staudt, L.M. & Smeland, E.B. (2007) Characterization of early stages of human B cell development by gene expression profiling. *J Immunol*, **179**, 3662-3671.
- Iida, S., Rao, P.H., Nallasivam, P., Hibshoosh, H., Butler, M., Louie, D.C., Dyomin, V., Ohno, H., Chaganti, R.S. & Dalla-Favera, R. (1996) The t(9;14)(p13;q32) chromosomal translocation associated with lymphoplasmacytoid lymphoma involves the PAX-5 gene. *Blood*, **88**, 4110-4117.
- Kallies, A., Hasbold, J., Fairfax, K., Pridans, C., Emslie, D., McKenzie, B.S., Lew, A.M., Corcoran, L.M., Hodgkin, P.D., Tarlinton, D.M. & Nutt, S.L. (2007) Initiation of plasma-cell differentiation is independent of the transcription factor Blimp-1. *Immunity*, **26**, 555-566.
- Kalnina, Z., Zayakin, P., Silina, K. & Line, A. (2005) Alterations of pre-mRNA splicing in cancer. *Genes Chromosomes Cancer*, **42**, 342-357.
- Katsura, Y. (2002) Redefinition of lymphoid progenitors. *Nat Rev Immunol*, **2**, 127-132.
- Kawamata, N., Ogawa, S., Zimmermann, M., Niebuhr, B., Stocking, C., Sanada, M., Hemminki, K., Yamatomo, G., Nannya, Y., Koehler, R., Flohr, T., Miller, C.W., Harbott, J., Ludwig, W.D., Stanulla, M., Schrappe, M., Bartram, C.R. & Koeffler, H.P. (2008) Cloning of genes involved in chromosomal translocations by high-resolution single nucleotide polymorphism genomic microarray. *Proc Natl Acad Sci USA*.
- Kawamata, N., Ogawa, S., Zimmermann, M., Sanada, M., Hemminki, K., Yamatomo, G., Nannya, Y., Koehler, R., Flohr, T., Miller, C.W., Harbott, J., Ludwig, W.-D., Stanulla, M., Schrappe, M., Bartram, C.R. & Koeffler, P.H. (2007) Rearrangement and Deletion of the PAX5 Gene in Pediatric Acute B-Cell Lineage Lymphoblastic Leukemia. *ASH Annual Meeting Abstracts*, **110**, 981-.
- Knudson, A.G. (1992) Stem cell regulation, tissue ontogeny, and oncogenic events. *Semin Cancer Biol*, **3**, 99-106.
- Kondo, M., Weissman, I.L. & Akashi, K. (1997) Identification of clonogenic common lymphoid progenitors in mouse bone marrow. *Cell*, **91**, 661-672.
- Konig, M., Reichel, M., Marschalek, R., Haas, O.A. & Strehl, S. (2002) A highly specific and sensitive fluorescence in situ hybridization assay for the detection of t(4;11)(q21;q23) and concurrent submicroscopic deletions in acute leukaemias. *Br J Haematol*, **116**, 758-764.
- Kozmik, Z., Wang, S., Dorfler, P., Adams, B. & Busslinger, M. (1992) The promoter of the CD19 gene is a target for the B-cell-specific transcription factor BSAP. *Mol Cell Biol*, **12**, 2662-2672.
- Krehan, D., Nebral, K., Konig, M. & Strehl, S. Monoallelic loss and frequent mutation of the second allele of PAX5 are genetic hallmarks of dic(9;20) childhood acute lymphoblastic leukemia (in preparation).
- Kroll, T.G., Sarraf, P., Pecciarini, L., Chen, C.J., Mueller, E., Spiegelman, B.M. & Fletcher, J.A. (2000) PAX8-PPARGgamma1 fusion oncogene in human thyroid carcinoma [corrected]. *Science*, **289**, 1357-1360.
- Kuiper, R.P., Schoenmakers, E.F., van Reijmersdal, S.V., Hehir-Kwa, J.Y., van Kessel, A.G., van Leeuwen, F.N. & Hoogerbrugge, P.M. (2007) High-resolution genomic profiling of childhood ALL reveals novel recurrent genetic lesions affecting pathways involved in lymphocyte differentiation and cell cycle progression. *Leukemia*, **21**, 1258-1266.

- Kwon, K., Hutter, C., Sun, Q., Bilic, I., Cobaleda, C., Malin, S. & Busslinger, M. (2008) Instructive role of the transcription factor E2A in early B lymphopoiesis and germinal center B cell development. *Immunity*, **28**, 751-762.
- Laiosa, C.V., Stadtfeld, M. & Graf, T. (2006) Determinants of lymphoid-myeloid lineage diversification. *Annu Rev Immunol*, **24**, 705-738.
- Lang, D., Powell, S.K., Plummer, R.S., Young, K.P. & Ruggeri, B.A. (2007) PAX genes: roles in development, pathophysiology, and cancer. *Biochem Pharmacol*, **73**, 1-14.
- Lin, H. & Grosschedl, R. (1995) Failure of B-cell differentiation in mice lacking the transcription factor EBF. *Nature*, **376**, 263-267.
- Maier, H. & Hagman, J. (2002) Roles of EBF and Pax-5 in B lineage commitment and development. *Semin Immunol*, **14**, 415-422.
- Mansson, R., Hultquist, A., Luc, S., Yang, L., Anderson, K., Kharazi, S., Al-Hashmi, S., Liuba, K., Thoren, L., Adolfsson, J., Buza-Vidas, N., Qian, H., Soneji, S., Enver, T., Sigvardsson, M. & Jacobsen, S.E. (2007) Molecular evidence for hierarchical transcriptional lineage priming in fetal and adult stem cells and multipotent progenitors. *Immunity*, **26**, 407-419.
- Martinez-Climent, J.A. (1997) Molecular cytogenetics of childhood hematological malignancies. *Leukemia*, **11**, 1999-2021.
- Mikkola, I., Heavey, B., Horcher, M. & Busslinger, M. (2002) Reversion of B cell commitment upon loss of Pax5 expression. *Science*, **297**, 110-113.
- Mitelman, F., Johansson, B. & Mertens, F. (2004) Fusion genes and rearranged genes as a linear function of chromosome aberrations in cancer. *Nat Genet*, **36**, 331-334.
- Mitelman, F., Johansson, B. & Mertens, F. (2007) The impact of translocations and gene fusions on cancer causation. *Nat Rev Cancer*, **7**, 233-245.
- Miyamoto, T., Iwasaki, H., Reizis, B., Ye, M., Graf, T., Weissman, I.L. & Akashi, K. (2002) Myeloid or lymphoid promiscuity as a critical step in hematopoietic lineage commitment. *Dev Cell*, **3**, 137-147.
- Mori, H., Colman, S.M., Xiao, Z., Ford, A.M., Healy, L.E., Donaldson, C., Hows, J.M., Navarrete, C. & Greaves, M. (2002) Chromosome translocations and covert leukemic clones are generated during normal fetal development. *Proc Natl Acad Sci U S A*, **99**, 8242-8247.
- Morrison, A.M., Jager, U., Chott, A., Schebesta, M., Haas, O.A. & Busslinger, M. (1998) Deregulated PAX-5 transcription from a translocated IgH promoter in marginal zone lymphoma. *Blood*, **92**, 3865-3878.
- Mullighan, C.G., Goorha, S., Radtke, I., Miller, C.B., Coustan-Smith, E., Dalton, J.D., Girtman, K., Mathew, S., Ma, J., Pounds, S.B., Su, X., Pui, C.H., Relling, M.V., Evans, W.E., Shurtleff, S.A. & Downing, J.R. (2007a) Genome-wide analysis of genetic alterations in acute lymphoblastic leukaemia. *Nature*, **446**, 758-764.
- Mullighan, C.G., Miller, C.B., Radtke, I., Phillips, L.A., Dalton, J., Ma, J., White, D., Hughes, T.P., Le Beau, M.M., Pui, C.H., Relling, M.V., Shurtleff, S.A. & Downing, J.R. (2008) BCR-ABL1 lymphoblastic leukaemia is characterized by the deletion of Ikaros. *Nature*, **453**, 110-114.
- Mullighan, C.G., Miller, C.B., Su, X., Radtke, I., Dalton, J.D., Song, G., Zhou, X., Pui, C.-H., Shurtleff, S.A. & Downing, J.R. (2007b) ERG Deletions Define a Novel Subtype of B-Progenitor Acute Lymphoblastic Leukemia. *Blood*, **110**, ASH Annual Meeting Abstracts, Abs. 691.
- Muratovska, A., Zhou, C., He, S., Goodyer, P. & Eccles, M.R. (2003) Paired-Box genes are frequently expressed in cancer and often required for cancer cell survival. *Oncogene*, **22**, 7989-7997.
- Nebral, K., Denk, D., Attarbaschi, A., Konig, M., Mann, G., Haas, O.A. & Strehl, S. Incidence and diversity of PAX5 fusion genes in childhood acute lymphoblastic leukemia. *Leukemia* (in press).
- Nebral, K., Konig, M., Harder, L., Siebert, R., Haas, O.A. & Strehl, S. (2007) Identification of PML as novel PAX5 fusion partner in childhood acute lymphoblastic leukaemia. *Br J Haematol*, **139**, 269-274.
- Nutt, S.L., Heavey, B., Rolink, A.G. & Busslinger, M. (1999a) Commitment to the B-lymphoid lineage depends on the transcription factor Pax5. *Nature*, **401**, 556-562.
- Nutt, S.L. & Kee, B.L. (2007) The transcriptional regulation of B cell lineage commitment. *Immunity*, **26**, 715-725.

- Nutt, S.L., Morrison, A.M., Dorfler, P., Rolink, A. & Busslinger, M. (1998) Identification of BSAP (Pax-5) target genes in early B-cell development by loss- and gain-of-function experiments. *Embo J*, **17**, 2319-2333.
- Nutt, S.L., Urbanek, P., Rolink, A. & Busslinger, M. (1997) Essential functions of Pax5 (BSAP) in pro-B cell development: difference between fetal and adult B lymphopoiesis and reduced V-to-DJ recombination at the IgH locus. *Genes Dev*, **11**, 476-491.
- Nutt, S.L., Vambrie, S., Steinlein, P., Kozmik, Z., Rolink, A., Weith, A. & Busslinger, M. (1999b) Independent regulation of the two Pax5 alleles during B-cell development. *Nat Genet*, **21**, 390-395.
- O'Neil, J. & Look, A.T. (2007) Mechanisms of transcription factor deregulation in lymphoid cell transformation. *Oncogene*, **26**, 6838-6849.
- O'Riordan, M. & Grosschedl, R. (1999) Coordinate regulation of B cell differentiation by the transcription factors EBF and E2A. *Immunity*, **11**, 21-31.
- Oppezzo, P., Dumas, G., Lalanne, A.I., Payelle-Brogard, B., Magnac, C., Pritsch, O., Dighiero, G. & Vuillier, F. (2005) Different isoforms of BSAP regulate expression of AID in normal and chronic lymphocytic leukemia B cells. *Blood*, **105**, 2495-2503.
- Orkin, S.H. & Zon, L.I. (2008) Hematopoiesis: an evolving paradigm for stem cell biology. *Cell*, **132**, 631-644.
- Panzer-Grumayer, E.R., Fasching, K., Panzer, S., Hettinger, K., Schmitt, K., Stockler-Ipsiroglu, S. & Haas, O.A. (2002) Nondisjunction of chromosomes leading to hyperdiploid childhood B-cell precursor acute lymphoblastic leukemia is an early event during leukemogenesis. *Blood*, **100**, 347-349.
- Parker, H., An, Q., Barber, K., Case, M., Davies, T., Konn, Z., Stewart, A., Wright, S., Griffiths, M., Ross, F.M., Moorman, A.V., Hall, A.G., Irving, J.A., Harrison, C.J. & Strefford, J.C. (2008) The complex genomic profile of ETV6-RUNX1 positive acute lymphoblastic leukemia highlights a recurrent deletion of TBL1XR1. *Genes Chromosomes Cancer*.
- Pasqualucci, L., Neumeister, P., Goossens, T., Nanjangud, G., Chaganti, R.S., Kuppers, R. & Dalla-Favera, R. (2001) Hypermutation of multiple proto-oncogenes in B-cell diffuse large-cell lymphomas. *Nature*, **412**, 341-346.
- Pieters, R., Schrappe, M., De Lorenzo, P., Hann, I., De Rossi, G., Felice, M., Hovi, L., LeBlanc, T., Szczepanski, T., Ferster, A., Janka, G., Rubnitz, J., Silverman, L., Stary, J., Campbell, M., Li, C.K., Mann, G., Suppiah, R., Biondi, A., Vora, A. & Valsecchi, M.G. (2007) A treatment protocol for infants younger than 1 year with acute lymphoblastic leukaemia (Interfant-99): an observational study and a multicentre randomised trial. *Lancet*, **370**, 240-250.
- Pongubala, J.M., Northrup, D.L., Lancki, D.W., Medina, K.L., Treiber, T., Bertolino, E., Thomas, M., Grosschedl, R., Allman, D. & Singh, H. (2008) Transcription factor EBF restricts alternative lineage options and promotes B cell fate commitment independently of Pax5. *Nat Immunol*, **9**, 203-215.
- Pridans, C., Holmes, M.L., Polli, M., Wettenhall, J.M., Dakic, A., Corcoran, L.M., Smyth, G.K. & Nutt, S.L. (2008) Identification of Pax5 target genes in early B cell differentiation. *J Immunol*, **180**, 1719-1728.
- Racz, A., Brass, N., Hofer, M., Sybrecht, G.W., Remberger, K. & Meese, E.U. (2000) Gene amplification at chromosome 1pter-p33 including the genes PAX7 and ENO1 in squamous cell lung carcinoma. *Int J Oncol*, **17**, 67-73.
- Robichaud, G.A., Nardini, M., Laflamme, M., Cuperlovic-Culf, M. & Ouellette, R.J. (2004) Human Pax-5 C-terminal isoforms possess distinct transactivation properties and are differentially modulated in normal and malignant B cells. *J Biol Chem*, **279**, 49956-49963.
- Robichaud, G.A., Perreault, J.P. & Ouellette, R.J. (2008) Development of an isoform-specific gene suppression system: the study of the human Pax-5B transcriptional element. *Nucleic Acids Res*, **36**, 4609-4620.
- Robson, E.J., He, S.J. & Eccles, M.R. (2006) A PANorama of PAX genes in cancer and development. *Nat Rev Cancer*, **6**, 52-62.
- Roessler, S., Gyory, I., Imhof, S., Spivakov, M., Williams, R.R., Busslinger, M., Fisher, A.G. & Grosschedl, R. (2007) Distinct promoters mediate the regulation of Ebf1 gene expression by interleukin-7 and Pax5. *Mol Cell Biol*, **27**, 579-594.

- Sadakane, Y., Zaitzu, M., Nishi, M., Sugita, K., Mizutani, S., Matsuzaki, A., Sueoka, E., Hamasaki, Y. & Ishii, E. (2007) Expression and production of aberrant PAX5 with deletion of exon 8 in B-lineage acute lymphoblastic leukaemia of children. *Br J Haematol*, **136**, 297-300.
- Schebesta, A., McManus, S., Salvagiotto, G., Delogu, A., Busslinger, G.A. & Busslinger, M. (2007) Transcription factor Pax5 activates the chromatin of key genes involved in B cell signaling, adhesion, migration, and immune function. *Immunity*, **27**, 49-63.
- Schebesta, M., Pfeffer, P.L. & Busslinger, M. (2002) Control of pre-BCR signaling by Pax5-dependent activation of the BLNK gene. *Immunity*, **17**, 473-485.
- Schoumans, J., Johansson, B., Corcoran, M., Kuchinskaya, E., Golovleva, I., Grander, D., Forestier, E., Staaf, J., Borg, A., Gustafsson, B., Blennow, E. & Nordgren, A. (2006) Characterisation of dic(9;20)(p11-13;q11) in childhood B-cell precursor acute lymphoblastic leukaemia by tiling resolution array-based comparative genomic hybridisation reveals clustered breakpoints at 9p13.2 and 20q11.2. *Br J Haematol*, **135**, 492-499.
- Sekine, R., Kitamura, T., Tsuji, T. & Tojo, A. (2007) Identification and comparative analysis of Pax5 C-terminal isoforms expressed in human cord blood-derived B cell progenitors. *Immunol Lett*, **111**, 21-25.
- Shaffer, A.L., Rosenwald, A. & Staudt, L.M. (2002) Lymphoid malignancies: the dark side of B-cell differentiation. *Nat Rev Immunol*, **2**, 920-932.
- Skotheim, R.I. & Nees, M. (2007) Alternative splicing in cancer: noise, functional, or systematic? *Int J Biochem Cell Biol*, **39**, 1432-1449.
- Souabni, A., Cobaleda, C., Schebesta, M. & Busslinger, M. (2002) Pax5 promotes B lymphopoiesis and blocks T cell development by repressing Notch1. *Immunity*, **17**, 781-793.
- Souabni, A., Jochum, W. & Busslinger, M. (2007) Oncogenic role of Pax5 in the T-lymphoid lineage upon ectopic expression from the immunoglobulin heavy-chain locus. *Blood*, **109**, 281-289.
- Strehl, S., Konig, M., Dworzak, M.N., Kalwak, K. & Haas, O.A. (2003) PAX5/ETV6 fusion defines cytogenetic entity dic(9;12)(p13;p13). *Leukemia*, **17**, 1121-1123.
- Stuart, E.T., Haffner, R., Oren, M. & Gruss, P. (1995a) Loss of p53 function through PAX-mediated transcriptional repression. *Embo J*, **14**, 5638-5645.
- Stuart, E.T., Kioussi, C., Aguzzi, A. & Gruss, P. (1995b) PAX5 expression correlates with increasing malignancy in human astrocytomas. *Clin Cancer Res*, **1**, 207-214.
- Thomas-Tikhonenko, A. & Cozma, D. (2008) PAX5 and B-cell neoplasms: transformation through presentation. *Future Oncol*, **4**, 5-9.
- Tsuzuki, S., Karnan, S., Horibe, K., Matsumoto, K., Kato, K., Inukai, T., Goi, K., Sugita, K., Nakazawa, S., Kasugai, Y., Ueda, R. & Seto, M. (2007) Genetic abnormalities involved in t(12;21) TEL-AML1 acute lymphoblastic leukemia: analysis by means of array-based comparative genomic hybridization. *Cancer Sci*, **98**, 698-706.
- Tsuzuki, S., Seto, M., Greaves, M. & Enver, T. (2004) Modeling first-hit functions of the t(12;21) TEL-AML1 translocation in mice. *Proc Natl Acad Sci U S A*, **101**, 8443-8448.
- Urbanek, P., Wang, Z.Q., Fetka, I., Wagner, E.F. & Busslinger, M. (1994) Complete block of early B cell differentiation and altered patterning of the posterior midbrain in mice lacking Pax5/BSAP. *Cell*, **79**, 901-912.
- van Zelm, M.C., van der Burg, M., de Ridder, D., Barendregt, B.H., de Haas, E.F., Reinders, M.J., Lankester, A.C., Revesz, T., Staal, F.J. & van Dongen, J.J. (2005) Ig gene rearrangement steps are initiated in early human precursor B cell subsets and correlate with specific transcription factor expression. *J Immunol*, **175**, 5912-5922.
- Venables, J.P. (2006) Unbalanced alternative splicing and its significance in cancer. *Bioessays*, **28**, 378-386.
- Wang, Q., Fang, W.H., Krupinski, J., Kumar, S., Slevin, M. & Kumar, P. (2008) Pax Genes in Embryogenesis and Oncogenesis. *J Cell Mol Med*.
- Welner, R.S., Pelayo, R. & Kincade, P.W. (2008) Evolving views on the genealogy of B cells. *Nat Rev Immunol*, **8**, 95-106.



Ying, H., Healy, J.I., Goodnow, C.C. & Parnes, J.R. (1998) Regulation of mouse CD72 gene expression during B lymphocyte development. *J Immunol*, **161**, 4760-4767.

## CHAPTER 8

### 8. APPENDIX

#### **8.1. *ETV6-NCOA2* fusion defines a new entity of T-lymphoid/myeloid progenitor acute leukemia**

Sabine Strehl, Karin Nebral, Margit König, Jochen Harbott, Stephanie Struski, Bella Bielorai, Michel Lessard, Herbert Strobl, Martin Zimmermann, Oskar A. Haas, Shai Izraeli

Clinical Cancer Research. 2008;14(4):977-83.

## Human Cancer Biology

### ETV6-NCOA2: A Novel Fusion Gene in Acute Leukemia Associated with Coexpression of T-Lymphoid and Myeloid Markers and Frequent NOTCH1 Mutations

Sabine Strehl,<sup>1</sup> Karin Nebral,<sup>1</sup> Margit König,<sup>1</sup> Jochen Harbott,<sup>4</sup> Herbert Strobl,<sup>2</sup> Richard Ratei,<sup>5</sup> Stephanie Struski,<sup>6</sup> Bella Bieloral,<sup>7,8</sup> Michel Lessard,<sup>6</sup> Martin Zimmermann,<sup>9</sup> Oskar A. Haas,<sup>3</sup> and Shai Izraeli<sup>7,8</sup>

**Abstract** **Purpose:** The *ETV6* gene has been reported to be fused to a multitude of partner genes in various hematologic malignancies with 12p13 aberrations. Cytogenetic analysis of six cases of childhood acute lymphoblastic leukemia revealed a novel recurrent t(8;12)(q13;p13), suggesting involvement of *ETV6*. **Experimental Design:** Fluorescence *in situ* hybridization was used to confirm the involvement of *ETV6* in the t(8;12)(q13;p13) and reverse transcription-PCR was used to identify the *ETV6* partner gene. Detailed immunologic characterization was done, and owing to their lineage promiscuity, the leukemic blast cells were analyzed for *NOTCH1* mutations. **Results:** We have identified a novel recurrent t(8;12)(q13;p13), which results in a fusion between the transcriptional repressor *ETV6* (*TEL*) and the transcriptional coactivator *NCOA2* (*TIF2*) in six cases of childhood leukemia expressing both T-lymphoid and myeloid antigens. The *ETV6-NCOA2* transcript encodes a chimeric protein that consists of the pointed protein interaction motif of *ETV6* that is fused to the COOH terminus of *NCOA2*, including the cyclic AMP – responsive element binding protein – binding protein (CBP) interaction and the AD2 activation domains. The absence of the reciprocal *NCOA2-ETV6* transcript in one of the cases suggests that the *ETV6-NCOA2* chimeric protein and not the reciprocal *NCOA2-ETV6* is responsible for leukemogenesis. In addition, *ETV6-NCOA2* leukemia shows a high frequency of heterozygous activating *NOTCH1* mutations, which disrupt the heterodimerization or the PEST domains. **Conclusions:** The *ETV6-NCOA2* fusion may define a novel subgroup of acute leukemia with T-lymphoid and myeloid features, which is associated with a high prevalence of *NOTCH1* mutations.

**Authors' Affiliations:** <sup>1</sup>Children's Cancer Research Institute, St. Anna Kinderkrebsforschung; <sup>2</sup>Institute of Immunology, Medical University of Vienna, Vienna Competence Center; <sup>3</sup>St. Anna Children's Hospital, Vienna, Austria; <sup>4</sup>Department of Pediatric Hematology and Oncology, Children's University Hospital, Giessen, Germany; <sup>5</sup>Department of Hematology, Oncology and Tumor Immunology, Robert-Rössle-Clinic at the HELIOS Klinikum Berlin, Charité Medical School, Berlin, Germany; <sup>6</sup>Laboratoire d'Hématologie, Hôpital de Hautepierre, Strasbourg, France; <sup>7</sup>Pediatric Hemato-Oncology, Cancer Research Center, Sheba Medical Center, Tel-Hashomer, Ramat Gan, Israel; <sup>8</sup>Faculty of Medicine, Tel Aviv University, Tel Aviv, Israel; and <sup>9</sup>Department of Pediatric Hematology/Oncology, Children's Hospital, Hannover Medical School, Hannover, Germany. Received 8/27/07; revised 10/16/07; accepted 11/9/07.

**Grant support:** Austrian Ministry of Science and Research grant GEN-AU II, GZ 200.136/1-VI/1/2005 (S. Strehl and O.A. Haas); St. Anna Kinderkrebsforschung; Israel Cancer Association; Israel Science Foundation (S. Izraeli); and Waxman Cancer Research Foundation (S. Izraeli).

The costs of publication of this article were defrayed in part by the payment of page charges. This article must therefore be hereby marked *advertisement* in accordance with 18 U.S.C. Section 1734 solely to indicate this fact.

**Note:** This is an International Berlin-Frankfurt-Münster Study Group study.

**Requests for reprints:** Sabine Strehl, Children's Cancer Research Institute, St. Anna Kinderkrebsforschung, Kinderspitalgasse 6, A-1090 Vienna, Austria. Phone: 43-1-40170-4490; Fax: 43-1-40170-7437; E-mail: sabine.strehl@ccri.at.

© 2008 American Association for Cancer Research.  
doi:10.1158/1078-0432.CCR-07-4022

Acute leukemia is subdivided into myeloid or lymphoid according to cytology and immunophenotyping. However, using these criteria, a minor proportion of acute leukemia is difficult to unambiguously assign because the blast populations do not allow classification in either a pure myeloid or lymphoid category (1). Such cases are designated as biphenotypic acute leukemia (BAL) or acute leukemia of ambiguous lineage.

In an effort to establish objective diagnostic criteria for defining such leukemias, several different immunologic classification and scoring systems, which are mostly based on the number and specificity of the lymphoid and myeloid markers expressed by the blast cells, have been introduced (1–4). Based on these categorizations, the prevalence of BAL has been determined to range from 2% to 5% in adult and childhood acute leukemia (5–7). Coexpression of myeloid and B-lymphoid antigens occurs in approximately 65% to 70%, whereas T-lymphoid and myeloid antigens account for 25% of all BAL and thus for ≤1% of acute leukemia (6).

As a basic principle, the classification of hematopoietic neoplasms should attempt to incorporate immunophenotypic, biologic, genetic, and clinical features to define specific disease

## Human Cancer Biology

entities. However, due to the lack of specific genetic features, BAL is defined by the application of arbitrary criteria (3). Genetic lesions such as t(9;22)(q34;q11)/BCR-ABL1, t(4;11)(q21;q23)/MLL-AF4/AFF1, and other 11q23 abnormalities seem to commonly concur with BAL of the myeloid/B-lymphoid type, whereas the specific genetic features of myeloid/T-lymphoid BAL remain widely elusive (6–10). Thus far, two NUP98 fusions (i.e., NUP98-RAP1GDS1 and NUP98-ADD3) seem to be associated with a subset of adult T-cell acute lymphoblastic leukemia (T-ALL) with variable expression of mature T-cell and myeloid markers (11–13). Furthermore, the PICALM-MLLT10 (CALM-AF10) fusion, which is mainly associated with immature T-ALL, has also been found in leukemia with a multilineage phenotype coexpressing T-cell and myeloid antigens (14). Recently, a specific subset of acute myeloid leukemia (AML) within the population of myeloid malignancies with coexpression of T-cell genes that is characterized by silencing of the CEBPA gene and recurring mutations in NOTCH1 has been described (15).

Activating NOTCH1 mutations that disrupt the heterodimerization and/or the PEST domains are present in >50% of childhood T-ALL but only in rare cases of AML, particularly in the context of lineage switch leukemia (15–18). In contrast to the well-established role of NOTCH1 in T-ALL pathogenesis (19), controversial results have been obtained with regard to NOTCH1 signaling in myeloid development. Enforced expression of constitutively activated NOTCH1 or treatment with NOTCH ligands results in the inhibition of granulocyte differentiation and an increase of immature precursors, suggesting a potential role of NOTCH signaling in the development of myeloid leukemia (20–23). However, NOTCH1 signaling has also been shown to irreversibly reduce the self-renewal capacity of multipotent progenitors and to induce multilineage myeloid differentiation (24).

We have identified a novel genetic subtype of acute leukemia with a recurrent t(8;12)(q13;p13), which fuses the ETV6 (TEL) and NCOA2 (TIF2) genes, and a high prevalence of NOTCH1 mutations. The combination of these two genetic lesions seems to be specifically associated with acute leukemia with a mixed T-lymphoid and myeloid immunophenotype.

## Materials and Methods

**Patients.** Bone marrow samples from children with newly diagnosed acute leukemia who were enrolled on either International Berlin-Frankfurt-Münster (BFM) or European Organization for Research and Treatment of Cancer (EORTC) protocols were obtained after informed consent of the patients or their legal guardians. Cytogenetic analysis of patients with acute leukemia enrolled in the Austrian AML-BFM 98 ( $n = 93$ , collected between 1998 and 2004; successfully karyotyped,  $n = 87$ ) and the ALL-BFM 2000 ( $n = 432$ , including  $n = 49$  T-ALLs, collected between 2000 and 2006; successfully karyotyped,  $n = 403$ ) studies identified two cases carrying a t(8;12)(q10-13;p10-13). Subsequently, additional patient samples with this specific translocation were collected from other study centers: two from Germany and one each from France and Israel.

**Conventional and molecular cytogenetics.** Samples were processed according to standard cytogenetic techniques and karyotypes were described according to the International System for Human Cytogenetic Nomenclature (25). ETV6 rearrangements were detected using differentially labeled ETV6 exon-specific cosmids 179A6 (exon 1A), 50F4 (intron 1 and exon 2), 50F4 (exon 2), 163E7 (exons 3-5), 54D5 (exons

5-8), and 148B6 (exon 8; kindly provided by P. Marynen, Center for Human Genetics, University of Leuven, Leuven, Belgium; ref. 26). Fluorescence *in situ* hybridization (FISH) was done as previously described (27).

FISH patterns were evaluated using an Axioplan fluorescent microscope (Zeiss) equipped with the appropriate filter sets for 4',6-diamidino-2-phenylindole (DAPI), FITC, and Cy3. Images were taken by means of a Plan Neofluar 100 $\times$ /1.3 oil immersion objective and a charge-coupled device camera (CH250, Photometrix Ltd.) using the IP Labs software (Vysis, Inc.). Using the same software, the images were split in the three color channels, and DAPI images were inverted and then again merged with the FITC and Cy3 images.

**Immunophenotyping.** Immunophenotyping was done on isolated bone marrow cells by means of flow cytometry with a panel of monoclonal antibodies. Immunologic data were determined in the facilities of the respective study centers, and thus, the antibody panels used were slightly different for the individual patient. Nevertheless, the most important markers that allow lineage assignment according to the European Group for the Immunological Classification of Leukemias (EGIL; ref. 2) criteria were analyzed: T-lymphoid markers, CD1a, CD2, cytoplasmic CD3 (cyCD3) and/or membrane CD3 (mCD3), CD5, CD7, CD4, CD8, and TdT; myeloid markers, MPO, CD13, CD33, CDw65, and CD117; natural killer marker, CD56; and progenitor marker, CD34.

**Reverse transcription-PCR analysis.** Total RNA was isolated from cryopreserved mononuclear cell or from methanol/acetic acid-fixed cells as previously described (28) using the RNeasy Mini kit (Qiagen) according to the manufacturers' recommendations. RNA was reverse transcribed with 200 units Moloney murine leukemia virus reverse transcriptase (Invitrogen) and 100 pmol random hexamers (GE Healthcare) at 42°C for 1 h. Primer sequences are listed in Table 1. All PCRs were done using Hot Start Taq (Qiagen). Gel images were taken using a Kodak Electrophoresis Documentation and Analysis System 120 and Kodak Digital Science 1 software (Kodak). PCR products were cleaned using the QIAquick PCR Purification kit (Qiagen) and sent to MWG-Biotech for direct sequencing.

**NOTCH1 mutation analysis.** Mutations in the N-terminal and COOH-terminal heterodimerization domains encoded by exons 26 and 27, respectively, and the PEST domain encoded by exon 34 of NOTCH1 were identified by direct sequencing of PCR-amplified cDNA. Primer sequences are listed in Table 1. PCRs were done using Hot Start Taq with an initial denaturation step at 95°C for 15 min, followed by 35 cycles (95°C for 30 s, 64°C for 30 s, 72°C for 45 s), and a final extension at 72°C for 7 min.

## Results

**Patient characteristics.** Clinical characteristics and cytogenetic data of the patients are summarized in Table 2. All patients displayed a t(8;12) with variable breakpoints that were difficult to assign accurately by conventional cytogenetics. In three cases (cases 1, 2, and 4), the t(8;12) was the sole karyotypic abnormality, whereas in two cases (cases 3 and 6) it occurred within complex karyotypes. In four of the patients, the morphology of the blast cells was consistent with ALL, whereas two cases were undifferentiated AML. Taking morphologic and immunologic criteria into consideration, patients were treated with the most appropriate therapy regimen. Irrespective of the treatment protocol, four of the patients (cases 1, 2, 3, and 5) are in complete remission 40 to 84 months after initial diagnosis. Case 4 was initially enrolled in the ALL IC-BFM 2002 study but responded very poorly to prednisone. Thus, the protocol was modified and more anti-AML drugs were administered and complete remission could be achieved in week 6 of therapy. In addition, this patient underwent stem cell transplantation from a matched sibling and is in continuous remission 17 months

## ETV6-NCOA2 Fusion in T-Lymphoid/Myeloid Leukemia

**Table 1.** Oligonucleotide primer sequences

Designation	Oligonucleotide sequence	Direction	Gene/exon*	Transcript
ETV6ex3-F1	TCCTGCTGCTGACCAAGAGG	Sense	ETV6/3	ETV6-NCOA2
TIF2ex17-R1	CAACTTCAGCATCGCCTCCA	Antisense	NCOA2/17	
TIF2ex14-F2	AGAATGGGCACCGCAGATTTC	Sense	NCOA2/14	
TIF2ex13-F1	TCAGCCAGGAATGATGGGTAATC	Sense	NCOA2/13	NCOA2-ETV6
ETV6ex6-R1	ACAGTCGAGCCAGTCCGTTG	Antisense	ETV6/6	
TIF2ex11-F1	GGAGATGAGCTTTGAGCCTGGTG	Sense	NCOA2/11	
TIF2ex9-F1	CCATGAGAGCAGCCATGAAACC	Sense	NCOA2/9	
TIF2ex7-F1	CAGTGCTTCGCTGTCTCTCAACC	Sense	NCOA2/7	
ETV6ex8-R1	CCCGCTGAGGTGGAAGTGTG	Antisense	ETV6/8	
NOTCH1ex25-F1	GCCTCTTCGACGGCTTTGAC	Sense	NOTCH1/25	NOTCH1
NOTCH1ex28-R1	TTGCTGGCCTCAGACACTTTG	Antisense	NOTCH1/28	
NOTCH1ex34-F1	TCCCCGTTCCAGCAGTCTC	Sense	NOTCH1/34	
NOTCH1ex34-R1	GCTCGGCTCTCCACTCAGG	Antisense	NOTCH1/34	
NOTCH1ex34-F2	AGCGCCCTGTCCAGATG	Sense	NOTCH1/34	
NOTCH1ex34-R2	GCACACAGACGCCGAAG	Antisense	NOTCH1/34	

\*Exon nomenclature according to the Ensembl Genome Browser exon information (<http://www.ensembl.org/>).

after diagnosis. Case 6 was treated according to the AML-BFM 93 protocol, relapsed 16 months after diagnosis, and died of progressive disease.

The patients analyzed were selected based on the availability of cytogenetic data in various study centers, and thus, it is difficult to estimate the overall frequency of the t(8;12)/ETV6-NCOA2 rearrangement. However, deduced from the numbers of patients enrolled in the Austrian AML-BFM 98 and ALL-BFM 2000 studies, in which one positive patient each was found, the t(8;12) is a rare but nevertheless recurrent genetic aberration. This finding agrees with previously reported cytogenetic data in childhood T-ALL (29).

**Immunophenotyping.** The percentages of blast cells positive for a specific immunologic marker are given in Table 3. According to the EGIL criteria (2), all patients had T-lymphoid scores of  $\geq 2$ , consistently expressed cyCD3 and CD7, and additional T-cell-specific markers, such as CD2 and CD5, to a variable extent. Except for case 3, the blast cells lacked expression of mCD3. In this leukemia, most of the cells (>50%) were devoid

of mCD3 expression and as such are defined as T-II. As a consequence of the myeloid antigen expression pattern, the patients were assigned to different EGIL subtypes (Table 3). True BAL is only considered when the scores are greater than two points for both the lymphoid and the myeloid lineage (2). Nevertheless, the blast cells of each patient expressed at least one myeloid marker, either MPO (EGIL score 2; three cases), CD33 (EGIL score 1; five cases), or CD13 (EGIL score 1; two cases) in combination with T-cell markers (Fig. 1). In case 6, two main subpopulations (i.e., cyCD3<sup>+</sup>/MPO<sup>dim</sup> and cyCD3<sup>dim</sup>/MPO<sup>bright</sup>) were observed (Fig. 1B) and a minor population expressing both markers. Together with the percentage of positive blast cells for the individual markers, this leukemia fulfills the EGIL criteria for BAL. In two of the samples, also expression of CD56, a marker specific for mature natural killer cells, was observed. The immature stage of the majority of the T-lymphoid/myeloid leukemias was supported by the double negativity for CD4/CD8 and, except for one case, the presence of CD34 (Table 3).

**Table 2.** Clinical characteristics and cytogenetic data of patients with coexpression of T-lymphoid and myeloid antigens

Case	Age (y)	Sex	FAB	Cytogenetics	Treatment protocol	Last follow-up from diagnosis
1	2.4	M	ALL	46,XY,t(8;12)(q13;p13)[15]/46,XY[5]	ALL-BFM 2000	60 mo + CR
2	8.5	F	AML-M1	46,XX,t(8;12)(q10;p10)[19]	AML-BFM 98	44 mo + CR
3	14.5	F	ALL	46,XX,del(5)(q23q32),r(7),t(8;12)(q12;p13), der(16)t(1;16)(?;?)[11]/46,XX[12]	EORTC 58951	40 mo + CR
4	2.0	M	ALL	46,XY,t(8;12)(q12;p12)[17]	ALL IC-BFM 2002, Interfant ALL 99 (modified)	17 mo + CR
5	2.5	M	AML-M1	47,XY,t(8;12)(q13;p11.2?),+22[4]	AML-BFM 87	84 mo CR*
6	10.9	M	ALL	46,XY,del(2)(p21),-4,del(5)(q3?4),add(5)(q2?3), del(6)(q21), t(8;12)(q11;p11),del(11)(q14), der(13)del(13)?(q14q22),-16,+?21,+?22[6]/46,XY[12]	AML-BFM 93	21 mo DOD

Abbreviations: FAB, French-American-British; BFM, Berlin-Frankfurt-Münster; CR, complete remission; EORTC, European Organization for Research and Treatment of Cancer; DOD, dead of disease.

\*Lost for follow-up.



**Table 3.** Immunophenotyping of blast cells with *ETV6-NCOA2* fusion and classification according to EGIL criteria

Case	CD34	CD4	CD8	CD1a	CD2	cyCD3	mCD3	CD5	CD7	TCR a/b	TCR g/d	TdT	MPO	CD13	CD33	CD65	CD117	CD56	EGIL
1	32	2	1	0	19	75	2	ND	94	ND	ND	2	1	36	59	13	1	ND	T-I/II/My+*
2	91	1	1	1	8	54	2	ND	56	ND	ND	18	16	3	95	10	15	86	BAL
3	98	3	2	0	58	99	37	94	95	59	5	34	0	9	14	34	2	ND	T-II/My+
4	0	0	0	0	ND	74	0	74	74	ND	ND	60	0	ND	40	ND	ND	30	T-II/My+
5	84	0	0	0	2	45	1	1	75	ND	ND	10	50	11	85	ND	ND	ND	BAL
6	76	4	6	1	15	70	16	78	88	10	1	3	14	17	73	3	30	ND	BAL

NOTE: Values in Table are expressed as percentage of positive blast cells.

Abbreviation: ND, not determined.

\*Due to the lack of CD5 data discrimination between T-I and T-II stage not possible.

**Identification of *NCOA2* as *ETV6* partner gene.** FISH analysis with *ETV6* exon-specific probes revealed disruption of this gene (Fig. 2A). To narrow down the breakpoint in 8q, FISH with various gene-specific probes located at 8q13.1-21.1 was carried out and the most likely breakpoint was determined to occur in chromosomal band 8q13.3 (data not shown). Out of the genes located in this chromosomal region, *NCOA2* was considered a likely candidate gene because it has already been identified as partner gene of *MYST3* (*MOZ*) in cases with an inv(8)(p11q13) (30). Fusion gene-specific reverse transcription-PCR experiments using primers located in exons 3 and 17 of *ETV6* and *NCOA2*, respectively, led to the identification of chimeric *ETV6-NCOA2* transcripts (Fig. 2B). Sequence analyses revealed an in-frame fusion between

*ETV6* exon 4 and *NCOA2* exon 15 in five of the six cases (cases 1, 2, 3, 5, and 6; Fig. 2C). In case 5, also an alternatively spliced transcript lacking exon 16 of *NCOA2* was detected. In the remaining case (no. 4), *ETV6* exon 5 was fused in-frame to *NCOA2* exon 14. Thus, the putative *ETV6-NCOA2* consensus fusion protein consists of the *ETV6* pointed domain (PNT) and the cyclic AMP-responsive element binding protein-binding protein (CBP) interaction (CID) and the AD2 (transactivation domain 2) domains of *NCOA2* (Fig. 2D). The splice variant lacking *NCOA2* exon 16 (case 5) would result in a partial deletion of the CID domain; however, the second transcript also encodes the putative consensus protein. Expression analysis for the reciprocal *NCOA2-ETV6* identified two different chimeric transcripts that fused *NCOA2* exon 14 to *ETV6* exons 5 or 6, respectively, thus showing alternative splicing of *ETV6* exon 5 (Fig. 2B). In case 4, despite all efforts using various primer combinations (see Table 1), no *NCOA2-ETV6* transcripts could be amplified, suggesting that the *ETV6-NCOA2* fusion gene is responsible for leukemogenesis.

**Detection of *NOTCH1* mutations.** The identification of activating *NOTCH1* mutations not only in T-ALL but also in rare cases of myeloid leukemia (15–18) prompted us to analyze our samples for the presence of *NOTCH1* mutations. Mutation analysis of the heterodimerization and PEST domains of *NOTCH1* revealed heterozygous *NOTCH1* mutations in four of five samples of which sufficient material was available. Mutations were detected in one sample in the heterodimerization domain, in two in the PEST domain, and in one in both domains. As previously described (18), heterodimerization domain mutations were missense, in-frame deletions and insertions, whereas the PEST domain mutations created premature termination codons (Table 4). The two heterodimerization domain mutations found in cases 2 and 3, and the PEST domain mutations of cases 1 and 6, have been previously described (18). A PEST domain mutation similar to that detected in case 2 has as well been reported (31).

## Discussion

In this study, we report six cases of childhood acute leukemia with a novel recurrent t(8;12), which results in a fusion of the repressor gene *ETV6* and the transcriptional coactivator *NCOA2*. The *ETV6-NCOA2* fusion concurs with a high prevalence of *NOTCH1* activating mutations and the coexpression

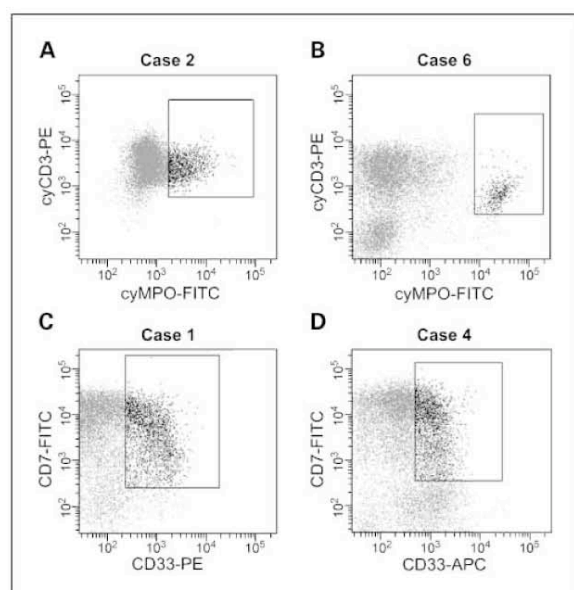


**Fig. 1.** Fluorescence-activated cell sorting data. A and B, coexpression of cyCD3 and cytoplasmic MPO (cyMPO) in a subpopulation of the blast cells of case 2 (A) and case 6 (B). C and D, coexpression of CD7 and CD33 in case 1 (C) and case 4 (D). PE, phycoerythrin; APC, allophycocyanin.

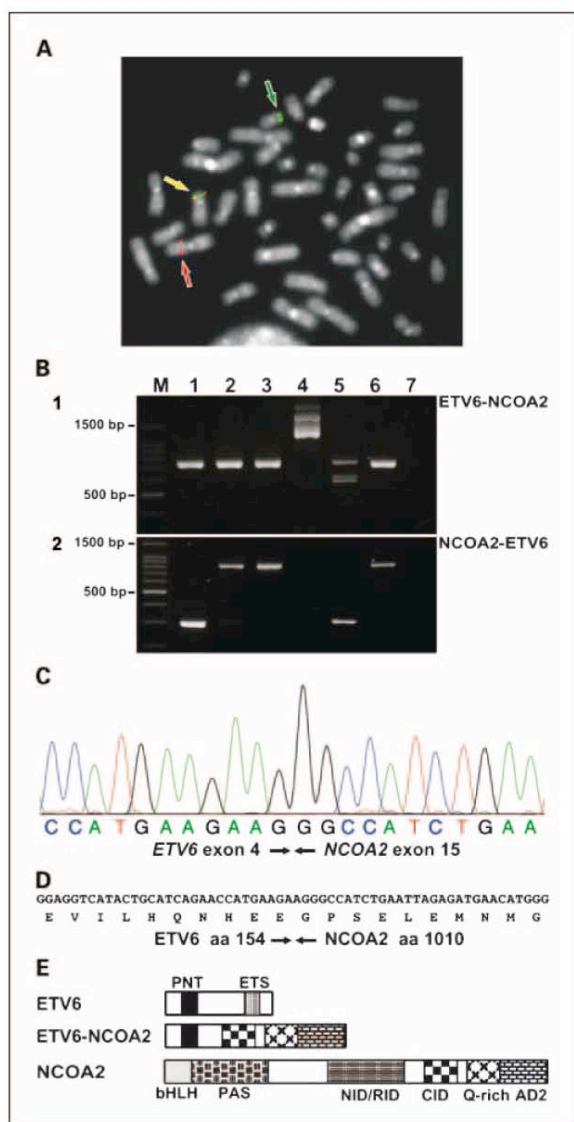


**Fig. 2.** *ETV6-NCOA2* fusion gene. **A**, FISH analysis of case 1 using *ETV6* exon-specific cosmid clones 50F4 (exon 2; green signals) and 148B6 (exon 8; red signals), showing disruption of the gene. **B**, reverse transcription-PCR analysis. M, 100-bp ladder (Promega); lanes 1 to 6, patient samples; lane 7, negative control. **B1**, reverse transcription-PCR analysis of the *ETV6-NCOA2* fusion transcript using primers located in exon 3 of *ETV6* (ETV6ex3-F1) and exon 17 of *NCOA2* (TIF2ex17-R1). **B2**, reverse transcription-PCR analysis of the reciprocal *NCOA2-ETV6* fusion transcript using primers located in exon 14 of *NCOA2* (TIF2ex14-F2) and exon 6 of *ETV6* (ETV6ex6-R1). The size differences are due to alternative splicing of *ETV6* exon 5. **C** and **D**, nucleotide and amino acid (aa) sequence of the *ETV6-NCOA2* fusion junction. **C**, sequence chromatogram of the *ETV6-NCOA2* fusion transcript of case 1 showing a fusion between exons 4 and 15 of *ETV6* and *NCOA2*, respectively. **D**, predicted amino acid sequence: amino acid 154 of *ETV6* is fused to amino acid 1010 of *NCOA2*. **E**, schematic representation of the putative consensus *ETV6-NCOA2* chimeric protein.

of T-cell-specific antigens (cyCD3 and CD7) and at least one myeloid marker (i.e., MPO, CD33, CD13, and CD65).

As a result of the t(8;12) translocation, the PNT protein interaction domain of *ETV6*, which is involved in homodimer-

ization and heterodimerization, is fused to the COOH terminus of *NCOA2*, including the CBP interaction domain and the AD2 activation domain. The same COOH-terminal domains of *NCOA2* are also retained in the previously identified MYST3-*NCOA2* fusion protein, which is generated by an inv(8)(p11q13) (30, 32). The absence of the reciprocal *NCOA2-ETV6* transcript in one of the cases, as well as the facts that MYST3-*NCOA2* is transforming and that the reciprocal *NCOA2-MYST3* is not expressed, suggests that the *ETV6-NCOA2* chimeric protein and not the reciprocal *NCOA2-ETV6* is responsible for leukemogenesis. However, this finding needs to be confirmed in a larger cohort of *ETV6-NCOA2*-positive cases.

The transforming properties of MYST3-*NCOA2* depend on the MYST3 MYST and the *NCOA2* CBP interaction domains, whereas the MYST3 PHD and the putative AD2 acetyltransferase motifs of *NCOA2* are not required for transformation (33). Expression of MYST3-*NCOA2* correlates with a depletion of CBP from PML bodies and reduced cellular levels of CBP. Thus, MYST3-*NCOA2* acts as a modulator of the transcriptional activity of CBP-dependent activators (34, 35). Future studies will determine whether the *ETV6-NCOA2* chimeric protein has similar properties or may recruit CBP to *ETV6* target genes resulting in their constitutive activation. In this respect, it is interesting to note that Ets pointed domains can also interact with the SRC1 interaction (CID) domain of CBP (36), suggesting a possible competition between *ETV6-NCOA2* and normal *ETV6* for CBP. Moreover, all NUP98 chimera, including those associated with a T/myeloid phenotype (11–13), retain the COOH-terminal FG repeats, which have the potential to bind CBP (37), indicating a probable involvement of CBP in these types of leukemia.

Bona fide transcriptional coactivators are rarely involved in leukemogenic translocations. Such fusion genes, which are expressed as a consequence of chromosomal translocations, include *MLL-CREBBP/CBP* (38–41), *MLL-EP300/p300* (41), *MYST3-CREBBP* (42), *MYST3-EP300* (43, 44), *MYST4/MORF-CREBBP* (45), and *MYST3-NCOA2* (30, 32). In contrast to MYST3-*NCOA2* and to all other rearrangements involving transcriptional coactivators, which are exclusively associated with AML, the *ETV6-NCOA2* irrespective of its occurrence in different morphologic and immunophenotypic leukemia subtypes determined by the FAB and EGIL classifications coincides with coexpression of T-lymphoid and myeloid markers.

Recently, a similar novel subtype of AML with coexpression of T-lymphoid markers characterized by *CEBPA* silencing through promoter hypermethylation and associated with frequent *NOTCH1* mutations has been identified (15). This subgroup of acute leukemia showed several cytogenetic abnormalities, none of which was common to all cases, suggesting that the *CEBPA/NOTCH1* and the *ETV6-NCOA2/NOTCH1* leukemia represent distinct entities.

Mixed myeloid and lymphoid T-cell-specific or B-cell-specific leukemia has been previously described and may either represent an unphysiologic transformation-related anomaly or, alternatively, reflect the immunophenotypic features of a physiologic common myeloid-lymphoid progenitor (46). The concurrence of the *ETV6-NCOA2* fusion with *NOTCH1* activating mutations raises the question whether this combination of genetic lesions or *ETV6-NCOA2* alone has instructive properties or at least one of them targets an uncommitted progenitor cell with a myeloid and T-lymphoid potential. In this context, the



**Table 4.** *NOTCH1* mutations in *ETV6-NCOA2* leukemia

Case	Domain	SNP	Nucleotide change	Amino acid change
1	HD	c.5097 C/T	—	—
	PEST	—	c.7403C>A	p.S2468X
2	HD	c.5097 C/T	c.5081C>T	p.F1694S
	PEST	—	c.7007_7008insT	p.2336 EHTGPLPAAWHGRPAAG
3	HD	—	c.5036T>C	p.L1679P
	PEST	—	—	—
4	HD	—	—	—
	PEST	—	—	—
6	HD	—	—	—
	PEST	—	c.7544_7545delCT	p.2515 RVP

Abbreviations: SNP, single nucleotide polymorphism; HD, heterodimerization.

presence of *NOTCH1* mutations in lineage infidelity (17) as well as in AML with T-lymphoid features (15) suggests that these mutations may occur in a leukemic stem cell that precedes both myeloid and T-lineage commitment (17). Accumulating evidence indicates that a myeloid potential accompanies early stages of T (also B and erythroid) development and that T-cell (and B-cell) progenitors are most likely produced from a common myeloid-lymphoid progenitor through intermediate bipotent or even multipotent stages (47–52). On the other hand, some fusion proteins encoded by translocations impart, through ectopic reactivation of genes associated with self-renewal, leukemia stem cell properties to committed hematopoietic progenitors (53, 54).

Although at this point the sequential or simultaneous occurrence of the two genetic events, fusion of *ETV6* to *NCOA2* and mutation of *NOTCH1*, remains indefinable, it is tempting to speculate that mutation of *NOTCH1* confers self-renewal capacity to early progenitors, which are then susceptible to the

accumulation of additional genetic hits such as fusion genes. Vice versa, the *ETV6-NCOA2* fusion might bestow transforming properties and the subsequent activation of *NOTCH1* may direct differentiation toward the T-cell lineage. Ectopic expression of *ETV6-NCOA2* will eventually reveal whether this chimeric protein reprograms progenitors or leads to expansion of a T/myeloid subset.

The eminent clinical question that derives from our findings is whether this type of leukemia should be treated as ALL or AML. The currently available rather limited information indicates that the affected patients have a decent prognostic outlook when treated with either ALL or AML therapy regimens. However, only the retrospective and prospective collection, evaluation, and comparison of treatment results of a larger number of such cases will provide a conclusive answer. The identification of the *ETV6-NCOA2* gene fusion and its accompanying *NOTCH1* mutations is thus the first essential step to achieve this goal.

## References

- Matutes E, Morilla R, Farahat N, et al. Definition of acute biphenotypic leukemia. *Haematologica* 1997; 82:64–6.
- Bene MC, Castoldi G, Knapp W, et al. Proposals for the immunological classification of acute leukemias. European Group for the Immunological Characterization of Leukemias (EGIL). *Leukemia* 1995;9:1783–6.
- Borowitz MJ, Bray R, Gascoyne R, et al. U.S.-Canadian Consensus recommendations on the immunophenotypic analysis of hematologic neoplasia by flow cytometry: data analysis and interpretation. *Cytometry* 1997;30:236–44.
- Vardiman JW, Harris NL, Brunning RD. The World Health Organization (WHO) classification of the myeloid neoplasms. *Blood* 2002;100:2292–302.
- Carbonell F, Swansbury J, Min T, et al. Cytogenetic findings in acute biphenotypic leukaemia. *Leukemia* 1996;10:1283–7.
- Owaidah TM, Al Beihany A, Iqbal MA, Elkum N, Roberts GT. Cytogenetics, molecular and ultrastructural characteristics of biphenotypic acute leukemia identified by the EGIL scoring system. *Leukemia* 2006;20:620–6.
- Rubio MT, Dhedin N, Boucheix C, et al. Adult T-biphenotypic acute leukaemia: clinical and biological features and outcome. *Br J Haematol* 2003;123: 842–9.
- Killick S, Matutes E, Powles RL, et al. Outcome of biphenotypic acute leukemia. *Haematologica* 1999; 84:699–706.
- Legrand O, Perrot JY, Simonin G, et al. Adult biphenotypic acute leukaemia: an entity with poor prognosis which is related to unfavourable cytogenetics and P-glycoprotein over-expression. *Br J Haematol* 1998; 100:147–55.
- Tiribelli M, Damiani D, Masolini P, Candoni A, Calistri E, Fanin R. Biological and clinical features of T-biphenotypic acute leukaemia: report from a single centre. *Br J Haematol* 2004;125:814–5.
- Lahortiga I, Vizmanos JL, Agirre X, et al. NUP98 is fused to adducin 3 in a patient with T-cell acute lymphoblastic leukemia and myeloid markers, with a new translocation t(10;11)(q25;p15). *Cancer Res* 2003;63: 3079–83.
- Hussey DJ, Nicola M, Moore S, Peters GB, Dobrovic A. The (4;11)(q21;p15) translocation fuses the NUP98 and RAP1GDS1 genes and is recurrent in T-cell acute lymphocytic leukemia. *Blood* 1999;94:2072–9.
- Mecucci C, La Starza R, Negrini M, et al. t(4;11)(q21;p15) translocation involving NUP98 and RAP1GDS1 genes: characterization of a new subset of T acute lymphoblastic leukaemia. *Br J Haematol* 2000;109:788–93.
- La Starza R, Crescenzi B, Krause A, et al. Dual-color split signal fluorescence *in situ* hybridization assays for the detection of CALM/AF10 in t(10;11)(p13;q14–21)-positive acute leukemia. *Haematologica* 2006;91: 1248–51.
- Wouters BJ, Alberich Jorda M, Keeshan K, et al. Distinct gene expression profiles of acute myeloid/T-lymphoid leukemia with silenced CEBPA and mutations in *NOTCH1*. *Blood* 2007;110:3706–14.
- Fu L, Kogoshi H, Nara N, Tohda S. *NOTCH1* mutations are rare in acute myeloid leukemia. *Leuk Lymphoma* 2006;47:2400–3.
- Palomero T, McKenna K, J ON, et al. Activating mutations in *NOTCH1* in acute myeloid leukemia and lineage switch leukemias. *Leukemia* 2006;20: 1963–6.
- Weng AP, Ferrando AA, Lee W, et al. Activating mutations of *NOTCH1* in human T cell acute lymphoblastic leukemia. *Science* 2004;306:269–71.
- Grabher C, von Boehmer H, Look AT. Notch 1 activation in the molecular pathogenesis of T-cell acute lymphoblastic leukaemia. *Nat Rev Cancer* 2006;6: 347–59.
- Carlesso N, Aster JC, Sklar J, Scadden DT. Notch1-induced delay of human hematopoietic progenitor cell differentiation is associated with altered cell cycle kinetics. *Blood* 1999;93:838–48.
- Jones P, May G, Healy L, et al. Stromal expression of Jagged 1 promotes colony formation by fetal hematopoietic progenitor cells. *Blood* 1998;92: 1505–11.
- Milner LA, Bigas A, Kopan R, Brashem-Stein C, Bernstein ID, Martin DI. Inhibition of granulocytic differentiation by mNotch1. *Proc Natl Acad Sci U S A* 1996;93:13014–9.
- Walker L, Lynch M, Silverman S, et al. The Notch/Jagged pathway inhibits proliferation of human hematopoietic progenitors *in vitro*. *Stem Cells* 1999;17: 162–71.
- Schroeder T, Kohlhof H, Rieber N, Just U. Notch signaling induces multilineage myeloid differentiation and up-regulates PU.1 expression. *J Immunol* 2003;170: 5538–48.
- Shaffer L, Mitelman F. ISCN 2005: an international



## ETV6-NCOA2 Fusion in T-Lymphoid/Myeloid Leukemia

- system for human cytogenetic nomenclature. Basel: Karger; 2005.
26. Baens M, Peeters P, Guo C, Aerssens J, Marynen P. Genomic organization of TEL: the human ETS-variant gene 6. *Genome Res* 1996;6:404–13.
  27. König M, Reichel M, Marschalek R, Haas OA, Strehl S. A highly specific and sensitive fluorescence *in situ* hybridization assay for the detection of t(4;11)(q21;q23) and concurrent submicroscopic deletions in acute leukaemias. *Br J Haematol* 2002;116:758–64.
  28. Strehl S, König M, Mann G, Haas OA. Multiplex reverse transcriptase-polymerase chain reaction screening in childhood acute myeloblastic leukemia. *Blood* 2001;97:805–8.
  29. Schneider NR, Carroll AJ, Shuster JJ, et al. New recurring cytogenetic abnormalities and association of blast cell karyotypes with prognosis in childhood T-cell acute lymphoblastic leukemia: a pediatric oncology group report of 343 cases. *Blood* 2000;96:2543–9.
  30. Carapeti M, Aguiar RC, Goldman JM, Cross NC. A novel fusion between MOZ and the nuclear receptor coactivator TIF2 in acute myeloid leukemia. *Blood* 1998;91:3127–33.
  31. Breit S, Stanulla M, Flohr T, et al. Activating NOTCH1 mutations predict favorable early treatment response and long-term outcome in childhood precursor T-cell lymphoblastic leukemia. *Blood* 2006;108:1151–7.
  32. Liang J, Prouty L, Williams BJ, Dayton MA, Blanchard KL. Acute mixed lineage leukemia with an inv(8)(p11q13) resulting in fusion of the genes for MOZ and TIF2. *Blood* 1998;92:2118–22.
  33. Deguchi K, Ayton PM, Carapeti M, et al. MOZ-TIF2-induced acute myeloid leukemia requires the MOZ nucleosome binding motif and TIF2-mediated recruitment of CBP. *Cancer Cell* 2003;3:259–71.
  34. Collins HM, Kindle KB, Matsuda S, et al. MOZ-TIF2 alters cofactor recruitment and histone modification at the RAR $\alpha$ 2 promoter: differential effects of MOZ fusion proteins on CBP- and MOZ-dependent activators. *J Biol Chem* 2006;281:17124–33.
  35. Kindle KB, Troke PJ, Collins HM, et al. MOZ-TIF2 inhibits transcription by nuclear receptors and p53 by impairment of CBP function. *Mol Cell Biol* 2005;25:988–1002.
  36. Matsuda S, Harries JC, Viskaduraki M, et al. A conserved  $\alpha$ -helical motif mediates the binding of diverse nuclear proteins to the SRC1 interaction domain of CBP. *J Biol Chem* 2004;279:14055–64.
  37. Kasper LH, Brindle PK, Schnabel CA, Pritchard CE, Cleary ML, van Deursen JM. CREB binding protein interacts with nucleoporin-specific FG repeats that activate transcription and mediate NUP98-HOXA9 oncogenicity. *Mol Cell Biol* 1999;19:764–76.
  38. Sobulo OM, Borrow J, Tomek R, et al. MLL is fused to CBP, a histone acetyltransferase, in therapy-related acute myeloid leukemia with a t(11;16)(q23;p13.3). *Proc Natl Acad Sci U S A* 1997;94:8732–7.
  39. Rowley JD, Reshmi S, Sobulo O, et al. All patients with the t(11;16)(q23;p13.3) that involves MLL and CBP have treatment-related hematologic disorders. *Blood* 1997;90:535–41.
  40. Taki T, Sako M, Tsuchida M, Hayashi Y. The t(11;16)(q23;p13) translocation in myelodysplastic syndrome fuses the MLL gene to the CBP gene. *Blood* 1997;89:3945–50.
  41. Ida K, Kitabayashi I, Taki T, et al. Adenoviral E1A-associated protein p300 is involved in acute myeloid leukemia with t(11;22)(q23;q13). *Blood* 1997;90:4699–704.
  42. Borrow J, Stanton VP, Jr., Andresen JM, et al. The translocation t(8;16)(p11;p13) of acute myeloid leukaemia fuses a putative acetyltransferase to the CREB-binding protein. *Nat Genet* 1996;14:33–41.
  43. Kitabayashi I, Aikawa Y, Yokoyama A, et al. Fusion of MOZ and p300 histone acetyltransferases in acute monocytic leukemia with a t(8;22)(p11;q13) chromosome translocation. *Leukemia* 2001;15:89–94.
  44. Chaffanet M, Gressin L, Preudhomme C, Soenen-Cornu V, Birnbaum D, Pebusque MJ. MOZ is fused to p300 in an acute monocytic leukemia with t(8;22). *Genes Chromosomes Cancer* 2000;28:138–44.
  45. Panagopoulos I, Fioretos T, Isaksson M, et al. Fusion of the MORF and CBP genes in acute myeloid leukemia with the t(10;16)(q22;p13). *Hum Mol Genet* 2001;10:395–404.
  46. Schmidt CA, Przybylski GK. What can we learn from leukemia as for the process of lineage commitment in hematopoiesis? *Int Rev Immunol* 2001;20:107–15.
  47. Adolfsson J, Mansson R, Buza-Vidas N, et al. Identification of Flt3<sup>+</sup> lympho-myeloid stem cells lacking erythro-megakaryocytic potential: a revised road map for adult blood lineage commitment. *Cell* 2005;121:295–306.
  48. Haddad R, Guardiola P, Izac B, et al. Molecular characterization of early human T/NK and B-lymphoid progenitor cells in umbilical cord blood. *Blood* 2004;104:3918–26.
  49. Katsura Y. Redefinition of lymphoid progenitors. *Nat Rev Immunol* 2002;2:127–32.
  50. Lai AY, Kondo M. Asymmetrical lymphoid and myeloid lineage commitment in multipotent hematopoietic progenitors. *J Exp Med* 2006;203:1867–73.
  51. Prohaska SS, Scherer DC, Weissman IL, Kondo M. Developmental plasticity of lymphoid progenitors. *Semin Immunol* 2002;14:377–84.
  52. Weerkamp F, Baert MR, Brugman MH, et al. Human thymus contains multipotent progenitors with T/B lymphoid, myeloid, and erythroid lineage potential. *Blood* 2006;107:3131–7.
  53. Huntly BJ, Shigematsu H, Deguchi K, et al. MOZ-TIF2, but not BCR-ABL, confers properties of leukemic stem cells to committed murine hematopoietic progenitors. *Cancer Cell* 2004;6:587–96.
  54. Krivtsov AV, Twomey D, Feng Z, et al. Transformation from committed progenitor to leukaemia stem cell initiated by MLL-AF9. *Nature* 2006;442:818–22.

## 8.2. Additional FISH clones

**Table 1. Additional FISH clones used for analysis**

Gene/Region	Locus	Clone	Accession Number/ Company
RSCD1-5'	01q24.2	RP3-455J7*	AL031733.3
RSCD1-3'	01q24.2	RP11-138P14*	AQ349162 and AQ385458 (BAC end pairs)
3p	03p	3p-arm-specific painting probe	NA
TOP2B	03p24.2	RP11-659P16 <sup>‡</sup>	AC093416
3q-subtelomere	03q subtelomere	196F4 <sup>#</sup>	NA
Chromosome 7	whole chromosome	pBS7	NA
AUTS2-5'	07q11.22	RP11-243F5*	AQ486680
AUTS2-3'	07q11.22	RP11-88H22*	AZ516257
ELN-5'	07q11.23	RP11-148M21*	AC093168
ELN-3'	07q11.23	RP11-349P21*	AQ528659
Chromosome 9	whole chromosome	pBS9	NA
5' of PAX5	09p13	RP11-397D12 <sup>‡</sup>	AL158155.24
5' of PAX5	09p13	RP11-3J10 <sup>‡</sup>	AL138752
3' of PAX5	09p13	RP11-84P7 <sup>‡</sup>	AL161792
LSI BCR/ABL Dual Color, Dual Fusion Translocation Probe Set	09q34 / 22q11.2	NA	Vysis (Abott)
ELP4-5'	11p13	RP5-1137O17*	AL133295
ELP4-3' and PAX6	11p13	RP11-307I15*	DX934410 and DX934411 (BAC end pairs)
WT1	11p13	RP11-74J1	Research Genetics - Invitrogen
BDNF-5'	11p14.1	RP11-52H5*	AQ083161 and AQ115784 (BAC end pairs)
KCNA4-3'	11p14.1	RP11-215H22*	AC021233.9
LGR4-3' and CCDC34	11p14.1	RP11-426P16*	AQ554326 and AQ554330 (BAC end pairs)

MUC15 and TMEM16C	11p14.2	RP11-283H3*	AC036114
LUZP2-3'	11p14.3	RP11-54J7*	AC087373
GAS2-5'	11p14.3	RP11-109H8*	AQ350699 and AQ323046 (BAC end pairs)
LUZP2-5'	11p14.3	RP11-372B5*	AC040968
NELL1-5'	11p15.1	RP11-3E17*	AC010811
NELL1-3'	11p15.1	RP11-116O9*	AC105190
E2F8	11p15.1	RP11-428C19*	AC009652
DKK3	11p15.3	RP11-313H5*	AC118656
GALNTL4-3'	11p15.3	RP11-75K2*	AQ267423
GALNTL4-5'	11p15.3	RP11-47D7*	AQ200362
LMO1	11p15.4	RP11-379P15*	AC091013
WEE1	11p15.4	RP11-16F15*	AC011979
SWAP70-3'	11p15.4	RP11-540A21*	AC026250.16
MRVI1	11p15.4	RP11-58H20*	AC009532
LSI® TEL/AML1	12p13 / 22q22	NA	Vysis (Abott)
Chromosome 14	whole chromosome	pBS14	NA
LSI® IGH DUAL break apart	14q32	NA	Vysis (Abott)
BCL11B-5'	14q32.2	RP11-431B1*	AC036222 and AC103702 (BAC end pairs)
BCL11B-3'	14q32.2	RP11-15E14*	AL352981

\*obtained from The Wellcome Trust Sanger Institute; <http://www.sanger.ac.uk>, Hinxton, Cambridge, United Kingdom.

‡obtained from M. Rocchi, Department of Cytogenetics, University of Bari, Bari, Italy.

#obtained from L. Kearney, MRC Medical Research Council, John Radcliffe Hospital, Molecular Haematology Unit, Headington, Oxford, United Kingdom.

NA, not applicable

### 8.3 Additional PCR primers

**Table 2. Additional oligonucleotide primer sequences**

Primer	Sequence (5' - 3')	Direction	Gene/Exon <sup>1</sup>
BDNFex2-R1	TTCTGGTCCTCATCCAACAGC	antisense	BDNF/2
BDNFex2-R2	CGGCAACAAACCACAACATTATC	antisense	BDNF/2
ELNex16-R1	GCACGCCAGGAACACCAG	antisense	ELN/16
ELNex18-R1	GCCCACCAGGCACTAAGC	antisense	ELN/18
ELNex6-R2	AGCAGCGTCAGCCACTCCAC	antisense	ELN/6
ETV6ex3-R1	CCTCTTTGGTCAGCAGCAGGAG	antisense	ETV6/3
FOXP1ex11-R1	TTGTTGCCTGTGGTTTCTTCTGC	antisense	FOXP1/11
FOXP1ex14-R1	GGCGGCTTTGGGTTCTGTAG	antisense	FOXP1/14
FOXP1ex8-R1	TGCTGGAGGAGAACCTGGAG	antisense	FOXP1/8
HIPK1ex8-F1	CTGCACCAGTTCCTGGAGTTGC	sense	HIPK1/8
PAX5ex3-F1	CCATGTTTGCCTGGGAGATCAG	sense	PAX5/3
PAX5ex5-F1	TACTCCATCAGCGGCATCC	sense	PAX5/5
PAX5ex6-7R1	TGGCTGAATACTCTGTGGTCTGCTC	antisense	PAX5/6-7
PAX5ex6-F1	CTGGACCGCGTGTTTGAGAG	sense	PAX5/6
PAX5ex7-R1	GGCCTTCATGTCGTCCAG	antisense	PAX5/7
PAX5ex9-10-R1	GCTATAATAGTAGGGGGAGCCAAGCA	antisense	PAX5/9-10
PAX5ex9-R2	ACGAGGAATACTGAGGGTGGCTGT	antisense	PAX5/9
PMLex1-F2	TCAGCTTCTCTTCACGCACTC	sense	PML/1
ZNF521ex4-R1	TGAGAGCCGTCCTTGTTCTC	antisense	ZNF521/4
ZNF521ex7-R1	CTGCTGCAACTTGTTTGCTTG	antisense	ZNF521/7

<sup>1</sup>Exon nomenclature according to the Ensembl Genome Browser exon information (<http://www.ensembl.org/>).

Fusion transcripts were amplified using the following primer combinations.

PAX5-BDNF:	PAX5ex5-F1 and BDNFex2-R1
	PAX5ex5-F1 and BDNFex2-R2
PAX5-ELN:	PAX5ex3-F1 and ELNex6-R2 or ELNex16-R1
	PAX5ex5-F1 and ELNex18-R1
PAX5-ETV6:	PAX5ex3-F1 and ETV6ex3-R1
PAX5-FOXP1:	PAX5ex6-F1 and FOXP1ex8-R1
	PAX5ex3-F1 and FOXP1ex11-R1
	PAX5ex5-F1 and FOXP1ex14-R1
PAX5-ZNF521:	PAX5ex3-F1 and ZNF521ex4-R1
	PAX5ex6-F1 and ZNF521ex7-R1
HIPK1-PAX5:	HIPK1ex8-F1 and PAX5ex6-7-R1
PML-PAX5:	PMLex1-F2 and PAX5ex7-R1

To identify novel *PAX5* fusion partner genes RACE was performed using various *PAX5* gene specific primers in combination with universal 5' or 3' primers provided by the Marathon Kit (Takara Bio Europe/Clontech, Saint-Germain-en-Laye, France) (Nebral *et al*, in press). Additional 5' RACE experiments were performed using PAX5ex9-10-R1 and AP1 for the first round of amplification, and PAX5ex9-R2 and AP2 for the nested second round of amplification. Alternatively, instead of a "touch down" PCR reaction a "one step" PCR was performed using the following cycling parameters: 95°C initial denaturation for 1min, 35 cycles of 94°C for 15sec, and 68°C for 5-8min, and final elongation at 68°C for 6min. The nested PCR was done for 30 cycles of 94°C for 15sec, and 68°C for 5-8min.

---

## DEUTSCHE ZUSAMMENFASSUNG

PAX5 ist ein Transkriptionsfaktor der Paired Box Genfamilie, welcher sowohl für die Entwicklung von B-Zellen aus hämatopoietischen Vorläuferzellen als auch für deren Fortbestand als reife B-Zellen von essentieller Bedeutung ist. Vor kurzem wurde gezeigt, dass PAX5 in B-Zell-Neoplasien häufig involviert ist. Die entsprechenden genetischen Alterationen umfassen Punktmutationen und Deletionen und, von besonderem Interesse im Zusammenhang mit meiner Arbeit, auch Genrearrangements. In B-Zell-Non-Hodgkin-Lymphomen mit einer t(9;14)(p13;q32), zum Beispiel, gelangt das *PAX5* Gen durch die Translokation in die Nähe des *IGH@* Locus, wodurch es zu einer Überexpression von *PAX5* kommt. Im Gegensatz dazu wurden bei akuten lymphatischen B-Vorläuferzell Leukämien ("B-cell-precursor"; BCP-ALL) Fusionen des *PAX5* Gens mit *FOXP1* (3p13), *AUTS2* (7q11), *ELN* (7q11), *ETV6* (12p13), *ZNF521* (18q11) und *C20orf112* (20q11) beschrieben, wobei die daraus resultierenden Fusionstranskripte für chimäre Proteine kodieren.

Das Ziel der vorliegenden Studie war es daher, die Häufigkeit und Art von *PAX5* Genrearrangements bei ALL im Kindesalter systematisch zu untersuchen, sowie neue *PAX5* Fusionspartner zu identifizieren und zu charakterisieren. Die 446 analysierten Proben stammen von konsekutiv in den österreichischen ALL-BFM 2000 und Interfant-99 Studien registrierten PatientInnen und repräsentieren daher eine unselektierte und klinisch gut charakterisierte Kohorte.

Zum Nachweis von potentiellen *PAX5* Genrearrangements wurden eigene Fluoreszenz in situ Hybridisierung (FISH) Assays entwickelt und die Interphase FISH Muster mithilfe der Metafer4-Metacyte Software (Metasystems) automatisch ausgewertet. Um alle im *PAX5* Gen möglichen Bruchpunkte zu erfassen (auch jene, die zu einer veränderten Expression des intakten *PAX5* Gens durch ein Partnergen führen) wurden primär das Gen flankierende zwei Farben FISH Sonden verwendet. Auffällige FISH Muster wurden weiter mit Gen-spezifischen Sonden abgeklärt. Anschließend wurden die Fusionspartner entweder mit FISH und/oder 3'-oder 5'-RACE (Rapid Amplification of cDNA ends) identifiziert und das Vorhandensein der chimären Transkripte mittels RT-PCR (Reverse Transcription-PCR) und Sequenzierung überprüft.

10 von 446 untersuchten Proben (2.2%) zeigten ein für ein *PAX5* Rearrangement charakteristisches FISH Muster. Ein Fall mit einer *PAX5-ETV6* Fusion war bereits aus Vorbefunden bekannt, bei einem weiteren wurde eine kürzlich in der Literatur beschriebene *PAX5-C20orf112* Genfusion gefunden und bei einem Patienten konnte die vorliegende *PAX5* Aberration trotz intensiver Analysen nicht vollständig aufgeklärt werden. Jedoch gelang es uns bei sieben Fällen sechs neue *PAX5* Fusionspartner zu identifizieren: *HIPK1* (1p13), *POM121* (7q11), *JAK2* (9p24), *DACH1* (13q21), *PML* (15q24) und *BRD1* (22q13.33). Mit Ausnahme von zwei *PAX5-JAK2* positiven Fällen, traten alle anderen Fusionen jeweils nur

---

einmal auf. Weiters konnten, zumindest bei der ALL im Kindesalter, keine *PAX5*-aktivierenden Translokationen gefunden werden. Aufgrund der großen Heterogenität der Fusionspartner ist die von uns etablierte FISH Strategie eine verlässliche und sinnvolle Screeningmethode mit der alle potentiellen *PAX5* Genfusionen systematisch erfasst werden können.

Aus dem Ergebnis meiner Studie kann man zusammenfassend ableiten, dass zirka 2.5% der BCP-ALL Fälle *PAX5* Genfusionen aufweisen, welche jedoch eine Vielzahl von Partnergenen betreffen, die nicht nur Transkriptionsfaktoren sondern auch Strukturproteine und eine Tyrosinkinase, einschließen. Die hypothetischen Fusionsproteine bestehen in allen Fällen zumindest aus der *PAX5*-paired DNA-Bindungsdomäne, die mit der C-terminalen Region oder sogar dem gesamten Protein des jeweiligen Partners fusioniert. Die Struktur der *PAX5* chimären Proteine legt nahe, dass diese zwar an *PAX5* Zielgene binden können, aber keine normale transkriptionelle Regulation ausüben und dadurch der intrinsischen *PAX5*-Aktivität entgegenwirken, was möglicherweise bei der Pathogenese der BCP-ALL eine Rolle spielt.

---

## CURRICULUM VITAE

### PERSÖNLICHE DATEN

**Name** Karin Nebral  
**Geburtsdatum** 28.10.1977  
**Geburtsort** Gmünd, Niederösterreich, Österreich  
**Staatsangehörigkeit** Österreich

### AUSBILDUNG

1984-1988 Volksschule Schwarzenau  
1988-1992 Sporthauptschule Waidhofen/Thaya  
1992-1996 Bundesrealgymnasium Zwettl  
06/1996 Reifeprüfung mit ausgezeichnetem Erfolg bestanden

### STUDIUM

10/1996-05/2004 Diplomstudium der Biologie, Studienzweig Anthropologie, Universität Wien  
09/2001-07/2002 Erasmusstipendium an der Universität Tor Vergata, Rom, Italien  
10/2002-05/2004 Diplomarbeit am CCRI, St. Anna Kinderkrebsforschung, Wien  
Gruppenleiter: Univ. Prof. Dr. Oskar A. Haas  
Thema: "Detection and characterization of *NUP98* rearrangements in leukemia"  
Supervisor: Dr. Sabine Strehl  
05/2004 2. Diplomprüfung mit Auszeichnung bestanden; Verleihung des akademischen Titels: Magistra der Naturwissenschaften (Mag. rer. nat.)  
11/2004-2008 Dissertation am CCRI, St. Anna Kinderkrebsforschung, Wien  
Gruppenleiterin: Dr. Sabine Strehl  
Thema: "Detection and characterization of *PAX5* aberrations in childhood acute lymphoblastic leukemia"  
10/2005-2008 Doktoratsstudium Biologie, Studienzweig Anthropologie, Universität Wien

### SONSTIGES

11.-12.9.2003  
12.-13.4.2005 Schulungen: Metafer4 Metacyte System (Metasystems)  
19.-20.6.2008  
06/2008 Travel Grant: 13th Congress of the EHA (European Hematology Association), Kopenhagen, Dänemark



---

## PUBLIKATIONSLISTE

**Nebral, K.**, Denk, D., Attarbaschi, A., Konig, M., Mann, G., Haas, O.A. & Strehl, S. (in press) Incidence and diversity of PAX5 fusion genes in childhood acute lymphoblastic leukemia. *Leukemia*.

**Nebral, K.**, Konig, M., Harder, L., Siebert, R., Haas, O.A. & Strehl, S. (2007) Identification of PML as novel PAX5 fusion partner in childhood acute lymphoblastic leukaemia. *Br J Haematol*, **139**, 269-274.

**Nebral, K.**, Konig, M., Schmidt, H.H., Lutz, D., Sperr, W.R., Kalwak, K., Brugger, S., Dworzak, M.N., Haas, O.A. & Strehl, S. (2005a) Screening for NUP98 rearrangements in hematopoietic malignancies by fluorescence in situ hybridization. *Haematologica*, **90**, 746-752.

**Nebral, K.**, Schmidt, H.H., Haas, O.A. & Strehl, S. (2005b) NUP98 is fused to topoisomerase (DNA) IIbeta 180 kDa (TOP2B) in a patient with acute myeloid leukemia with a new t(3;11)(p24;p15). *Clin Cancer Res*, **11**, 6489-6494.

Strehl, S., **Nebral, K.**, Konig, M., Harbott, J., Strobl, H., Ratei, R., Struski, S., Bielecki, B., Lessard, M., Zimmermann, M., Haas, O.A. & Izraeli, S. (2008) ETV6-NCOA2: a novel fusion gene in acute leukemia associated with coexpression of T-lymphoid and myeloid markers and frequent NOTCH1 mutations. *Clin Cancer Res*, **14**, 977-983.

Steiner, M., Attarbaschi, A., Konig, M., **Nebral, K.**, Gadner, H., Haas, O.A. & Mann, G. (2005) Equal frequency of TEL/AML1 rearrangements in children with acute lymphoblastic leukemia with and without Down syndrome. *Pediatr Hematol Oncol*, **22**, 229-234.

---

## DANKSAGUNG

Ein großes DANKE an all jene, die mich während der letzten Jahre begleitet haben – einerseits allen KollegInnen des CCRI, die mir immer mit Rat & Tat zur Seite standen und die den Arbeitsalltag mit einer positiven sozialen Komponente erfüllten - andererseits allen Freunden, die mit mir durch Ups & Downs gegangen sind, mir in den Phasen des Zweifels zugehört haben und die mir gezeigt haben, dass es auch noch ein anderes Leben neben der Arbeit gibt, das es zu genießen & zu leben heißt.

Einzelne Namen zu nennen ist schwierig (ich hoffe, es ist niemand beleidigt, der nicht genannt wird):

Oskar, der mir die Tür ins CCRI geöffnet hat, dem ich diesen wissenschaftlichen Werdegang verdanke & den ich für sein unglaubliches Wissen und sein Selbstverständnis für die Bedeutung des Lernens und Lehrens bewundere und den ich auch privat sehr schätze.

Sabine, eine Betreuerin, die mensch kein zweites Mal findet! Sie hat mich immer mit großem Engagement & einem unendlichen Wissen geleitet. Auch wenn es manchmal hart war, die Dinge richtig zu machen, so war es das Endergebnis immer wert. Sie hat mich sowohl wissenschaftlich als auch sozial geprägt und mich immer voll & ganz unterstützt, auch wenn es mir mal nicht so gut ging.

Weiters allen meinen lieben Labor-KollegInnen für Hilfe im Laboralltag, für gemeinsame Kaffeepausen, für das freundschaftliche und respektvolle Miteinander:

Anne, Barbara, Bettina, Bettina, Brigitte, Brigitte, Dagmar, Daniela, Eva, Gudrun, Margit, Markus, Nicky, Ulli, Susanna, Trude  
& allen aus dem Labor 7

für die Freundschaft, die angeregten Diskussionen & die Unterstützung bei Experimenten, sowie die Hilfestellung bei klinischen Fragen: Andrea, Gerd, Ruth & Renate und Andishe.

sowie für methodische und gerätetechnische Unterstützung, Tipps & Tricks ein Dank an das gesamte CCRI!

Vielen Dank auch an mein PhD-Komitee: Ulrich Jäger, Berthold Streubel und Johannes Schmid, die mich durch positives Feedback und konstruktive Diskussion immer sehr motivierten.

Von meinen Freunden besonders Marc, Sascha, Erich, Susi & Dani.

Der größte Dank gehört meiner Familie, der Basis meines Lebens. Danke für das Verständnis, die immerwährende Unterstützung, dass wir alle füreinander da sind!

Ich widme diese Dissertation meinem Opa, der mich immer wieder fragte, wann ich nun endlich fertig sei, und der leider die Antwort auf diese Frage "jetzt!" nicht mehr miterleben durfte.